THE APPLICATION OF CAPILLARY PRESSURES IN DETERMINING THE SEAL CAPACITY OF EROMANGA BASIN CAP-ROCKS

Thesis Submitted to the Faculty of Science,
University of Adelaide

In
Partial Fulfilment of the Requirement for

the
M. Sc Degree

in

Petroleum Geology and Geophysics,

the University of Adelaide

by Catherine J. Solomon
1992

STATEMENT OF AUTHENTICITY

To the best of my knowledge and belief this thesis contains no material which has been accepted for the award of any other degree or diploma in any University, nor does it contain any material previously published or written by another person, except where due reference is made in the text.

I consent to this thesis being made available for loan or for photocopying as required.

ACKNOWLEDGEMENTS

I would like to thank all those at SANTOS Ltd who assisted me during both the planning and research stages of this project. In particular, I wish to thank Dr. R. Heath, G. Solomon, S. McIntyre and N. Tupper for their valuable advice and discussion throughout. I also thank M. Madey for the preparation of the diagrams and plates within the thesis.

Special thanks to D. Sisely of Gearhart for his time and effort in preparing my core samples and for his help with the planning and supervising of all the core analyses.

I am grateful to Dr. W. Stuart and Professor L. Frakes for their constructive comments and suggestions on thesis content and preparation of the manuscript.

I also thank all those others too numerous to mention who have helped me during the last few years with discussions and with the production of the final manuscript.

TABLE OF CONTENTS

FIGURES

APPENDIX 1

1. Routine Core Analysis
2. Eromanga Basin Oil Densities

APPENDIX 2

1. Crossplots of the Year drilled against the analyses results
2. Crossplots of Routine Core Analyses against Mineralogy
3. Crossplots of Threshold Pressure against Mineralogy

ABSTRACT

The seal capacity, measured in terms of the height of oil column a seal can hold, has been determined for several Eromanga Basin cap-rock samples from mercury injection capillary pressure measurements. The threshold or breakthrough pressure has been estimated from the mercury saturation versus injection pressure curves and converted to reservoir conditions. Using an equation that relates the threshold pressure to the reservoir and oil densities, the theoretical oil column height has been calculated.

Calculated oil column heights for the Eromanga Basin samples range from 288 feet (88m) up to 5,550 feet (1692m) indicating good to excellent sealing capacity. These silty mudstones from the Murta and Namur Members of the Mooga Formation and the Birkhead Formation are composed primarily of quartz, illite and kaolinite, with minor amounts of chlorite, siderite and feldspar.

Microporosity constitutes 90 to 100 per cent of the measured porosity and occurs between oriented platy clay and mica grains, as observed under Scanning Electron Microscope. Although measured porosities range from less than one per cent up to 14.9 per cent, permeabilities are consistently very low. All samples were reported to have values less than 0.09 millidarcies.

Calculated oil column heights were compared to the actual columns intersected in the Eromanga Basin to determine the role of seal capacity in controlling the size and distribution of oil pools.

Many Eromanga Basin structural closures are only a few hundred feet or less from the crest to the spill point. Most oil pools contained in these structures are small, with oil columns far less than those predicted by the experimental results. Oil columns rarely exceed 50 feet (15m) and are generally less than the structural closure. Although the

experimental results show that the mudstone layers can be excellent seals, only a few Eromanga Basin oil pools are interpreted to be filled to structural spill. The occurrence of multiple, stacked oil pools within the sequence indicates that either quantities of oil are leaking through the seals or that there could be multiple sources for the oil.

Although some oil pools may have received a contribution from Eromanga Basin source rocks, current evidence from both well and regional data suggests that most of the oil trapped within the Eromanga Basin sequence is being sourced from the underlying Permian Cooper Basin sequence and is migrating into suitable Eromanga Basin traps where the lower regional seals are eroded or faulted.

The size and distribution of oil pools within the Eromanga Basin can be explained in part, by poor lateral continuity of the seals, which allows leakage of oil from one horizon to another. This is probably caused by rapid facies changes within the finely interbedded sealing intervals. Mudstones grade into siltstones or sandstones which have lower sealing capacities. Another major factor in disrupting the lateral seal continuity is faulting and fracturing caused by either burial compaction or later tectonic events.

1. INTRODUCTION

Successful exploration for Eromanga Basin oil has been difficult in some areas of the Eromanga Basin in PEL's 5 and 6 and ATP 259 P due to a poor understanding of the origin of the oil and the mechanisms that control the lateral and vertical distribution of accumulations. This is evidenced by the poor success ratio for wells with exploration targets in the Eromanga Basin sequences.

The presence of reservoir, seal and an oil source within the study area has been proven. Extensive sandstones with moderate to excellent reservoir quality, capped by thin silty mudstones occur within the Jurassic to Early Cretaceous sequence. The presence of oil accumulations within these reservoirs proves that an oil source is available. One aspect of the hydrocarbon potential of the basin that has not been evaluated is the quality of the sealing rocks.

The aim of this study was to measure the seal capacity of the Eromanga Basin cap-rocks and thus to determine the importance of seal capacity in controlling the distribution and size of oil accumulations. This is the first study of its kind within the Eromanga Basin and one of the first to be undertaken in Australia.

Eromanga Basin seals are generally perceived to be poor cap-rocks because oil pools are small, with known oil columns generally less than 50 feet (15m) and nearly always less than the mapped closure. Structures containing multiple, stacked oil pools are common, but are often found adjacent to fields containing single oil pools or structures that are dry. This distribution of oil pools could be related to the volume of oil that is available for migration and entrapment or to poor seal capacity. This has important implications for exploration within the study area as the size of oil accumulations could be limited by the quality of the sealing intervals.

This study investigates the seal capacity of cap-rock samples from the main sealing units in the Murta and Namur Members of the Mooga Formation and the Birkhead Formation. The intervals within each formation that contain mudstones have been examined to determine the seal capacity of the best sealing lithologies. Theoretical oil column heights calculated from the experimental results have been compared to the actual oil columns observed within the Eromanga Basin.

The methods used to measure seal capacity are special mercury injection capillary pressure techniques. X-Ray Diffraction (XRD) and Scanning Electron Microscopy (SEM) have been used for determining the sample mineralogy and together with conventional porosity and permeability measurements, help define the relationship of grains and pore throats.

It is noted that the distribution and size of Eromanga Basin oil pools could also be the result of a combination of many other factors. One of the most important controls, the origin of the oil reservoired in the Eromanga Basin, is discussed in Section 2.3.

2. REGIONAL SETTING

2.1 STRATIGRAPHY

The Eromanga Basin lies in the central part of the Australian continent and consists of Jurassic to Late Cretaceous marine and non-marine sediments. The basin covers an area of approximately one million square kilometres. The study area is a small region in the central part of the basin covered by PEL's 5 and 6 (South Australia) and ATP 259 (Queensland) (Fig. 1). In this area, the thickness of the basin sequence reaches a maximum of over 8,000 feet (2500m). Over most of the study area, the Eromanga Basin overlies the Permo-Triassic Cooper Basin sequence. A relatively thin veneer of Tertiary sediments overlies the Eromanga Basin.

The Jurassic to Late Cretaceous Eromanga Basin can be separated into three main sequences within the study area. A lower non-marine sandstone, siltstone, shale and coal sequence is overlain by marginal-marine to marine shale, siltstone and sandstone and capped by a further non-marine cycle of fluvial to lacustrine sediments, as shown diagrammatically in Fig. 2.

Significant amounts of hydrocarbons were first discovered in the Eromanga Basin in the mid 1970's, after several minor indications of oil were encountered during drilling (Sprigg, 1986). However, it was not until the early 1980's that a major effort was made in the exploration for Eromanga Basin oil. To date, all the economic oil discoveries have been made in the Late Jurassic to Early Cretaceous non-marine Eromanga Basin sequences, with the greatest volumes of oil being contained in the Hutton Sandstone, the Birkhead Formation and the Namur and Murta Members of the Mooga Formation (Fig. 2). Major Eromanga Basin oil fields have been discovered in sandstones of all formations within this section and only this Jurassic to Early Cretaceous sequence, relevant to the study, will be discussed further.

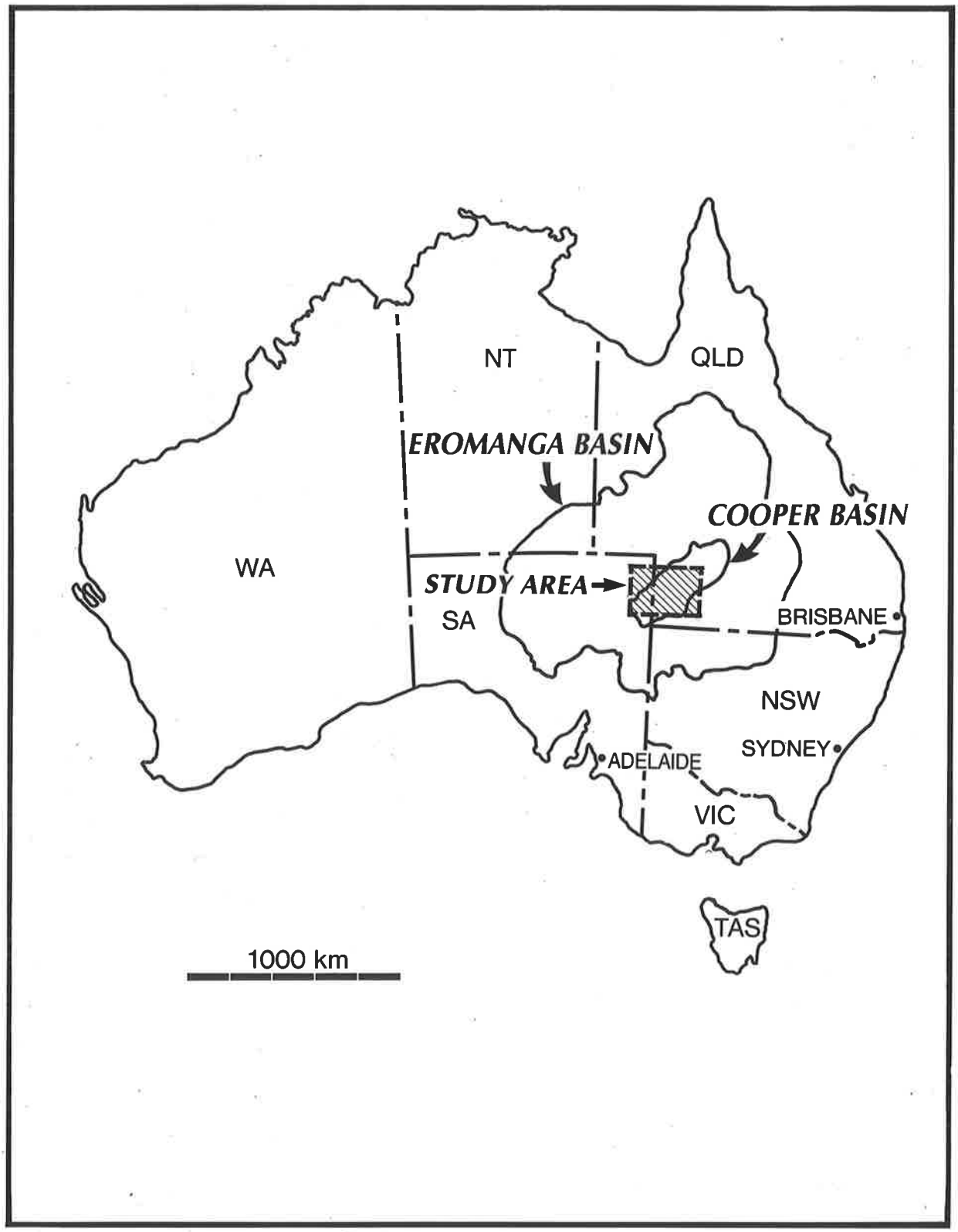

Fig. 1 Location map of the Eromanga, Cooper Basins and study area, Central Australia.

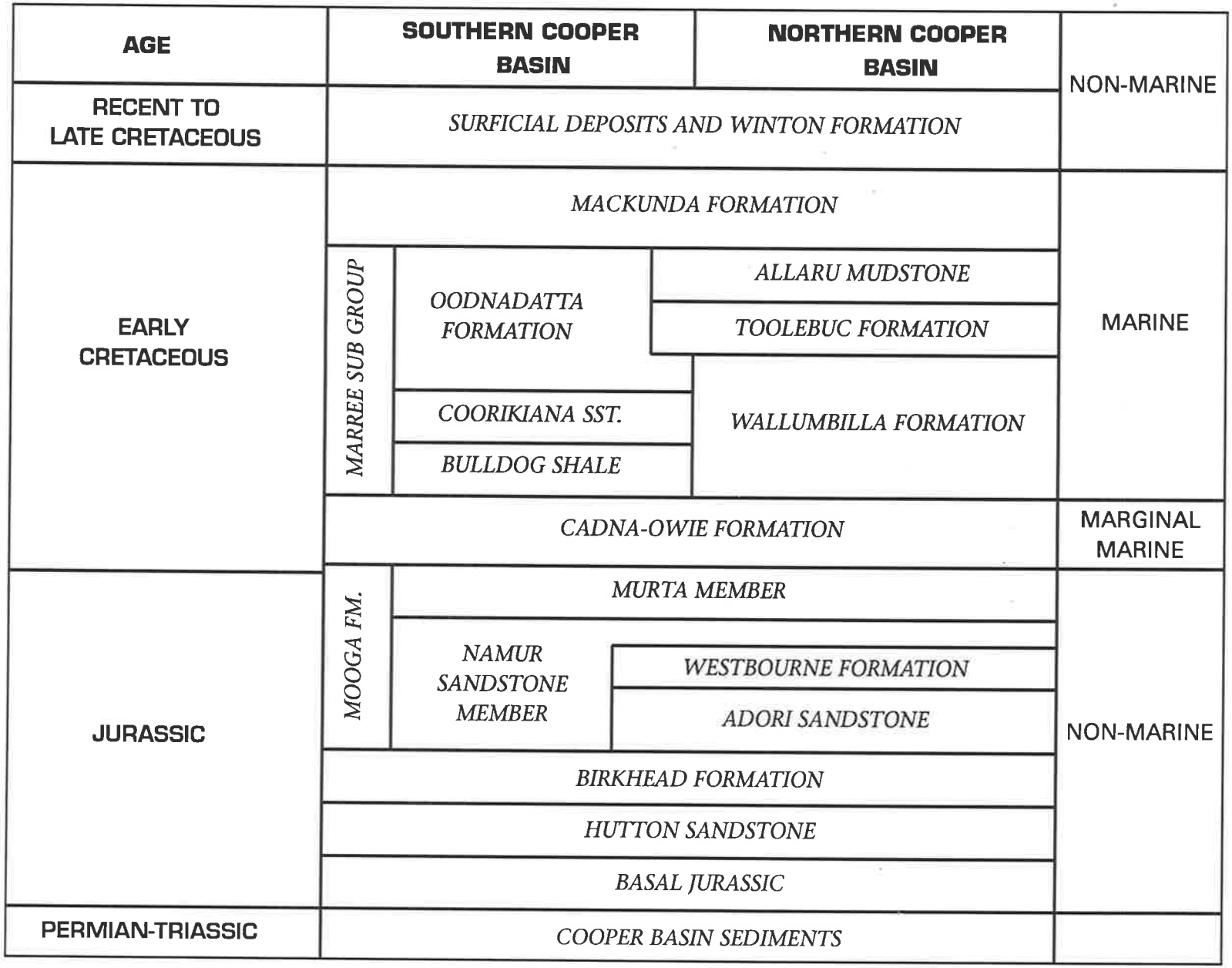

Fig. 2 Stratigraphy of the Eromanga Basin in South Australia and Queensland.

The stratigraphic cross-section displayed in Fig. 3 shows the variation in thickness of the stratigraphic units from west to east. The main sealing intervals of the Murta Member and the Birkhead Formation have higher gamma ray log values resulting from the greater concentration of radioactive minerals such as clays, feldspar and mica. The mudstones and siltstones are shaded to highlight these lithologies.

There are several excellent works on the stratigraphy of the Eromanga Basin, some of which are contained in the volumes, Moore and Mount (1982), Gravestock et al. (1986) and O'Neil (1989). The following is a brief discussion of the lower Eromanga Basin stratigraphy as it relates to this study.

2.1.1 LOWER EROMANGA BASIN SEQUENCE - JURASSIC TO EARLY CRETACEOUS

The earliest depositional unit of the Eromanga Basin is the Early Jurassic Poolowanna Formation. The Poolowanna Formation was deposited on a major unconformity surface following uplift and erosion of underlying Cooper Basin sediments at the end of the Triassic. Topographically low areas were gradually infilled. This can be seen on seismic sections where the Poolowanna Formation and lower Hutton Sandstone reflectors onlap older highs along the margins of the deeper troughs within the study area.

The Poolowanna Formation consists of fine to medium grained sandstones with interbedded shales, coals and siltstones deposited in deltaic to fluvial environments.

Thickness of the Poolowanna Formation, where present, ranges from less than 50 feet (15m) up to 500 feet (152m) across the study area and can vary considerably from one field to another due to facies changes. The Poolowanna Formation is locally an important reservoir unit in the western part of the study area (Fig. 4 and 5). Thin, interbedded mudstones and silty mudstones, usually grey in colour, micaceous and containing minor

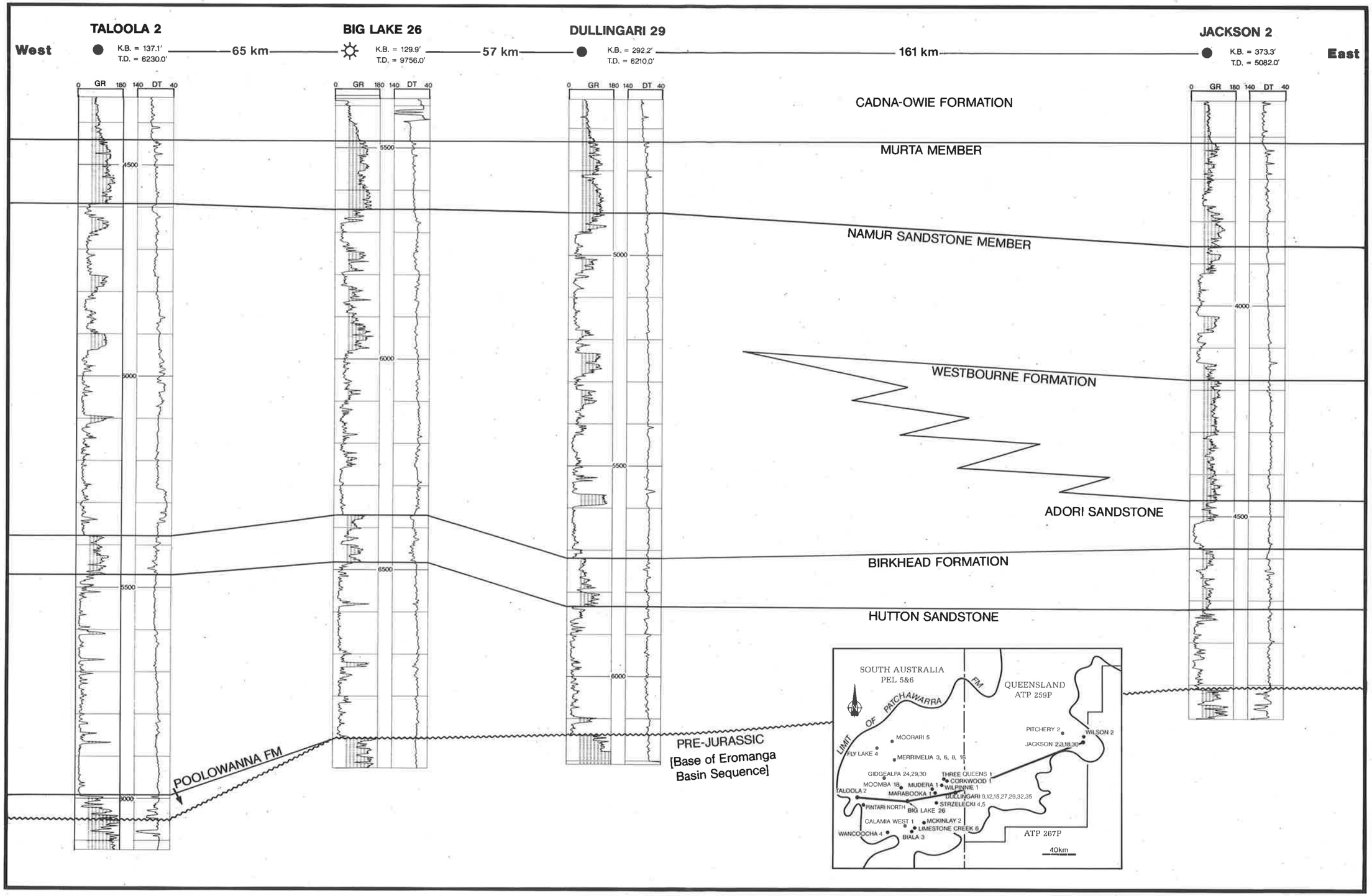

Figure 3 : Stratigraphic cross-section across the study area showing the lower Eromanga Basin sequence from west to east.

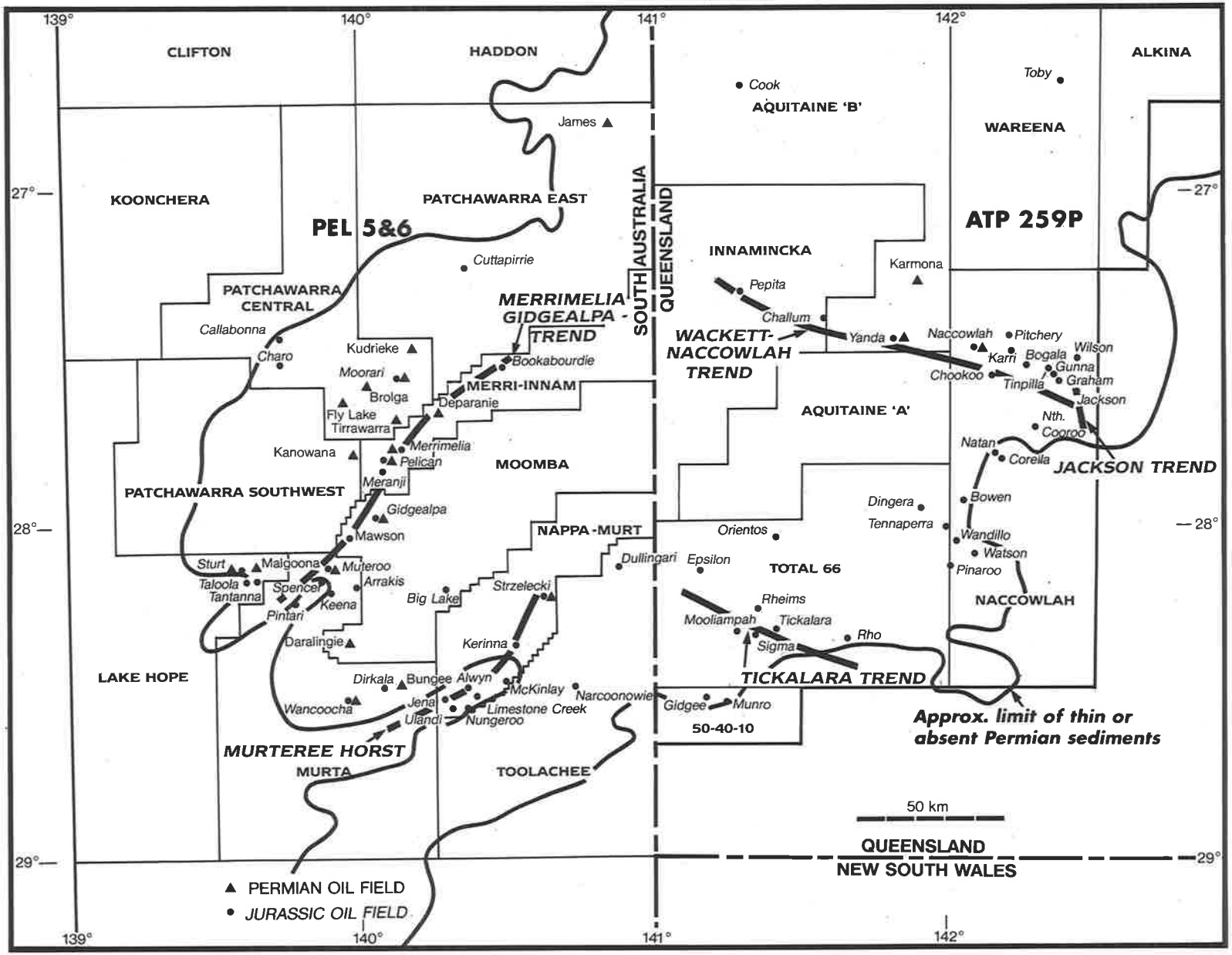

Fig. 4 Location map of Eromanga and Cooper Basin oil fields.

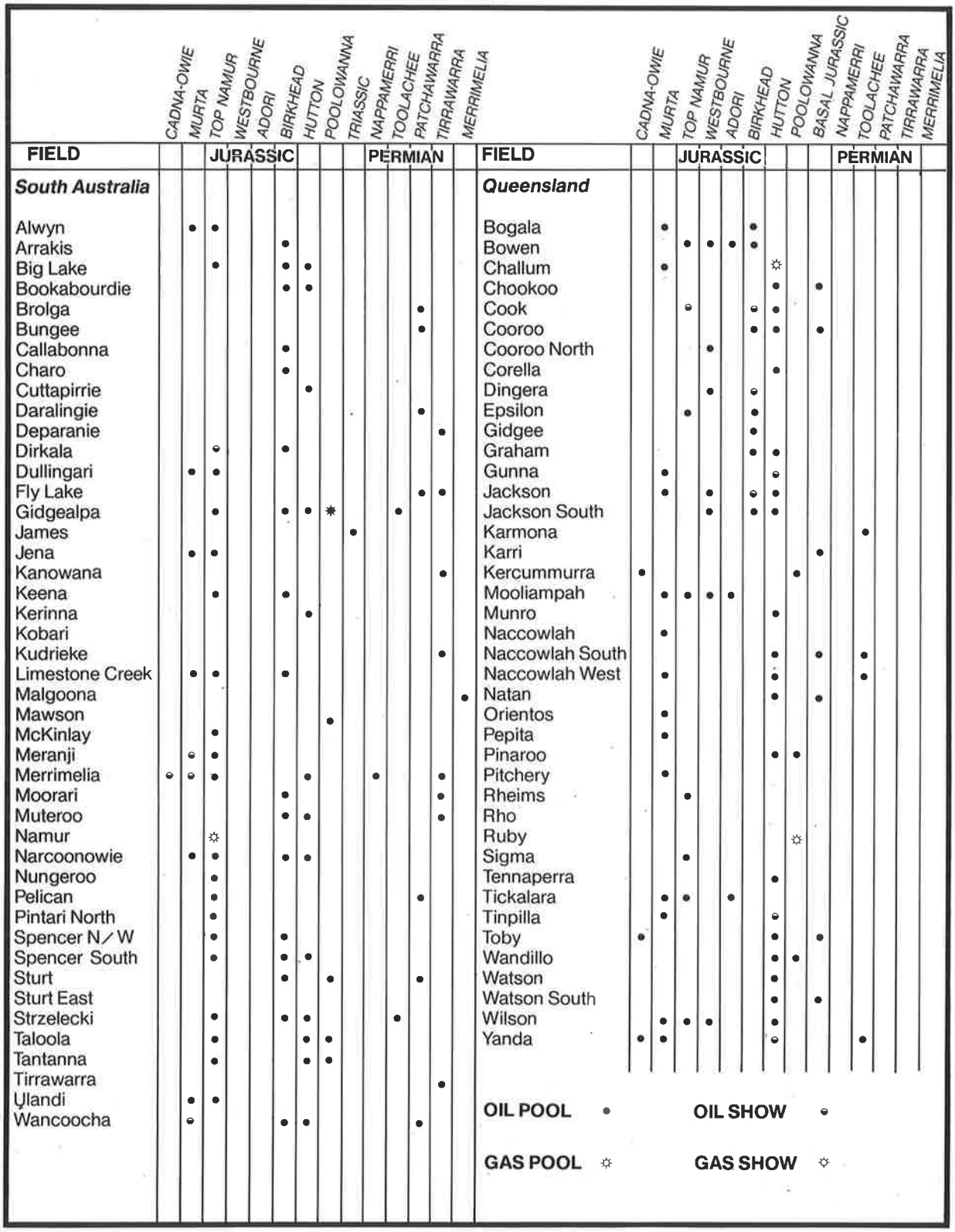

Fig. 5 Stratigraphic distribution of Eromanga Basin hydrocarbons and Cooper Basin oil fields. (modified after Heath et al (1989))

to abundant carbonaceous material, form the seals to sandstone reservoirs.

The conformably overlying Early to Middle Jurassic Hutton Sandstone, is a laterally extensive unit consisting of a series of stacked braided stream sandstones with occasional thin interbedded siltstones and mudstones. It contains some of the best reservoir rocks in the basin, with porosities often greater than 20 per cent and permeabilities greater than one hundred millidarcies.

Thicknesses range from around 50 feet (15m) on the south eastern margin of the study area to 800 feet (244m) in the centre. Thin mudstones and siltstones, representing abandoned channel and reworked overbank deposits, are occasionally present in parts of the section and often cannot be correlated for any great distance, even within the same field.

The contact between the Hutton Sandstone and the overlying Birkhead Formation is often gradational, although a sharp contact is not uncommon. The Middle to Late Jurassic Birkhead Formation reaches thickness of around 350 feet (107m) in the centre of the study area. It consists of siltstones, interbedded with silty mudstones, sandstones and coals that were deposited in fluvial, deltaic and lacustrine environments. These siltstones and mudstones form the cap-rocks to many large oil fields. The mudstones are grey to brown/grey and often silty and carbonaceous. Individual mudstone bed thicknesses rarely exceed 10 feet (3m) in the full-hole cores. Core photographs of the Birkhead Formation are presented in Figs. 6e and 6f.

Although predominantly composed of silty mudstone, siltstone, mudstone and coal, the Birkhead Formation can also contain good reservoir sandstones. In contrast to the Hutton Sandstone, sandstones of the Birkhead Formation are generally finer grained, more argillaceous and have lower porosities and permeabilities. These sandstones are sealed by intraformational mudstones and silty mudstones.

The Birkhead Formation is conformably overlain by the Late Jurassic Adori Sandstone in the eastern part of the study area. The Adori Sandstone is a sequence of sandstones deposited in a braided to meandering stream environment which attains thicknesses up to 300 feet (91m). The sandstones are generally medium grained, with good porosity and permeability.

Finely interbedded siltstones, sandstones and silty mudstones of the lacustrine to fluvial Westbourne Formation overlie and seal the Adori Sandstone. The Westbourne Formation is Late Jurassic in age and reaches a maximum thickness of 500 feet (152m) in the east of the study area. To the west it intertongues with the Namur Sandstone Member (Fig. 3). Although both the Adori Sandstone and Westbourne Formation contain oil pools in the eastern part of the area, they hold relatively small volumes of oil basin-wide (Fig. 5).

The finer clastics of the Westbourne Formation are laterally equivalent to the coarser, braided sandstones of the Namur Sandstone Member. The underlying Adori Sandstone and the Westbourne Formation are not differentiated in the western and southern parts of the Eromanga Basin (Fig. 3).

The Late Jurassic to Early Cretaceous Namur Member of the Mooga Formation consists of sandstones that are fine to very coarse grained, slightly more argillaceous than the Hutton Sandstone sediments and may contain thick carbonate cemented zones in the lower section. The Namur Member ranges in thickness from 100 feet (30m) in the west and north to 800 feet (244m) in the south of the study area. Many oil pools have been discovered in the reservoirs of the upper Namur Member, trapped below the fine-grained sediments of the lower Murta Member. Examples of these fine-grained intervals are given in the core photographs, (Figs. 6c and 6d). Small oil columns have also been intersected below thin mudstones within the Namur Sandstone. Hence, the thin Namur mudstones may have better lateral continuity, compared to that inferred from observations of siltstone-mudstone interbeds within the Hutton Sandstone.

The upper contact of the Namur Member with the Early Cretaceous Murta Member of the Mooga Formation is commonly gradational, with the sandstones becoming micaceous and finer grained towards the top. This interval of radioactively 'hot' sandstone and siltstone has been informally called the McKinlay Member in some areas of South Australia and locally is an important reservoir rock.

The Murta Member consists of deltaic to lacustrine siltstones, sandstones and mudstones that are very thinly bedded and often bioturbated (Figs. 6a to 6d). It ranges in thickness from less than 50 feet (15m) to a maximum thickness of 350 feet (107m) in the study area. Most of the lower section has no reservoir potential and forms a thick sealing interval to the Namur Sandstone. The sequence also contains hard bands of sandstone cemented by siderite and calcite. In the full-hole cores examined, some sections were extensively bioturbated and showed signs of soft sediment deformation such as slumping. Microfaults were also noted in several of the cores. Individual mudstone and silty mudstone layers are generally less than one foot (0.3m) thick.

Within the upper part of the Murta Member, highly permeable sandstones interpreted as reworked shoreline and lacustrine fan deposits with thicknesses from a few inches (5cm) up to two feet (0.6m), can form good to excellent reservoir rocks. The thicker, coarsening upwards sandstones have lower permeability due to higher clay and silt contents. Interbedded mudstones and silty mudstones form the seals within this unit.

The transition from non-marine to marine conditions is associated with deposition of the Neocomian Cadna-Owie Formation, previously informally called the 'Transition Beds'. It consists of a 100 to 350 feet (30 to 107m) thick sequence of coarsening upwards siltstones and fine sandstones with minor mudstones. Reservoir potential is generally very low in the study area due to silica and carbonate cementation of the fine grained sandstones and high clay and silt contents. Small oil and gas discoveries have been made in the both the eastern and western parts of the study area (Fig. 4 and 5).

The Cadna-Owie Formation grades upwards into the open marine shales of the Wallumbilla Formation (Bulldog Shale equivalent), marking the base of the middle part of the Eromanga Basin sequence.

2.2 STRUCTURE

The Eromanga Basin has been described by Passmore (1989) as a broad, intracratonic basin which developed primarily in response to continental thermal sag. This gentle downwarping was later modified by a period of regional uplift during the Late Cretaceous to Tertiary which is responsible for much of the present-day relief (Gilby and Mortimore, 1989).

The Permo-Triassic Cooper Basin and the older pre-Permian Warburton Basin sequences are blanketed by the Eromanga Basin sediments over the entire study area. Much of the lower Eromanga Basin sequence was deposited under conditions of relative tectonic stability. This is evidenced by the Cadna-owie Formation to Hutton Sandstone isopachs which vary gradually from over 1000 feet (305m) in the south west, up to 1600 feet (488m) in the north and deeper parts of the basin within the study area. The upper part of the Eromanga Basin was deposited during a period of increased subsidence during the Aptian to Cenomanian, resulting in the accumulation of several thousand feet of sediment in the basin depocentre.

Structural features displayed by the Eromanga Basin generally reflect those of the underlying Cooper and Warburton Basins. The dominant expression of structural development of the Jurassic and Cretaceous sequences is broad, gentle folding which formed in response to Tertiary tectonic activity and to drape and compaction over pre-existing structures. Basement horst blocks uplifted during several tectonic events in the Devonian, Permian and Triassic form the basis of the major highs such as the Nappacoongee-Murteree, Gidgealpa-Merrimelia and the Wackett-Jackson trends. These

horst blocks are often bounded by high-angle normal faults on one flank and a more gently dipping surface on the other and can be observed on several seismic sections.

The lower part of the Eromanga Basin sequence generally displays a different style of faulting to the upper part. The throw on the deep basement faults that cut the Cooper Basin appears to diminish significantly upon reaching the base of the Jurassic Eromanga Basin sequence. However, occasionally these normal faults can be seen on seismic to extend as high as the Birkhead or even the Cadna-Owie Formation. Faults or fracture zones may commonly extend beyond this level but the variable nature of the sediments results in many discontinuous reflectors obscuring the evidence for faults with small throws at this level.

Post-depositional fracturing and folding of the Eromanga Basin sequence occurred during a period of compression during the Tertiary (Passmore, 1989). Major basement faulting was probably reactivated during this period, extending the lower faults up into the Jurassic sequence.

This tectonic activity also resulted in the development of folds and some listric and keystone style faulting within the upper Eromanga Basin sequence. This part of the sequence contains a higher proportion of finer grained lithologies and is less compacted. Faulting often occurs directly overlying the edges of faulted basement horst blocks and generally soles out before reaching the upper part of the Cadna-Owie Formation.

2.3 DISTRIBUTION OF KNOWN OIL FIELDS

2.3.1 GEOGRAPHICAL DISTRIBUTION

Eromanga Basin oil accumulations have been found predominantly in structural traps overlying the margins of the Triassic and Permian sequences of the Cooper Basin (e.g. Jackson, Tantanna, Taloola, Wancoocha and Watson). Many fields are also located on,

or close to major structural trends such as the Nappacoongee-Murteree High, the Gidgealpa-Merrimelia High and the Wackett-Jackson High, (e.g. Biala, Limestone Creek, Gidgealpa, Narcoonowie and Merrimelia). The underlying Cooper Basin sequences, which include major regional mudstone seals, are thin or absent over these older Pre-Permian basement highs due to onlap during deposition or erosion. The locations of many Eromanga Basin and Cooper Basin oil fields are shown in Fig. 4.

Almost all of the oil discovered in the study area has been found in the structural settings described above. Other Eromanga Basin oil fields such as Dullingari, Big Lake, Bookabourdie, Meranji and Moorari are underlain by thick sequences of Permian and Triassic strata which includes the thick regional mudstone seals of the Nappamerri Formation and the Murteree and Roseneath Shale. These structures often have either associated complex faulting over the anticlines or major regional faults cutting the flanks of the structural highs.

Although most Eromanga Basin oil fields are found clustered around the Cooper Basin margins, it is not uncommon to find structures containing several oil pools located immediately adjacent to structures that are water saturated in all Jurassic horizons. Some of those located in South Australia are Kurunda and Mawson, Nealyon and Tantanna. Gas discovered in significant quantities within the Jurassic sequences is reservoired in the Namur Member or the lower Hutton Sandstone and Poolowanna Formation, in structures above faulted regional highs, as in Namur and Gidgealpa in South Australia and Chookoo in Queensland.

The geographical distribution of hydrocarbon accumulations is related to the location of mature source rocks and is influenced by secondary migration and concentrating mechanisms. Hydrocarbon generation generally occurs initially in the deeper parts of a basin where potential source rocks will mature first. A liquids or oil prone generative stage will often be followed by wet gas and then dry gas as temperatures and pressures

increase in the central parts of a basin. Horizons higher in the sequence will likewise also go through the oil and gas windows, but at later stages. As the hydrocarbons are generated and migrate out of the basin centre, concentric zones with varying liquids content should form outwards from the basin centre as well as vertically through the section. This of course assumes a relatively constant variation in conditions (e.g. geothermal gradient and slope) across the basin.

The pattern of varying liquids content with location is very pronounced in the Permian Cooper Basin (Hunt et al., 1989). Dry gas is found in the deeper parts of the basin, grading outwards to liquids-rich gas and eventually oil at the basin margins where source rocks have lower maturity. However, there appears to be no regular pattern in the regional distribution of Jurassic hydrocarbon pools. Oil pools lie in a rather thin band around the edges of the Cooper Basin and along major structural trends (Fig. 4).

The few gas pools discovered are trapped in structures that also contain oil pools (e.g. Gidgealpa) or in structures that are in close proximity to major oil and Permian gas fields (e.g. Namur).

2.3.2 STRATIGRAPHIC DISTRIBUTION

The vertical distribution of oil pools in the Eromanga Basin is erratic, with both multiple, stacked pools and single pools being common. From the stratigraphic diagram showing the location of many of the oil pools within the Jurassic and Early Cretaceous sequence (Fig. 5), it is clear that the largest number of oil pools have been discovered in the top of the Hutton Sandstone and in the Namur Member.

No patterns can be observed with depth of burial or with position in the basin, except where there are a number of culminations with the same features closely spaced along a structural trend such as the Limestone Creek, Alwyn, Biala, Ulandi and Jena region.

Approximately 80 kilometres to the north-west of the Limestone Creek area, lie oil fields which are closely spaced and which have very similar structural and stratigraphic features. However, oil pools occur in different horizons within each culmination. In the Tantanna Field, oil has been discovered in the Poolowanna, Hutton and Namur reservoirs, but only in the Poolowanna and Namur reservoirs in the adjacent Taloola Field. The Sturt and Sturt East Fields lie on a parallel trend to the north of the Tantanna and Taloola Fields. Oil has been found in the Poolowanna Formation and the Birkhead Formation in Sturt, but only in the Poolowanna Formation in Sturt East. A recently drilled culmination, Malgoona, located further into the basin from the Tantanna Field, discovered oil within the lower part of the Cooper Basin sequence, the Merrimelia Formation. Another nearby structure has oil reservoired in fractured Pre-Permian volcanic rocks. This oil is believed to have migrated into the trap from a Permian source.

2.4 CURRENT MODELS FOR THE ORIGIN OF EROMANGA BASIN OIL

The origin of the Eromanga Basin oil pools has been discussed in several recent papers (Sprigg, 1986, Heath et al., 1989, Jenkins, 1989, Michaelsen and McKirdy, 1989, Tupper and Burckhardt, 1990). At present there are two models for the origin of the hydrocarbons reservoired in the Eromanga Basin. One is a Permian source model, the other is a Jurassic or Early Cretaceous source model.

Currently, it is considered likely that most of the oil reservoired in the Eromanga Basin is sourced from the underlying Cooper Basin and the evidence for this is discussed in the next section. However, the extent to which the Jurassic or Early Cretaceous sequences are contributing to the accumulations is still unknown. Michaelsen and McKirdy (1989), believe that many of the Murta Member oil pools have been sourced in situ.

Differentiating Permian derived oils from those generated from Jurassic source rocks is

not a simple task, as potential source rocks in both the Jurassic and the Permian contain predominantly land plant derived (Type 11 & 111) kerogens that have similar geochemical characteristics and the same conventional biomarker distributions (Jenkins, 1989).

The geographical location of known oil pools immediately above breached Permian reservoirs (Gidgealpa, Jackson, Limestone Creek and Tantanna are just some of these), suggests that the main migration direction was vertical and that little lateral migration has taken place. On the other hand, if the Eromanga Basin sequences are sourcing significant volumes of oil, then lateral migration may have had a greater influence on the distribution of oil pools. The small oil column heights observed could then be a result of poor quality or limited source rocks or low volumes of generated hydrocarbons rather than leaky seals.

No single model adequately explains the distribution, sizes and characteristics of all the Eromanga Basin oil pools discovered to date and the following section discusses some of the arguments for the origin of Eromanga Basin oil.

2.4.1 MODEL 1 - PERMIAN SOURCE

The location of many Eromanga Basin oil fields above truncated, thin, or faulted Cooper Basin rocks that are more mature, contain excellent source rock characteristics and which have known hydrocarbon generating potential, strongly suggests that most of the Eromanga Basin oil pools have been sourced from the underlying Permian sequences and has leaked into suitable structures in the overlying section (Heath et al., 1989, McIntyre, 1987).

Almost all oil fields discovered to date are located crestally within anticlinal structures with four-way dip closure that are located in a position that will trap leaking Permian hydrocarbons.

Hydrocarbons generated within mature Permian sequences, most likely the Patchawarra Formation or possibly the Toolachee Formation, migrate upwards and outwards from the deeper parts of the basin and into the overlying Jurassic at or near the edges of the Lower Permian or Triassic regional seals. The occurrence of Permian oil pools or high liquids-content gas pools directly underlying or in close proximity to oil bearing Jurassic closures provides a strong argument for this model (e.g. Merrimelia, Gidgealpa, Yanda and Naccowlah).

The oils reservoired in the Eromanga Basin have very low gas-oil ratios and are low in water-soluble aromatic compounds. This could be attributed to water-washing, which strips the hydrocarbons of gaseous and other water-soluble molecules as they migrate vertically up through firstly the Hutton Sandstone and then the Namur Formation aquifers (Heath et al., 1989).

2.4.2 MODEL 2 - JURASSIC SOURCE

The abundance of multiple, stacked oil pools with small oil columns in the Eromanga Basin may also indicate a limited volume of source rock available within the Jurassic and Early Cretaceous sequences. The presence of Murta and Namur oil pools located above thick, competent Birkhead sealing intervals could also be explained by a Murta Member source. Cook (1982), Jenkins (1989), Michaelsen and McKirdy (1989), Tupper and Burckhardt (1990) and others, have conducted studies of Eromanga Basin source rocks to determine kerogen types, geochemical characteristics, source potential and maturity levels. Some of these studies suggest that a few of the oil accumulations in the Jurassic sequences may be derived predominantly from Jurassic or Early Cretaceous source rocks.

Potential Eromanga Basin source rocks have been identified primarily in the Murta Member, but the carbonaceous intervals within the Birkhead and Poolowanna Formations

also have some potential (McKirdy, 1982). The lacustrine Murta Member contains organic matter that is algal in origin, in addition to the land plant material common to Jurassic and Permian source rocks. Some Murta reservoired oils have higher pristane/ phytane ratios that are considered to reflect these differences in source material (Michaelsen and McKirdy, 1989).

In most parts of the Eromanga Basin, particularly around the margins of the Cooper Basin where many oil discoveries have been made, the maturity of potential Eromanga source rocks is low. Vitrinite reflectance studies performed primarily by Keriaville Consultants and Amdel Ltd give an indication of maturity levels in some wells. The Murta Member reaches a Rv = 0.7 per cent only in the centre of the study area, (Kantsler et al., 1982) and Rv = 0.4 - 0.6 per cent around the Limestone Creek area. The measured vitrinite reflectances of the Birkhead Formation are around Rv = 0.5 - 0.65 per cent at the Cooper Basin edge in the Spencer, Muteroo, Limestone Creek, Watson and Jackson wells. The start of the oil generative window is considered to be in the range Ro = 0.5 - 0.7 per cent (Tissot and Welte, 1978). However, most vitrinite reflectances are below those for the generation and expulsion of significant liquid hydrocarbons from land-plant derived source rocks, which is from Ro = 0.7 to 0.9 per cent (Thomas, 1982; Heath et al., 1989).

Michaelsen and McKirdy (1989) describe some low maturity oils that they believe have been generated from the Early Cretaceous Murta and Namur Members at equivalent vitrinite reflectance levels of Ro = 0.5 - 0.6 per cent. This conclusion is based upon the analysis of alkane biomarkers and methylphenanthrene indexes (MPI) as maturation indicators. The method for determining maturity levels of oils and potential source rocks obtained by the MPI molecular maturity indicator is given in Tupper and Burckhardt (1990).

Tupper and Burckhardt (1990) considered a Jurassic reservoired oil to be sourced in situ if the maturity of the oil and the reservoir rocks was comparable and the biomarker distributions were favourable for a Jurassic source. Jenkins (1989) used similar criteria to establish the origin of Eromanga Basin reservoired oils. These workers conclude that Cooper and Eromanga Basin oils have been expelled at various maturities, which could be as low as an equivalent vitrinite reflectance of Ro = 0.6 per cent.

If Murta Member or Birkhead Formation source rocks are mature away from the basin centre and oil is being generated locally, it follows that gas and wet gas accumulations should be found in the deeper parts of the basin where temperatures and pressures are greater. No gas fields that can be attributed to an Eromanga source have been found in these areas to date. The gas in the Nanima, Gidgealpa, Marabooka and Namur Fields in South Australia and the Chookoo Field, in Queensland, is interpreted to have leaked up from the Cooper Basin via faults. This is based on the compositional affinity with adjacent Permian gas pools (Rigby and Smith, 1981).

The small number of gas pools discovered within the Jurassic sequence could be attributed to water-washing or the stripping of lighter hydrocarbons by moving groundwaters. The lighter fractions are particularly easily dissolved in the fresh water contained within the aquifers, which would disperse it and effectively prevent the accumulation of gas pools (Heath et al., 1989).

However, it is the process of water washing that also provides some evidence for the Permian source model. The composition of oil pools tends to vary in a regular way with depth in multiple, vertically stacked accumulations, implying leakage from one horizon to another from below. Many of these oils have a greater affinity with others in the same field, rather than with the oils in a nearby field in the same horizon (Heath et al., 1989) suggesting vertical migration from below.

Futhermore, gas pools within the Jurassic section are most commonly located in the Poolowanna Formation and lower Hutton Sandstone (e.g. Gidgealpa), which are closest to the point of leakage from the Permian reservoirs below. Gas can locally saturate the waters in these horizons, before further migration allows it to be swept away.

The small number of wells drilled in a position that could investigate the gas or oil potential of Jurassic closures in the centre of the basin could also account for the low number of Eromanga Basin gas discoveries.

There are only a few Eromanga Basin oil fields that cannot be easily explained by a Permian source model. The Dullingari Oil Field is one of these. Oil is reservoired in the Murta and Namur Members above a water saturated Hutton Sandstone and Birkhead Formation. Dullingari lies in a position where the Jurassic and Early Cretaceous intervals are considered to be marginally mature for oil generation (Ro = 0.6 to 0.7 per cent). Oil could have migrated from Murta source rocks in the deeper parts of the basin or have been generated in situ (Jenkins, 1989, Michaelsen and McKirdy, 1989). However, it may also have migrated along the Tickalara fault zone from lower horizons.

2.4.3 SUMMARY

Most of the evidence discussed previously suggests that the Cooper Basin is the main source for the oil discovered in the Eromanga Basin. However, there is the possibility of some contribution of hydrocarbons from potential source rocks in the Eromanga Basin sequence itself. The main evidence against the Jurassic model is the local immaturity of Eromanga Basin source rocks and the lack of indications of longer range migration. In addition, if Eromanga Basin rocks are capable of sourcing and expelling oil at low levels of maturity, the quantities are likely to be low unless a very large area is involved. Volumetrically, the Early Cretaceous coal and carbonaceous mudstone intervals are only a fraction of those known to exist in the Permian sequence.

Although no oil or gas fields have been found in the deeper areas of the Eromanga basin, many oil shows have been observed. This may indicate that some Jurassic oil may have been generated but has not yet reached a level at which it can be expelled (Heath et al., 1989). It has been suggested by Jenkins (1989) that some Jurassic mudstones are rich enough in organic matter to generate oil, but they may have low expulsion efficiencies.

Many studies have been conducted in the last few years to find biomarkers either in the oils or in the source rocks in an effort to determine the origin of the oils. Age dependent biomarkers have been identified in rocks of the Eromanga Basin, but no unique biomarkers for the Cooper Basin rocks have been found (Jenkins, 1989). The presence of an Eromanga biomarker in a particular oil, however, does not preclude a Permian source. Some Jurassic carbonaceous intervals may have generated oil, little or none of which has yet been expelled. The mixing of these hydrocarbon molecules can occur as the Permian oil migrates through the rocks, attracting them and leaving a Jurassic fingerprint.

The origin of the oil is a major influence on the distribution of Eromanga Basin oil pools. At this time a significant contribution from Jurassic source rocks cannot be proven. Heath et al. (1989) have suggested that for oil derived from a Permian source, the distribution of Eromanga oil pools is controlled in part by the thickest, most competent seal found lower-most in the Eromanga sequence. The nature and location of effective seals within this sequence is discussed in the following sections.

3. SAMPLING

3.1 DETERMINATION OF THE SEALING INTERVALS

The location of oil pools trapped predominantly beneath the finer grained intervals of the Murta and Namur Members and the Birkhead Formation means that sealing lithologies exist within these formations. The variable pool sizes and the distribution of accumulations raises the fundamental question of what constitutes an effective Eromanga Basin seal.

Effective seals are described by Downey (1984, p. 1752) as "typically thick, laterally continuous, ductile rocks with high capillary entry pressures". However, no thick regional mudstone units have been identified that could provide such seals to the oil accumulations in the Eromanga Basin. The massive reservoir sandstones of the Namur Member, Hutton Sandstone and the thin highly permeable sandstones of the Murta Member are overlain by sequences consisting of finely interbedded and often bioturbated silty mudstones, siltstones and sandstones. Photographs of these sealing intervals for several wells are given in Figs. 6a to 6f.

Examples of sealing lithologies from the Murta Member in Figs. 6a and 6b show much thinner bedding than the sealing sections in the Birkhead Formation (Figs. 6e and 6f). The lower part of the Murta Member, which forms the sealing unit to the Namur Member (Figs. 6c and 6d), is very similar to the upper Murta Member. Siderite content is much higher in the Namur Member seals and can be seen in the photographs, appearing as pale yellow or honey coloured bands and nodules.

The almost flat bedding in all the cores reflects the gentle dips on many of the structures in the Eromanga Basin. Cross-bedding, microfaulting and bioturbation are common and can be seen throughout the cored intervals. As no thick mudstone seals can be identified from the core, an alternative definition of a seal is needed. One definition given by

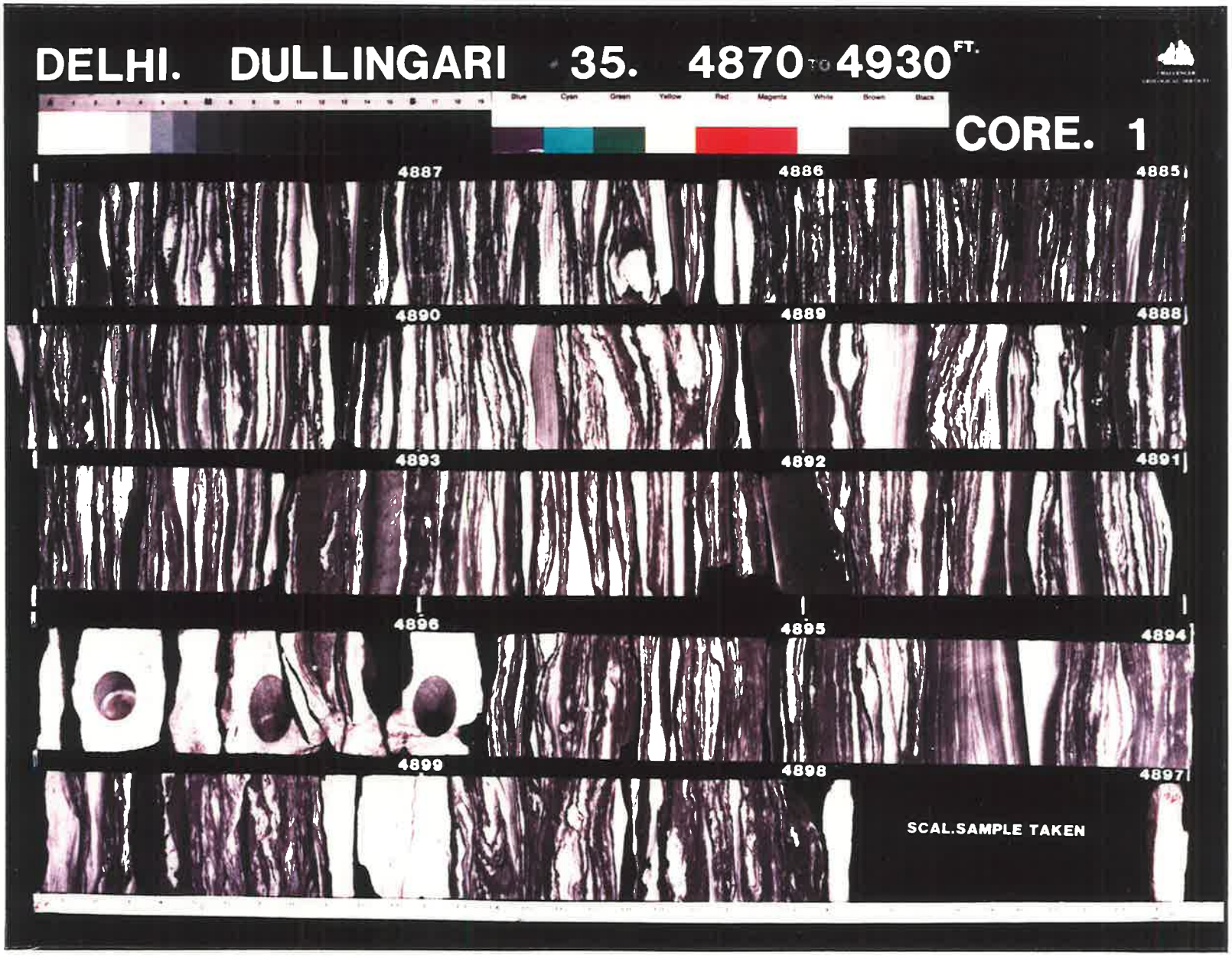

Fig. 6(a) Core photograph, Dullingari 35, Murta Member.

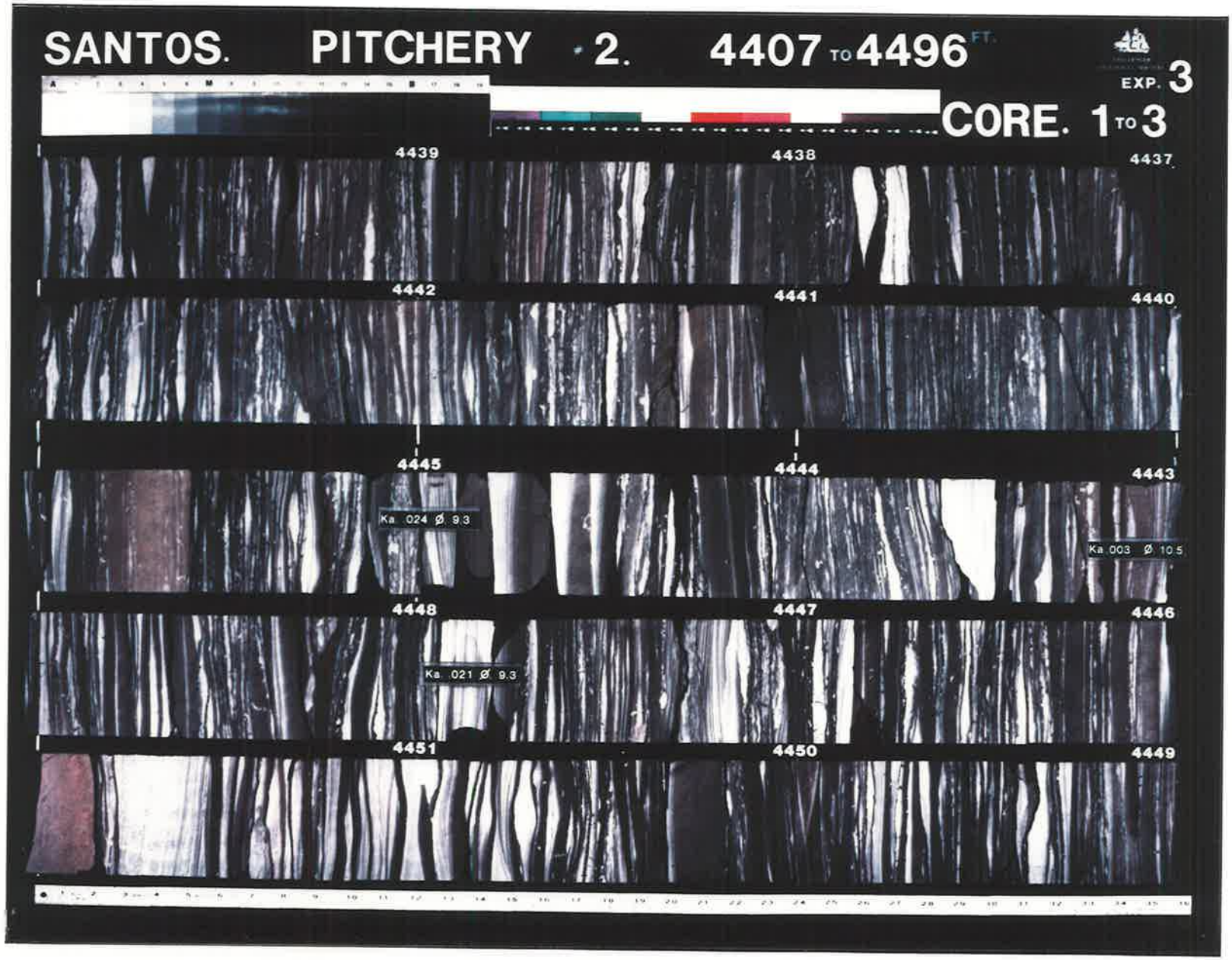

Fig. 6(b) Core photograph, Pitchery 2, Murta Member.

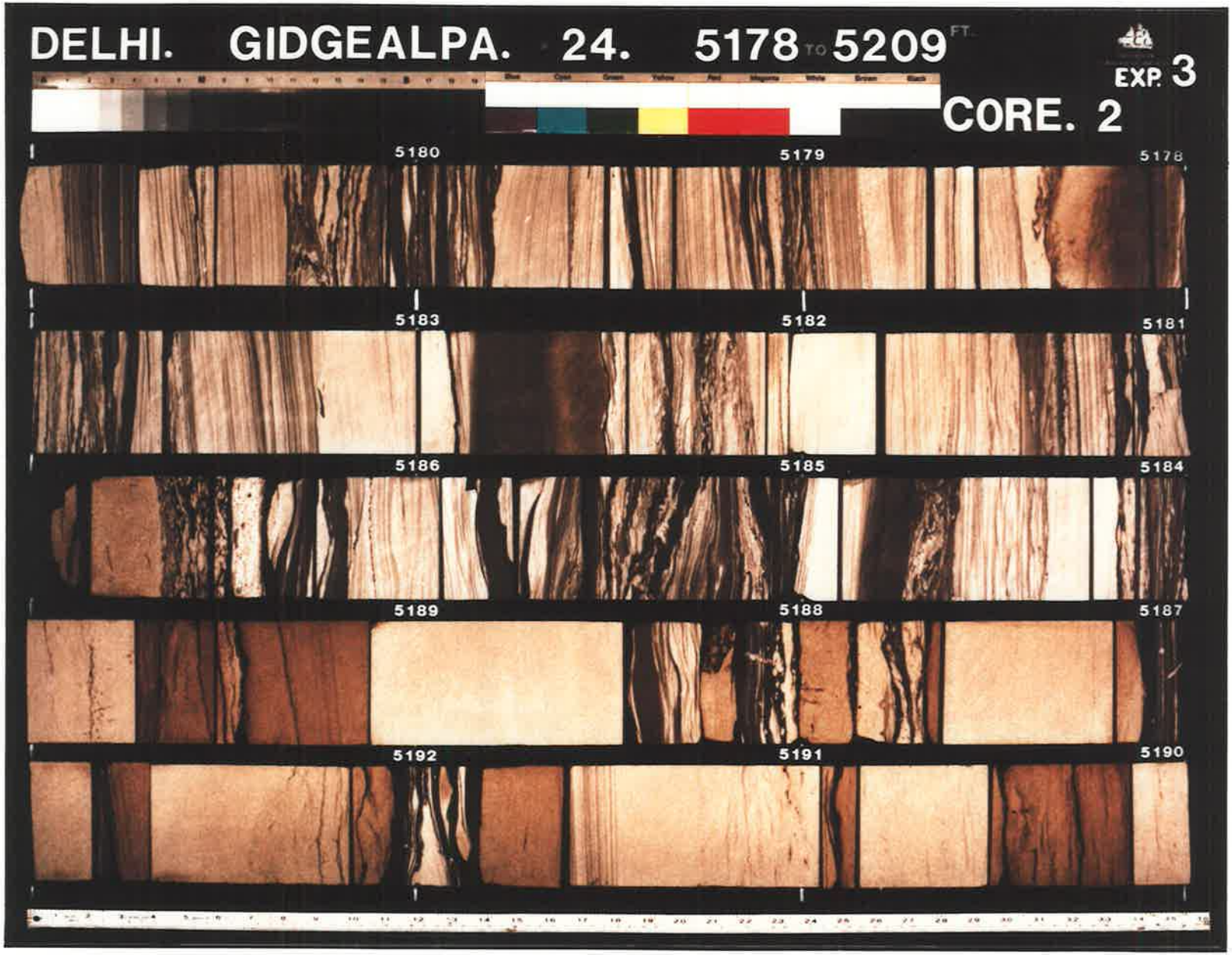

Fig. 6(c) Core photograph, Gidgealpa 24, Namur Member.

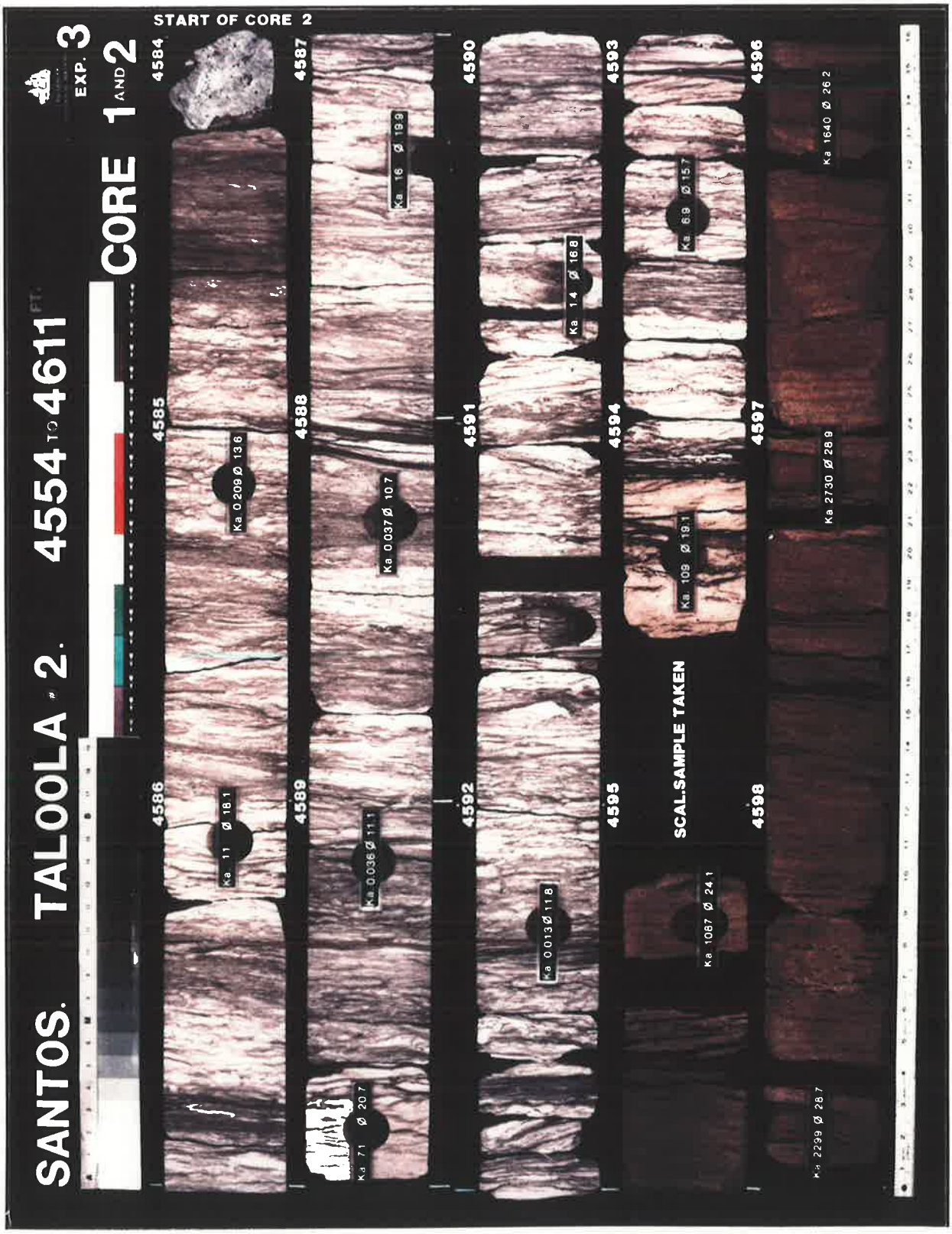

Fig. 6(d) Core photograph, Taloola 2, Namur Member.

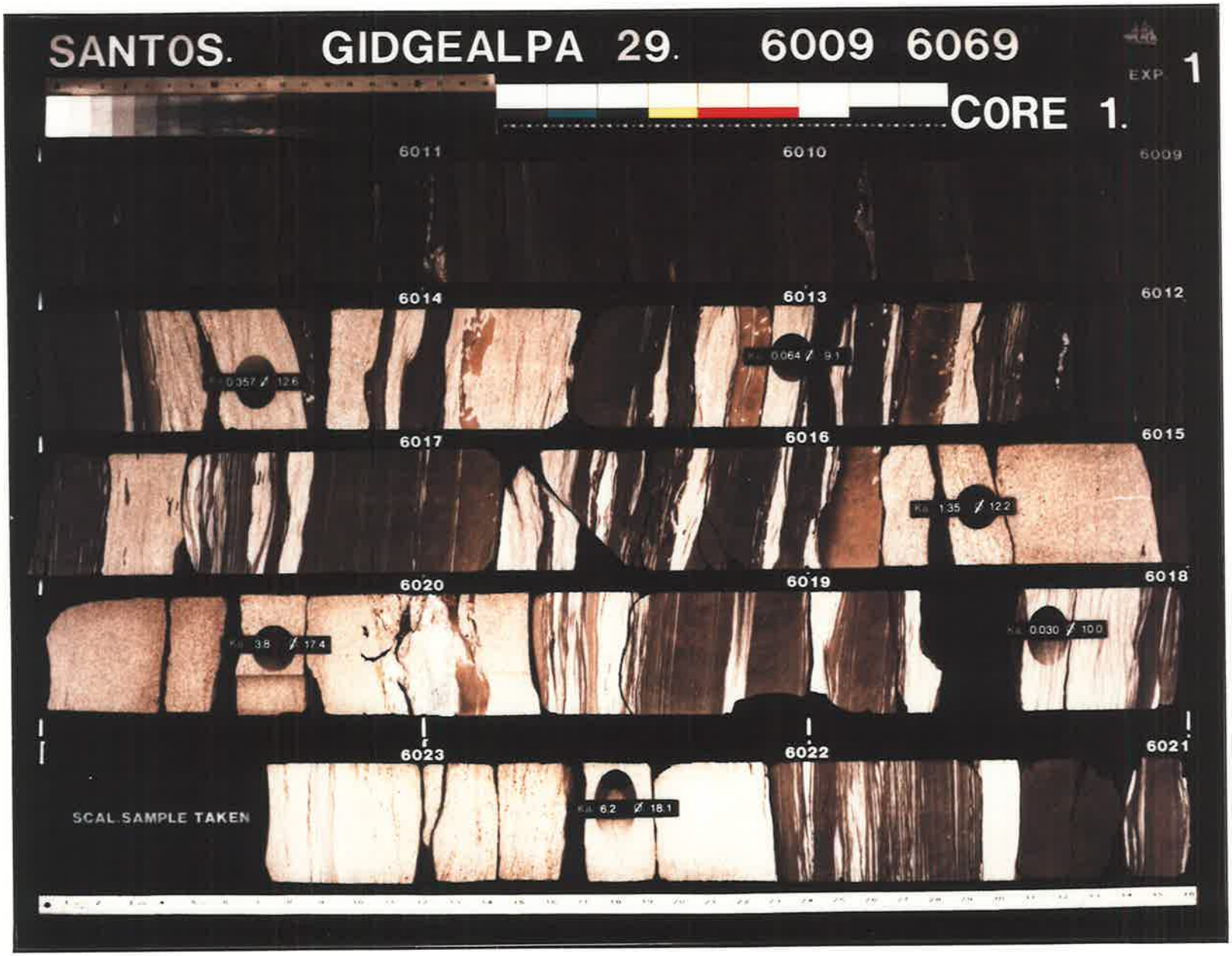

Fig. 6(e) Core photograph, Gidgealpa 29, Birkhead Formation.

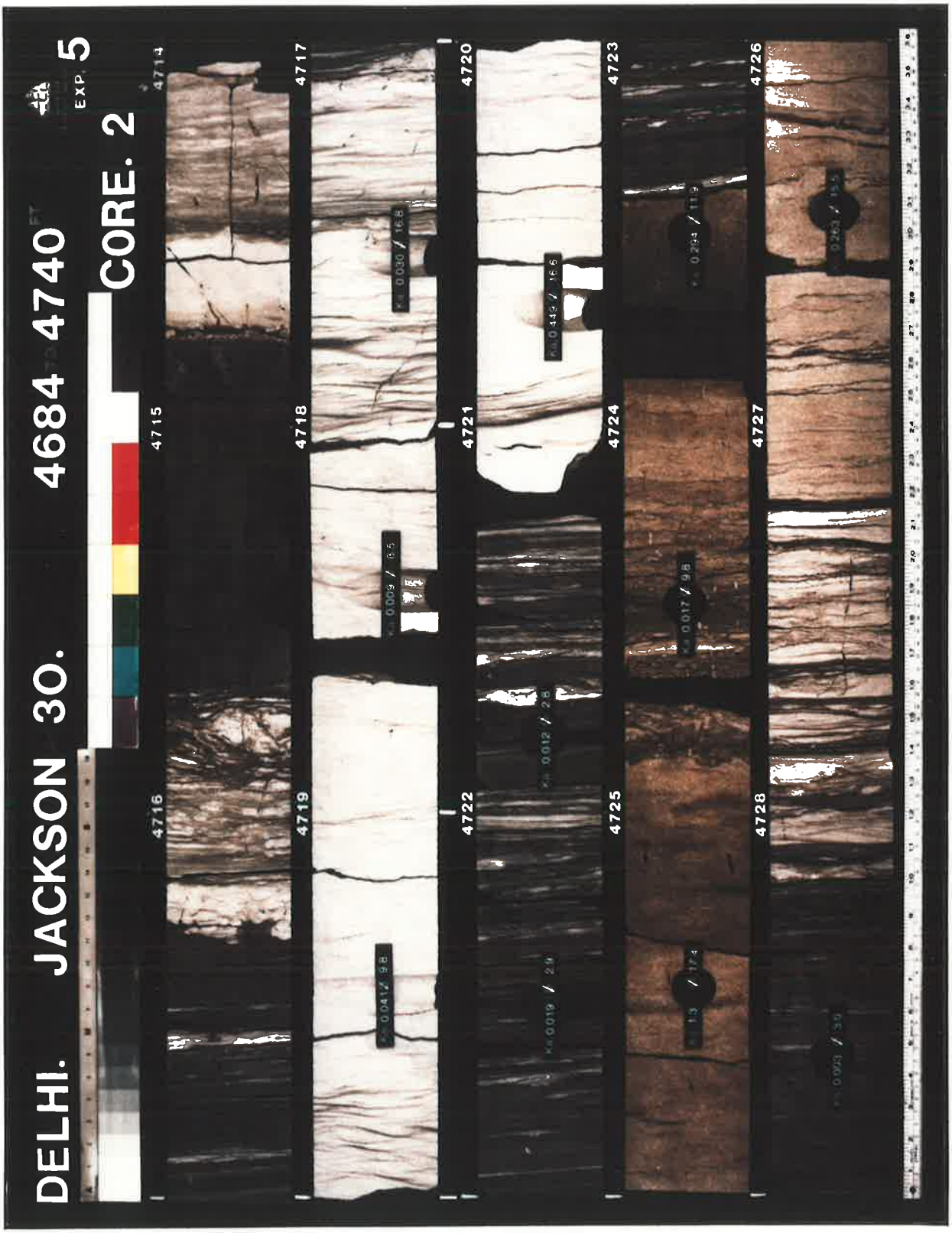

Fig. 6(f) Core photograph, Jackson 30, Birkhead Formation.

Berg (1975, p. 944), states that "a barrier facies may be porous and permeable and yet trap a significant oil column". Although this kind of cap-rock would be considered poor, it will hold a finite column of oil. The examples shown in the core photographs could be described in this way.

Hence, the entire interbedded sequence that overlies a reservoir could be providing the seal, due to the reduction in pore throat size from the highly porous and permeable reservoir sandstones to the tighter, interbedded siltstone sequence above. Berg (1975) examined and identified examples of porous and permeable rocks that appear to form a barrier to oil migration due to the difference in capillary pressures, which is related to pore throat size and distribution between the reservoir and barrier rock types.

Several full-hole cores from the Eromanga Basin show alternating bands of oil saturated sandstones and water saturated sandstones with no traces of hydrocarbons. The absence of oil in parts of the sequence could be attributable in some cases to finer grain size and tighter porosity.

However, in other cores, many of the thin, tighter siltstones and sandstones in the interbedded sequence above the main reservoir zones do have some oil saturation, although it is low. These rocks act either as part of the reservoir or as the reservoir waste zone (a zone of poor permeability and porosity that is oil saturated, but which will not produce significant quantities of oil). Hence, oil may have been prevented from entering particular sandstone layers of the sequence not only because of low permeability, but also because sandstones are encased by mudstone beds that are acting as local seals.

From these observations, it is likely that the series of thin silty mudstones is providing the seal in most of the wells studied. However, identifying the exact mudstone seal for the oil accumulations was not possible from either the wireline logs or from the cored intervals in these instances, due to the extreme lateral and vertical variation in lithology

and the number of mudstone bands present in each of the cores. Several mudstones and silty mudstones were observed between oil saturated sandstones, implying that some of the mudstones form a seal and others do not. Therfore, the seal capacity of any mudstones within the sequence is assumed to give an indication of the maximum sealing capacity of the entire interval, even though many of the mudstone layers may not be continuous. Mineralogical work, reported later, show that all the mudstone samples have very similar compositions and that the above assumption appears to be valid.

3.2 SAMPLE SELECTION

The wells selected for the study were those in which full-hole cores had been cut. The choices were limited as most full-hole cores are usually taken only in the reservoir sections, rather than in the mudstones and siltstones of the overlying sealing intervals.

Full-hole cores that included sections from above the reservoir sandstones for the Murta Member, the Namur Sandstone Member, the Birkhead Formation and the Hutton Sandstone were initially selected for the study. The study allowed for approximately fifty plug samples to be analysed. Hence, cores from wells with oil pools and wells which had recorded oil recoveries on drill-stem testing were given priority.

A total of 38 wells were finally selected and 90 vertical core plugs were cut from the mudstone and silty mudstone layers in each of the cores examined. From the 90 core plugs, 54 eventually proved suitable for the seal capacity work, the rejections are described below. Well locations are shown in Fig. 7 and the sample numbers and depths are listed in Table 1. Analyses were performed on vertical plugs cut from full-hole cores, because they would give the most reliable results and allow the full range of tests (including vertical permeability) to be conducted. Drill cuttings were not used as the large surface area to volume ratio of cuttings and the possibility of contamination can lead to less reliable values of capillary pressure (Jennings, 1987). Also, vertical

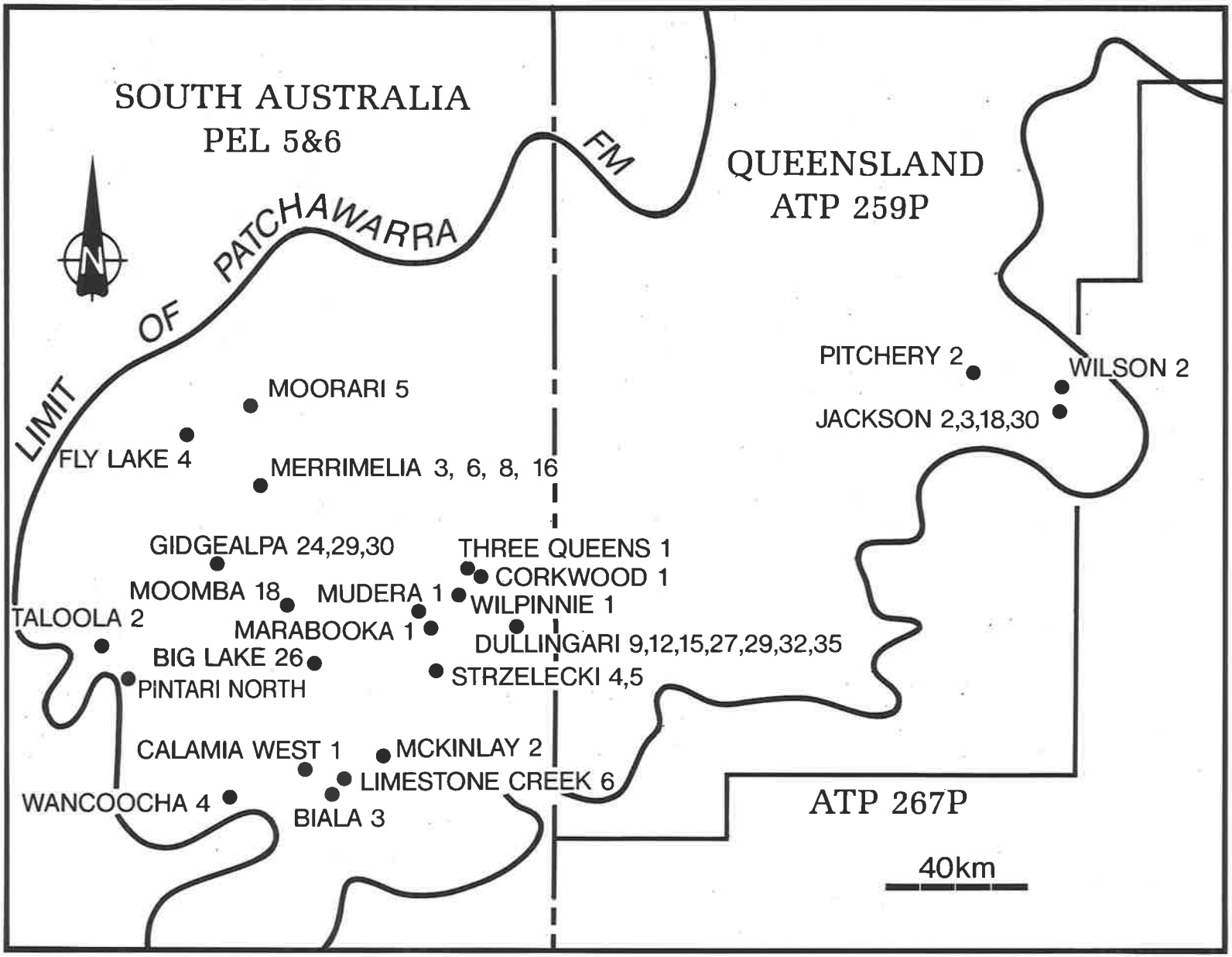

Fig. 7 Location map showing the distribution of core plug samples.

TABLE 1 - CORE PLUG SAMPLE DEPTHS

WELL NAME AND NUMBER	FORMATION SEALS	CORE PLUG NO.	DEPTH DRLR (FT)	CORR	DEPTH LOGR (FT)
BIG LAKE 26	BIRKHEAD	1	6450.0	4	6454.0
BIG LAKE 26	BIRKHEAD	2	6457.0	4	6461.0
BIG LAKE 26	BIRKHEAD	3	6473.5	4	6477.5
BIG LAKE 26	BIRKHEAD	4	6457.0	4	6461.0
BIG LAKE 26	BIRKHEAD	5	6471.0	4	6475.0
CORKWOOD 1	BIRKHEAD	6	5515.5	4	5519.5
CORKWOOD 1	BIRKHEAD	7	5514.5	4	5518.5
CORKWOOD 1	BIRKHEAD	8	5530.0	4	5534.0
GIDGEALPA 29	BIRKHEAD	9	6010.0	-3	6007.0
GIDGEALPA 29	BIRKHEAD	10	6011.0	-3	6008.0
GIDGEALPA 30	BIRKHEAD	11	5984.0	2	5986.0
GIDGEALPA 30	BIRKHEAD	12	5998.0	2	6000.0
GIDGEALPA 30	BIRKHEAD	13	6017.5	2	6019.5
MOORARI 5	BIRKHEAD	14	7057.5	-4	7053.5
MOORARI 5	BIRKHEAD	15	7062.0	-4	7058.0
WANCOOCHA 4	BIRKHEAD	16	5132.0	5	5137.0
WANCOOCHA 4	BIRKHEAD	17	5130.0	5	5135.0
WANCOOCHA 4	BIRKHEAD	18	5132.5	5	5137.5
DULLINGARI 9	MURTA MBR	19	4824.0	-5	4819.0
DULLINGARI 9	MURTA MBR	20	4835.0	-5	4830.0
DULLINGARI 9	MURTA MBR	21	4846.5	-5	4841.5
DULLINGARI 12	MURTA MBR	22	4927.0	4	4931.0
DULLINGARI 12	MURTA MBR	23	4916.5	4	4920.5
DULLINGARI 12	MURTA MBR	24	4904.5	4	4908.5
DULLINGARI 15	MURTA MBR	25	4816.5	4	4820.5
DULLINGARI 15	MURTA MBR	26	4804.0	4	4808.0
DULLINGARI 15	MURTA MBR	27	4829.0	4	4833.0
DULLINGARI 27	MURTA MBR	28	4879.5	3	4882.5
DULLINGARI 27	MURTA MBR	29	4888.0	3	4891.0
DULLINGARI 35	MURTA MBR	30	4877.0	5	4882.0
DULLINGARI 35	MURTA MBR	31	4895.0	5	4900.0
DULLINGARI 35	MURTA MBR	32	4891.5	5	4896.5
FLY LAKE 4	MURTA MBR	33	5885.0	-9	5876.0
FLY LAKE 4	MURTA MBR	34	5896.0	-9	5887.0
LIMESTONE CK 6	MURTA MBR	35	3988.0	-6	3982.0
LIMESTONE CK 6	MURTA MBR	36	3981.5	-6	3975.5
THREE QUEENS 1	MURTA MBR	37	4788.0	2	4790.0
THREE QUEENS 1	MURTA MBR	38	4797.5	2	4799.5
THREE QUEENS 1	MURTA MBR	39	4807.0	2	4809.0
WILPINNIE 1	MURTA MBR	40	4677.0	1	4678.0
WILPINNIE 1	MURTA MBR	41	4686.0	1	4687.0
MERRIMELIA 3	BIRKHEAD	42	6334.0	0	6334.0
MERRIMELIA 3	BIRKHEAD	43	6343.0	0	6343.0
MULAPULA 1	BIRKHEAD	44	4006.0	-3	4003.0
MULAPULA 1	BIRKHEAD	45	4007.0	-3	4004.0
MULAPULA 1	BIRKHEAD	46	4013.0	3	4010.0
MULAPULA 1	BIRKHEAD	47	4019.5	-3	4016.5
STRZELECKI 4	BIRKHEAD	48	5489.0	2	5491.0
STRZELECKI 4	BIRKHEAD	49	5509.5	2	5511.5
STRZELECKI 4	BIRKHEAD	50	5522.0	2	5524.0

TABLE 1 - CORE PLUG SAMPLE DEPTHS

WELL NAME AND NUMBER	FORMATION SEALS	CORE PLUG NO.	DEPTH DRLR (FT)	CORR	DEPTH LOGR (FT)
STRZELECKI 5	BIRKHEAD	51	5507.0	4	5511.0
STRZELECKI 5	BIRKHEAD	52	5525.0	4	5529.0
STRZELECKI 5	BIRKHEAD	53	5513.0	4	5517.0
STRZELECKI 5	BIRKHEAD	54	5531.0	4	5535.0
CALAMIA WEST 1	NAMUR MBR	55	4060.0	2	4062.0
CALAMIA WEST 1	NAMUR MBR	56	4070.5	2	4072.5
CALAMIA WEST 1	NAMUR MBR	57	4077.5	2	4079.5
BIALA 3	NAMUR MBR	58	4024.5	-2	4022.5
BIALA 3	NAMUR MBR	59	4030.0	-2	4028.0
DULLINGARI 29	NAMUR MBR	60	4902.5	4	4906.5
DULLINGARI 29	NAMUR MBR	61	4924.0	4	4928.0
DULLINGARI 29	NAMUR MBR	62	4926.0	4	4930.0
DULLINGARI 32	NAMUR MBR	63	4940.5	4	4944.5
DULLINGARI 32	NAMUR MBR	64	4949.5	4	4953.5
GIDGEALPA 24	NAMUR MBR	65	5182.5	6	5188.5
GIDGEALPA 24	NAMUR MBR	66	5182.7	6	5188.7
GIDGEALPA 24	NAMUR MBR	67	5205.5	6	5211.5
MARABOOKA 1	NAMUR MBR	68	4760.0	3	4763.0
MCKINLAY 2	NAMUR MBR	69	4073.5	6	4079.5
MERRIMELIA 6	NAMUR MBR	70	5196.0	5	5201.0
MERRIMELIA 6	NAMUR MBR	71	5221.0	5	5226.0
MERRIMELIA 8	NAMUR MBR	72	5237.0	0	5237.0
MERRIMELIA 8	NAMUR MBR	73	5239.0	0	5239.0
MERRIMELIA 16	NAMUR MBR	74	5247.5	2	5249.5
MOOMBA 18	NAMUR MBR	75	5792.0	-1	5791.0
MUDERA 1	NAMUR MBR	76	4960.0	4	4956.0
JACKSON 2	MURTA MBR	77	3624.5	0	3624.5
JACKSON 2	MURTA MBR	78	3630.5	0	3630.5
JACKSON 3	MURTA MBR	79	3650.5	2	3648.5
JACKSON 3	MURTA MBR	80	3646.0	-2	3644.0
WILSON 2	MURTA MBR	81	3736.5	4	3740.5
JACKSON 18	BIRKHEAD	82	4780.0	3	4783.0
JACKSON 18	BIRKHEAD	83	4770.0	3	4773.0
JACKSON 30	BIRKHEAD	84	4716.5	-1	4715.5
JACKSON 30	BIRKHEAD	85	4723.0	-1	4722.0
PITCHERY 2	MURTA MBR	86	4448.5	-6	4442.5
PITCHERY 2	MURTA MBR	87	4449.5	-6	4443.5
TALOOLA 2	NAMUR MBR	88	4561.5	-2	4559.5
TALOOLA 2	NAMUR MBR	89	4565.0	-2	4563.0
TALOOLA 2	NAMUR MBR	90	4591.5	-2	4589.5

permeability tests cannot be conducted on drill cuttings to supplement the capillary measurements. Sidewall cores, although quite suitable for capillary pressure measurements, are unsuitable for vertical permeability measurements due to the orientation of the cores and the induced fractures caused by the force of the bullet striking the formation.

Any shale above the known oil reservoir that appeared likely to form a seal was sampled. A few samples were also taken in the hard, siderite cemented bands that are prevalent in the intervals above the Namur Member and also in some of the more silty sections adjacent to the mudstone layers, for comparison. Hence, nearly all samples chosen were biased towards the best sealing lithologies.

Only one fresh core (Taloola 2) was available at the time of sample selection for use as a control. Obvious changes in the older cores were the development of fractures and partings along bedding planes caused by the drying out of the cores. Sample selection was made difficult by the weathered state of some of the full-hole cores, with some zones being too badly fractured to consider. The most preserved sections were sent to Gearhart Laboratories, Adelaide, where one inch diameter vertical plugs were cut from the centres of the slabbed full-hole cores. The samples were then sealed in foil and wax and selected samples were shipped to the Gearhart Laboratories at Fort Worth, USA, for analysis. Duplicate samples were taken for mineralogical analyses.

3.2.1 EFFECT OF INITIAL SAMPLE PREPARATION

Care was taken to minimise the effect of re-saturating the core while cutting plugs by keeping the amount of water low and sealing them before they could dry out. Despite this, some samples did arrive at the Fort Worth laboratories in a state that was reported as unsuitable for further work, as fine fractures had developed in some of the plugs.

The effects of age and weathering on the clay particles and the surrounding pore throats and the magnitude of changes to permeability and capillary measurements cannot be determined without several control samples of fresh core. These were not available at the time of the study, as the more shaley parts of the cores are not routinely preserved at the well-site by seal-pealing. Crossplots of the age of the cores versus the routine and special core analysis results are given in Appendix Fig. 1 and show that the values obtained for the older cores were well within the minimum and maximum values for all of the samples.

Richardson et al. (1955) and Omoregie (1986) considered the problem of deterioration of samples, but were concerned with capillary pressures at low water saturation values (used for determining the irreducible water saturations in reservoir rocks). Both authors noted that air drying of samples resulted in a lower reading of irreducible water saturation than fresh samples. The samples used by Richardson et al. (1955), had been stored in open containers and were extracted with solvents before analysis, as were the samples for this study.

This study is concerned with pressure values at the other end of the scale, where breakthrough or leakage occurs. From Figs. 1 and 2 in Richardson et al. (1955), the changes to the pressures at the higher water saturation values appear to be varied and the differences to threshold pressure measurements cannot be determined. The examples given by Omoregie (1986) in Figs. 4 and 6 show only small differences in magnitude of the threshold pressures. Due to the varied and inconclusive results, no correction could be applied to the measurements obtained in this study.

Further work, using both fresh and weathered core, is required to determine if drying of the cores will produce a significant error in the capillary pressure results and to determine the magnitude of any correction if required.

4. MINERALOGY

4.1 X-RAY DIFFRACTION (XRD)

The samples used for the bulk rock XRD analysis were taken from the same full hole core interval as the vertical plugs used for the conventional core analysis and capillary pressure measurements. Only samples for the South Australian wells were analysed as the full-hole cores for the six wells located in Queensland reside in that state.

Contamination from drilling mud should be negligible as invasion of mud solids into the full hole cores in fine-grained tight sediments is small. The plugs were cut from the centre of the full hole cores to ensure this would not be a problem. The lack of smectite or swelling clays, a common additive to drilling muds, identified in the analysed samples suggests that no significant contamination has occurred.

Small pieces of core were gently crushed for twenty seconds in a tungsten-carbide mill using ethanol, then transferred to beakers and dried in an oven at low temperature. The dried, crushed samples were then placed in aluminium holders and analysed using Co Kα radiation. The angle of investigation was from 0 to 75 degrees 2 theta, which is sufficient to identify most minerals commonly found in sedimentary rocks. An XRD trace from Wancoocha 4, for a typical mudstone sample, is shown in Fig. 8a. The main peaks are identified on the plot. A correlation of wireline logs and XRD analysis for Calamia West 1 (Fig. 8b) shows that in this case, although the siderite cemented layer is thin, it can be identified on the logs by the higher sonic transit time values.

Various minerals were identified based upon the recognition of collections of peaks which correspond to reflections from various crystal faces within that mineral. A computer plotting programme was used to overlay all the peaks for common minerals on the XRD traces for the samples as a quality check.

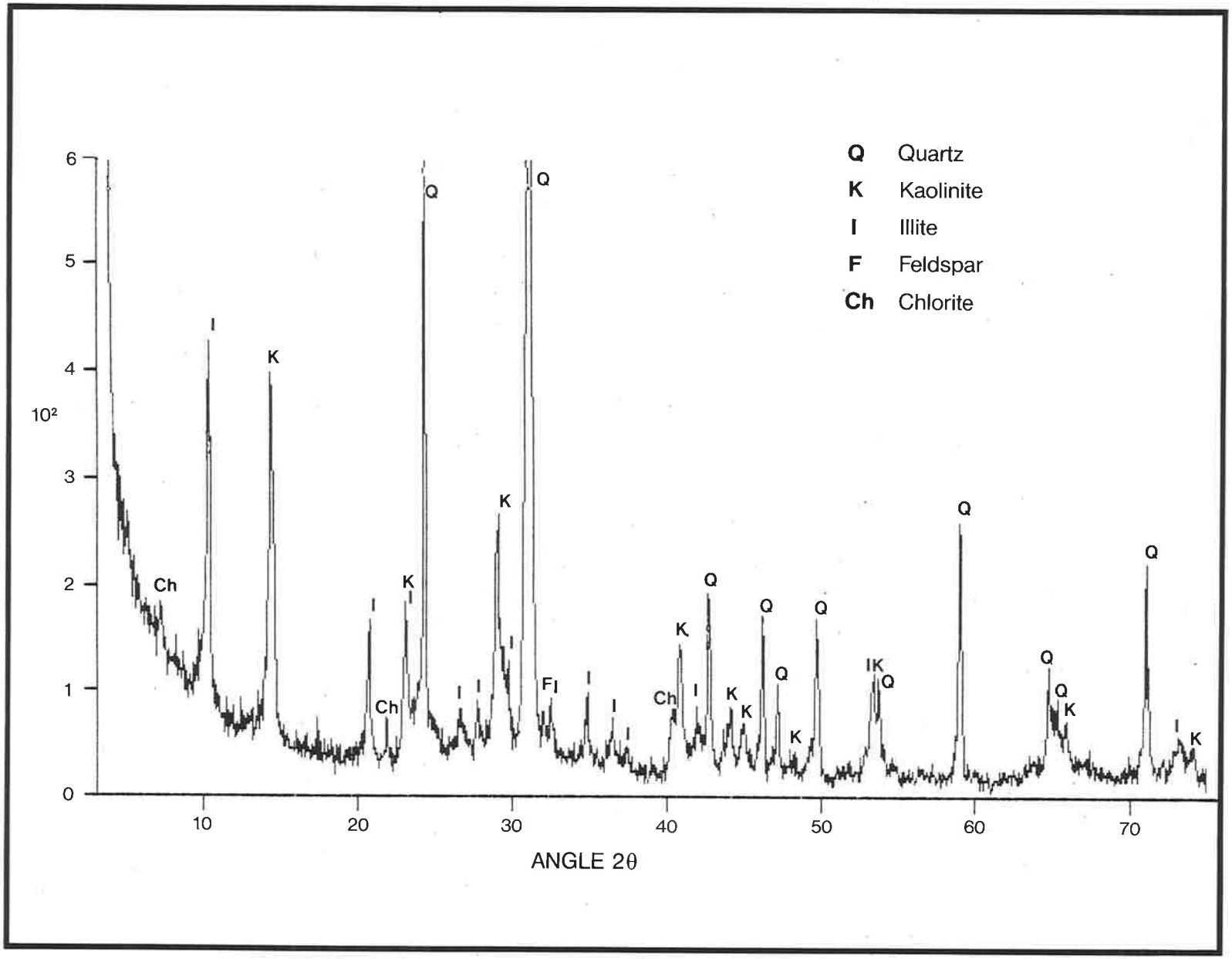

Fig.8(a) Interpreted X-ray diffraction trace for Wancoocha 4, mudstone sample, Birkhead Formation.

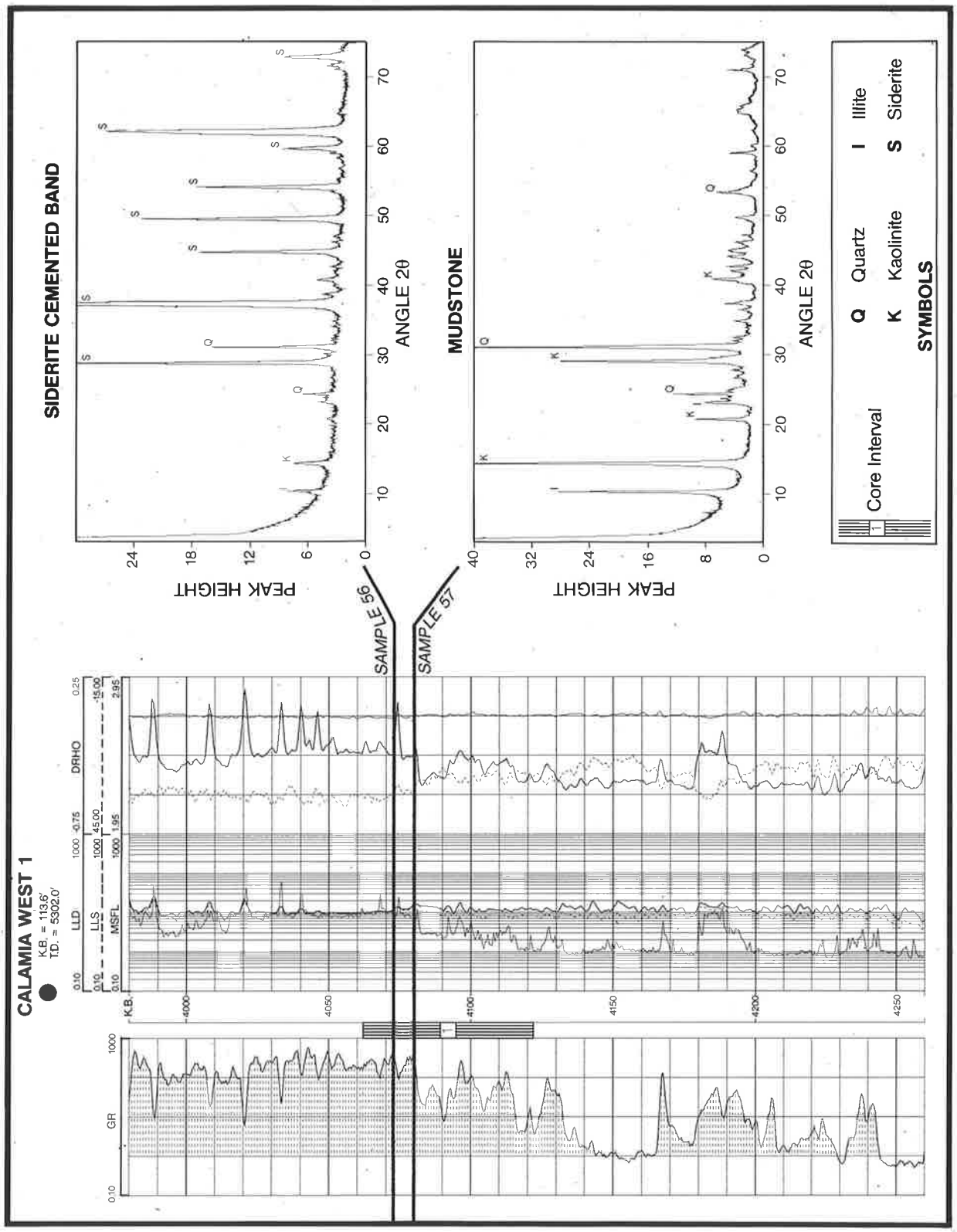

Fig. 8(b) X-ray diffraction traces correlated with the wireline logs for Calamia West 1, Namur member.

A summary of the major peaks used to identify the minerals in each of the samples is given in Table 2.

TABLE 2 - X-RAY DIFFRACTION ANALYSIS

MINERAL	D-SPACING	2 THETA	
QUARTZ	4.2442	24.35	
	3.3389	31.10	
KAOLINITE	7.1418	14.40	
	3.5689	29.05	
ILLITE/MICA	9.9718	10.30	
	4.9822	20.70	
SIDERITE	2.7918	37.40	
	2.1300	49.70	
CHLORITE	14.0603	7.30	
	4.7016	21.95	
FELDSPAR			
ALBITE	3.1987	32.50	
OLIGOCLASE	3.2035	32.45	
MICROCLINE	3.2424	32.05	
	3.1892	32.60	
SMECTITE	< 10.0203	< 10.00	(BROAD PEAK)

The results of the bulk rock XRD showed a surprisingly similar composition for all of the mudstone samples analysed. Quartz, kaolinite and illite/mica are the most abundant minerals. Minor to trace amounts of feldspar (albite, microcline and oligoclase), siderite and chlorite are present in approximately half the samples examined. Traces of smectite clays were identified in only a few samples.

In addition to the mudstone samples, several samples of the hard, cemented bands from the top of the Namur Sandstone were analysed. These are composed predominantly of siderite with quartz and minor amounts of kaolinite and illite/mica. A trace of feldspar was observed in only one of the samples. The interpreted mineralogy of each of the samples is given in Table 3.

TABLE 3 - X-RAY DIFFRACTION MINERALOGY

	SAMPLE NUMBER																	
MINERAL	1	5	8	9	11	13	15	16	21	26	27	28	29	32	33	35	36	43
QUARTZ	D	D	D	D	D	D	D	D	D	D	D	D	D	D	D	D	D	D
KAOLINTE	A	A	A	A	A	A	M	A	A	A	A	A	A	A	A	A	A	A
ILLITE/MICA	M	A	A	M	M	M	A	A	A	M	A	A	A	A	A	A	A	M
SIDERITE						TR			TR						M			
CHLORITE							TR	TR	M	TR	TR	TR	TR	TR	TR	TR	TR	
FELDSPAR	M	M		M	M		TR		TR	M	TR	TR		TR	TR	TR		M
SMECTITE	TR			TR	TR	TR				TR								TR

	SAMPLE NUMBER																	
MINERAL	49	50	51	53	56	57	58	59	60	62	65	66	68	70	71	72	73	76
QUARTZ	D	D	D	D	A	D	A	D	D	D	A	D	D	D	D	A	D	D
KAOLINTE	A	A	A	A	M	A	M	A	A	A	A	A	A	A	A	A	A	A
ILLITE/MICA	A	A	A	A	M	A	M	A	A	A	M	A	A	A	A	A	A	A
SIDERITE					D	TR	D	TR	TR	M	D	TR		M	TR	D	TR	TR
CHLORITE									TR	TR		TR	TR	TR	TR	TR	TR	TR
FELDSPAR								TR	TR		TR	M	M	TR	TR			M
SMECTITE																		

D - DOMINANT A - ABUNDANT M - MINOR TR - TRACE

To enable crossplots of mineralogy against depth to be produced, a measure of the mineral content was taken as the peak height from the XRD traces. This is a semi-qualitative method and gives only an indication of the relative abundance of minerals as the height and sharpness of the peak is the result of both the orientation and the crystallinity of the mineral particles analysed. The crossplots of mineralogy against depth (Figs. 9a to 9d) show that both illite and kaolinite decrease with depth and quartz content increases with depth.

The decrease in clay content in the deeper Birkhead Formation samples could be related to differences in depositional processes or could be a direct consequence of depth and diagenesis. Although the samples all consist of fine grained minerals that have been deposited in low energy environments, lithological variations can occur with changes in provenance. The Birkhead Formation samples contain either more clay-sized quartz grains or are slightly more silty than the Murta and Namur Member samples. No increase of illite with decreasing kaolinite content with depth was noted, which might be expected with diagenetic alteration.

Analysis of the clay fraction (< 5 μm) was not performed, as the initial XRD results showed a monotonous mineralogy and a correlation with the capillary pressure analyses showed no significant trends. The crossplots of mineralogy against threshold pressure are given in Appendix 2, Fig. 3. Further tests were considered unlikely to present any further information that would be significant to this study.

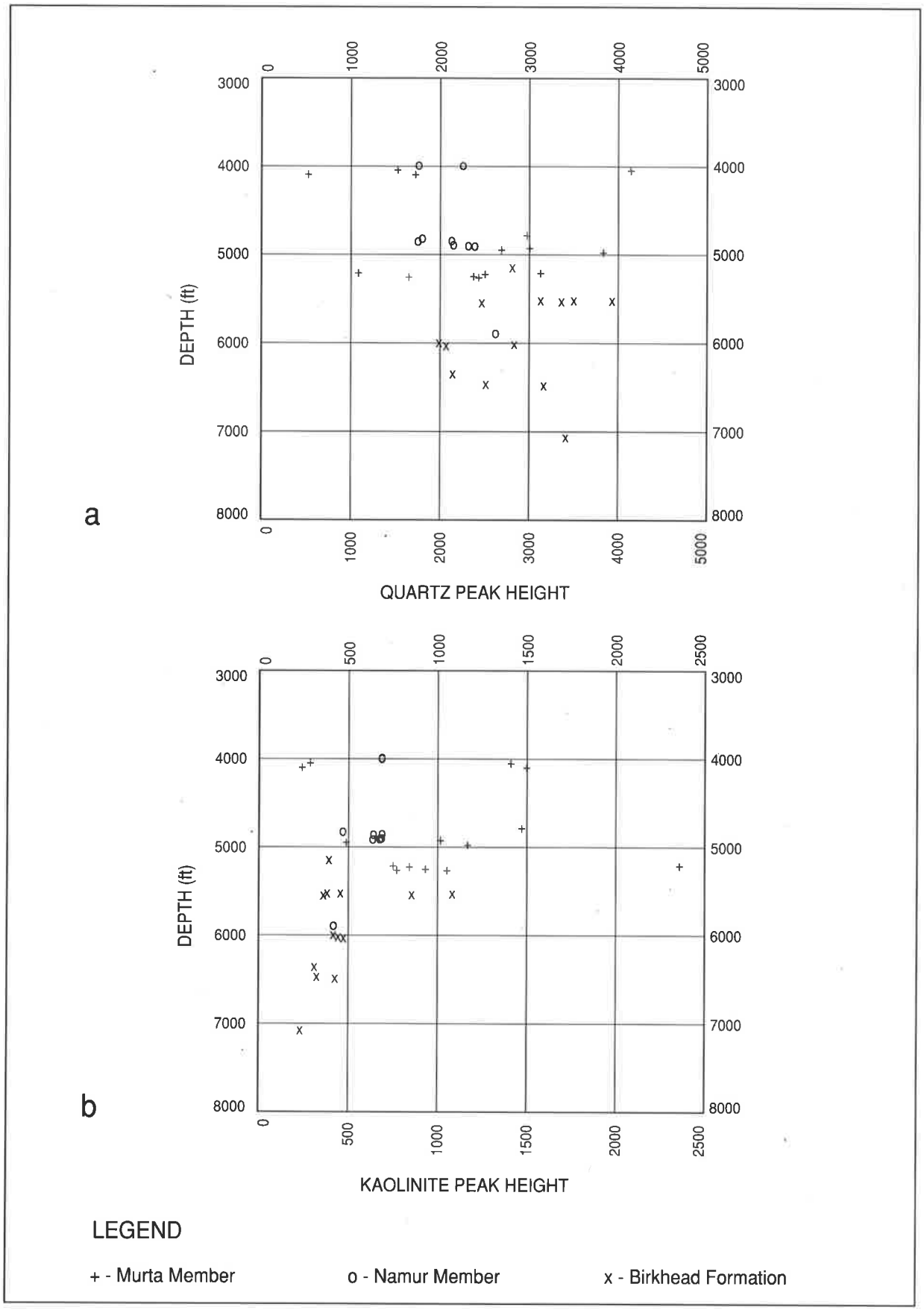

FIG. 9 : Crossplots of X-Ray Diffraction Mineral Peak Heights a) Quartz, b) Kaolinite against the Depth of Origin of the Sample.

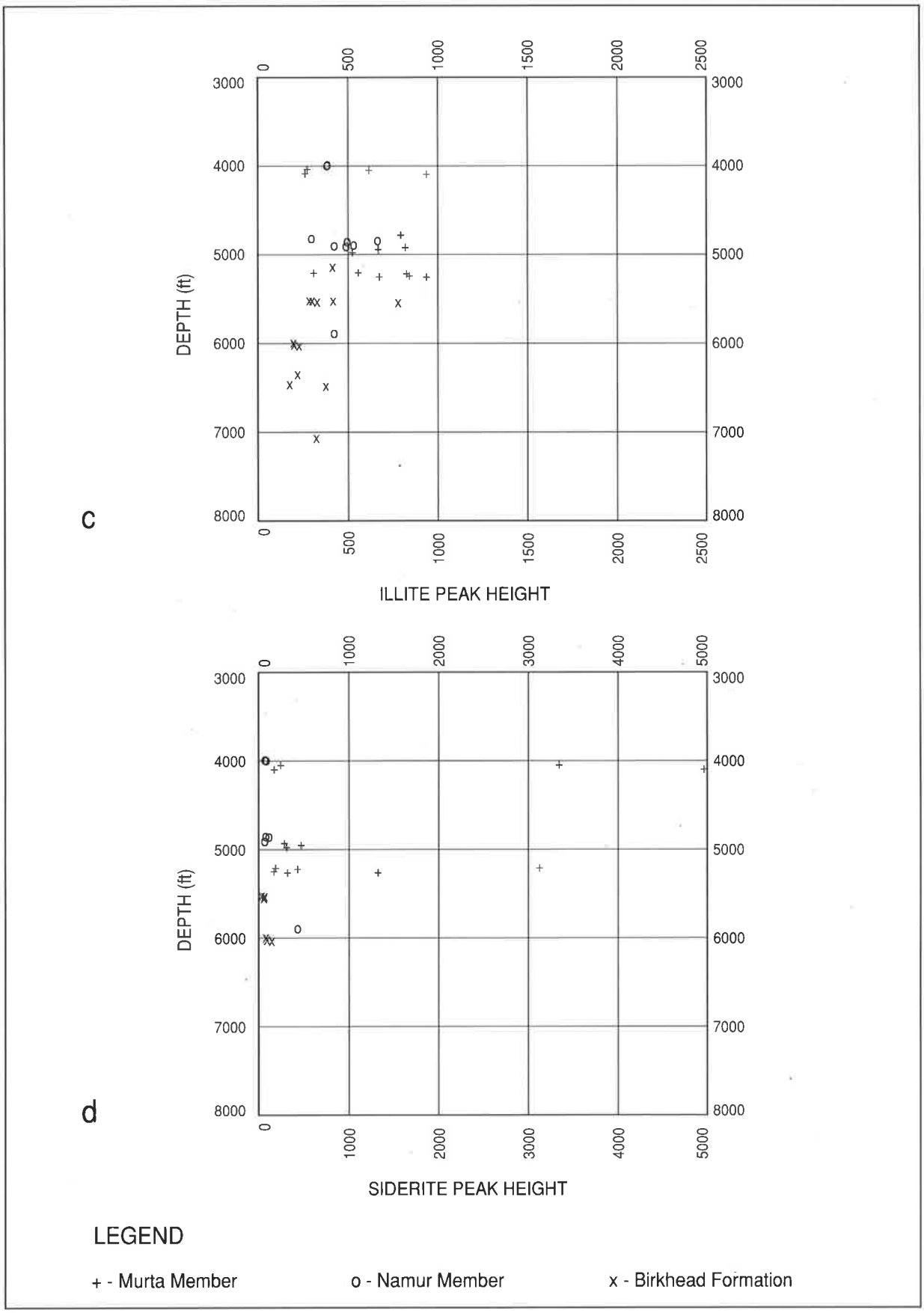

FIG. 9 : CONT. Crossplots of X-Ray Diffraction Mineral Peak Heights c) Illite, d) Siderite against the Depth of Origin of the Sample.

Figure 10 - SEM Micrographs.

(a) Authigenic quartz showing well developed crystal faces. Fine-grained kaolinite (K) can be seen on the left of the micrograph as small, bright grains with poorly developed crystal faces.
Limestone Creek 6, sample 35.

(b) Extensive quartz overgrowths (Q) surround coarse-grained booklets of kaolinite (K). Much of the porosity and permeability is reduced by these overgrowths.
Corkwood 1, sample 8.

(c) Small quartz overgrowths and coarse-grained booklets of kaolinite in-filling pore spaces of a more silty lens within the mudstone sample.
Limestone Creek 6, sample 35.

(d) Typical view of a mudstone sample showing the very fine, bright crystals identified as kaolinite (K). The large platy grain is mica, surrounded by layered illite (I).
Dullingari 35, sample 32.

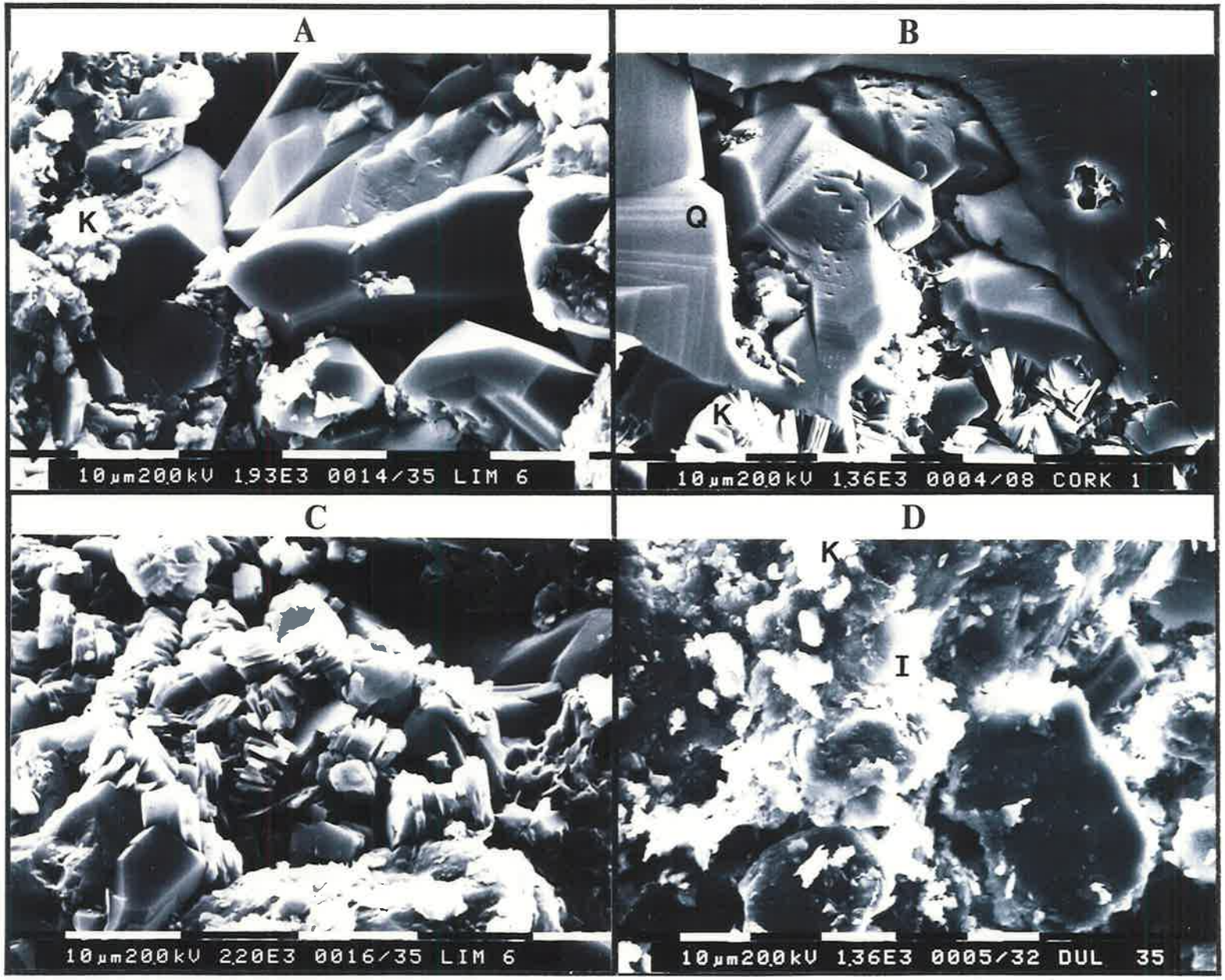
A
K
10µm20.0kV 1.93E3 0014/35 LIM 6
B
Q
K
10µm20.0kV 1.36E3 0004/08 CORK 1
C
10µm20.0kV 2.20E3 0016/35 LIM 6
D
K
I
10µm20.0kV 1.36E3 0005/32 DUL 35

Figure 10 - SEM Micrographs.

(e) Close-up of oriented platy illite and fine mica grains.
Porosity is low, occuring between the sheets of illite.
Fly Lake 4, sample 33.

(f) Representative view of a mudstone sample. Mica and fine,
platy illite grains are closely packed. Pore throats are
very small and micro-porosity predominates.
Illite to kaolinite ratios are high for this mudstone.
Corkwood 1, sample 8.

(g) A view of smectite clay (S) which appears as irregular crystals
often described as "lettuce leaves". It is associated with
fine, poorly developed authigenic kaolinite crystals (K).
Gidgealpa 24, sample 67.

(h) A large mica grain surrounded by finer grained illite.
Gidgealpa 30, sample 13.

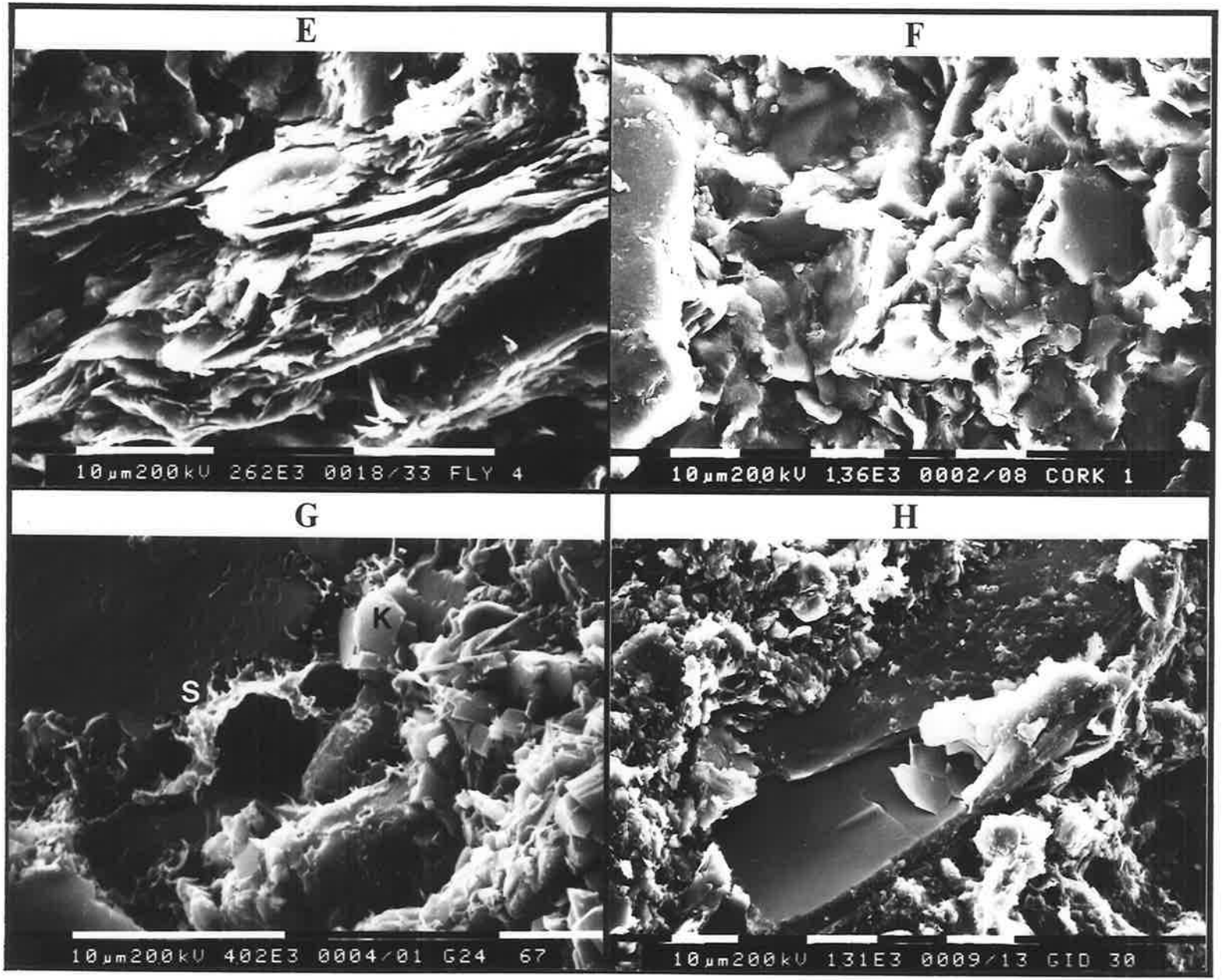
E
10µm200kV 262E3 0018/33 FLY 4
F
10µm200kV 1.36E3 0002/08 CORK 1
G
K
S
10µm200kV 402E3 0004/01 G24 67
H
10µm200kV 131E3 0009/13 GID 30

Figure 10 - SEM Micrographs.

(i) Close-up of chlorite crystals (C) lining a pore. The Chlorite crystals are platy to needle-like and arranged in a distinctive pattern, perpendicular to the pore wall.
Dullingari 35, sample 32.

(j) Authigenic chlorite coating a quartz grain with overgrowths.
Fly Lake 4, sample 33.

(k) Massive micritic siderite cement. Very little porosity or permeability can be observed in this sample.
Calamia West 1, sample 56

(l) Siderite showing two distinct forms. A massive micritic cement can be seen surrounding and in close contact with rhombohedral crystals of siderite. This could represent either the replacement of another carbonate mineral or a change from micritic to more coarsely crystalline siderite.
Mudera 1, sample 76.

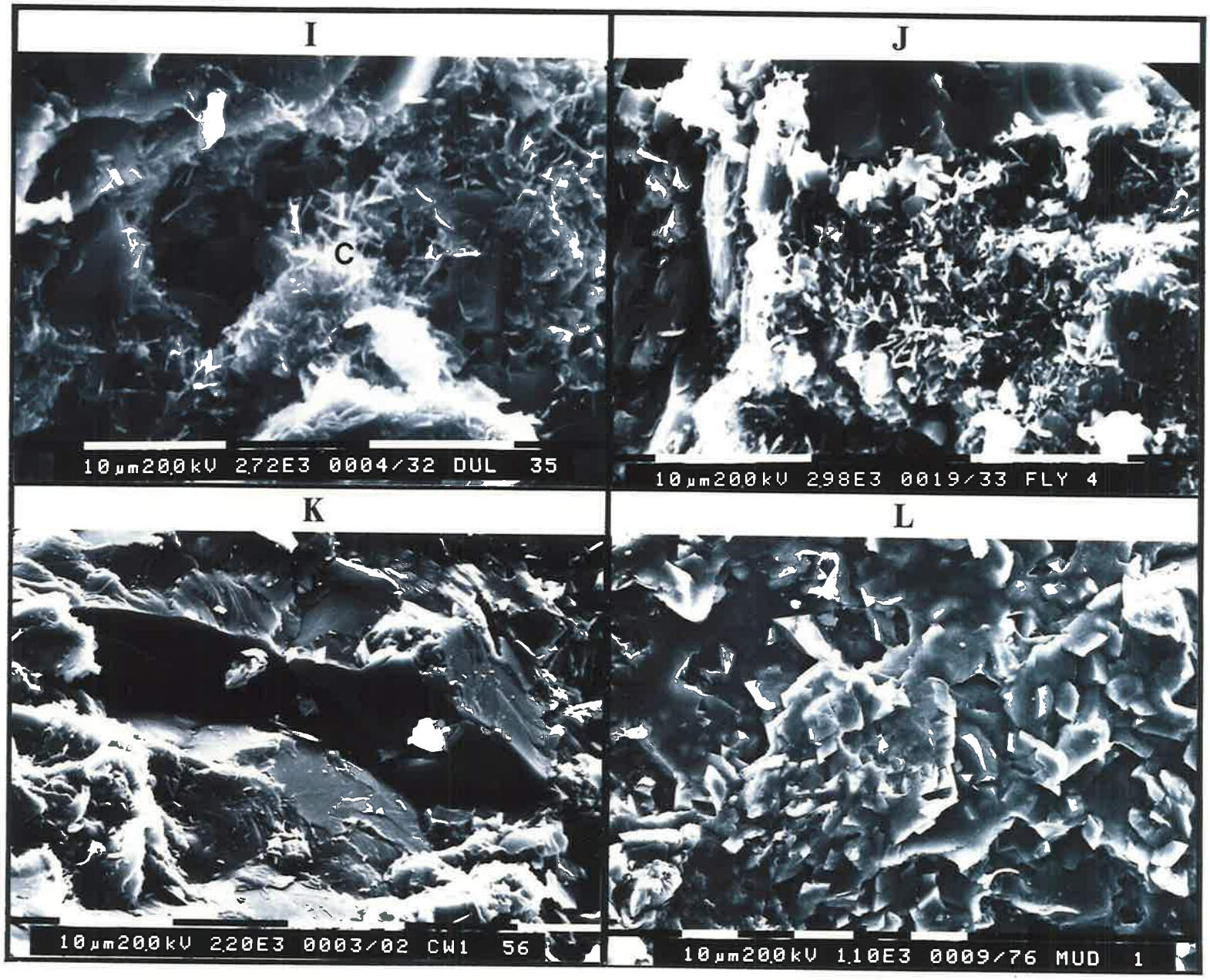
I
C
10µm20.0kV 2.72E3 0004/32 DUL 35
J
10µm20.0kV 2.98E3 0019/33 FLY 4
K
10µm20.0kV 2.20E3 0003/02 CW1 56
L
10µm20.0kV 1.10E3 0009/76 MUD 1

brighter, fine crystals in Figs. 10a, 10d and 10g. Figs. 10b and 10c show coarser grained, authigenic kaolinite, more commonly found in porous sandstones. It is confined here to the larger pore spaces in the very fine lenses of silt or sand within the mudstones.

Detrital illite and fine mica is more readily identified than kaolinite in the samples that were examined. Both minerals show a platy grain morphology. Much of the illite is also inter-layered with coarser grained micas, both muscovite (Fig. 10h) and biotite. Figs. 10e and 10f show typical views of the detrital illite seen in most of the samples. Authigenic illite, which appears as fine hair-like grains, is rare.

Minor smectite can be observed in Fig. 10g. It appears as uneven, lettuce-like grains.

Rare weathered feldspar grains were observed. Limited secondary porosity, presumably due to the dissolution of such grains was observed.

Iron-rich chlorite lines some pore spaces and can be identified by its distinct platy, honeycomb crystal habit (Figs. 10i and 10j).

Siderite appears as a very fine crystalline mass that replaces other minerals and destroys all other textures and reduces porosity and permeability in the samples in which it is common (Figs. 10k and 10l).

4.3 PETROGRAPHIC SUMMARY

There appears to be no significant variation in mineralogy with geographical location. All mudstone samples contained varying amounts of quartz, kaolinite and illite/mica. Feldspar, chlorite and siderite occur sporadically and traces of smectite were observed in only a few samples. The samples with abundant siderite cement are from the top Namur or lower Murta Member only.

Plots of mineralogy with depth show a minor trend of increasing quartz content and decreasing kaolinite and illite content with formation, or depth of the sample. This increase in quartz content with a correspondingly lower clay content may either reflect a more silty nature of the Birkhead Formation samples, due to a slight difference in depositional environment, or indicate the presence of significant clay sized quartz particles. Alternatively, there may have been some bias in the sampling procedures.

Porosity within the mudstones is predominantly micro-porosity developed between platy grains of detrital illite/mica and between kaolinite grains. Macro-porosity is present, but occurs as isolated pores often associated with the dissolution of larger unstable grains such as feldspar.

5. CONVENTIONAL CORE ANALYSIS

5.1 POROSITY, PERMEABILITY AND GRAIN DENSITY

Small wafers of the one inch diameter core plugs were used to perform the routine measurements of helium injection porosity and vertical air permeability at surface conditions. The wafers (approximately half inch, 1cm in length) were placed in soxhlet extractors for 48-72 hours and than dried in an oven to remove residual fluids. The porosity for each of the samples was determined by injecting helium into the plug and the pore volume was calculated using Boyle's Law.

Permeability was determined by forcing air through the sample, measuring the flow rate and then correcting for Klinkenberg effects. The results are reported as equivalent liquid permeabilities. A summary of the results is presented in Table 4. Appendix Table 1 contains the full list of routine core analysis results.

As expected with fine grained samples, permeabilities are generally very low and range from 0.001 to 0.09 md. This is due to the very small pore throats and the limited connection of micro-pores present between the platy illite and mica grains observed in the SEM micrographs.

Porosities vary from less than 1 up to 15 per cent. The higher porosities observed in some samples may be due to either the large proportion of micro-porosity present between clay particles or the presence of macro-pores occurring around larger detrital grains of quartz or feldspar. The Murta Member and Namur Member samples from shallower depths have higher average porosities than the Birkhead Formation samples. The effects of compaction on the more ductile mica and illite grains may result in lower porosity values with increasing depth.

TABLE 4 - ROUTINE CORE ANALYSIS RESULTS

A) POROSITY IN PERCENT

FORMATION SEALS	MINIMUM	MAXIMUM	AVERAGE
MURTA MEMBER	6.6	13.8	10.4
NAMUR MEMBER	3.1	14.9	7.6
BIRKHEAD FORMATION	0.7	7.0	3.8
TOTAL	**0.7**	**14.9**	**7.2**

B) PERMEABILITY IN MILLIDARCIES

FORMATION SEALS	MINIMUM	MAXIMUM	AVERAGE
MURTA MEMBER	0.0024	0.0347	0.0055
NAMUR MEMBER	0.0024	0.0320	0.0053
BIRKHEAD FORMATION	0.0021	0.0872	0.0094
TOTAL	**0.0021**	**0.0872**	**0.0068**

C) GRAIN DENSITY IN GRAMS PER CUBIC CENTIMETRE

FORMATION SEALS	MINIMUM	MAXIMUM	AVERAGE
MURTA MEMBER	2.61	2.92	2.69
NAMUR MEMBER	2.55	3.30	2.79
BIRKHEAD FORMATION	2.43	2.68	2.61
TOTAL	**2.43**	**3.30**	**2.69**

Sample grain densities range from 2.4 gm/cc up to 3.3 gm/cc. The density of siderite is 3.89 gm/cc and the samples with the higher grain densities (56, 58, 65 and 72) have correspondingly higher siderite contents, indicated by the XRD analyses. The samples

with lower grain densities (49, 50 and 51) are mudstone samples with lower percentages of mica, feldspar and chlorite which have higher densities than quartz and kaolinite.

5.2 OVERBURDEN PERMEABILITY

The vertical permeability measurements were repeated under overburden pressures to simulate reservoir conditions. As precise overburden pressure data were not available, a value (in psi) of 0.3 * depth (feet) was suggested by the Reservoir Engineering Department of Santos Ltd.

The permeabilities determined under overburden conditions were substantially less that those measured under ambient conditions and some were below the resolution of the permeameter which was reported to be accurate to 0.001 millidarcy. Nearly all of the samples showed a reduction in permeability of 90 per cent or more from the ambient value. However, it is significant to note that the permeability of fresh core (Taloola 2, sample 89) was reduced by approximately 50 per cent. This sample was more silty than many of the other samples and may have been compacted less than the mudstone samples. However, at these small values of permeability, the ability to resolve these differences may be beyond the capabilities of the equipment used.

5.3 SUMMARY

The mudstone samples constituting the Eromanga Basin seals have variable porosities, ranging from 0.7 to 14.9 per cent and permeabilities which are less than 0.09 millidarcies. There is no trend of increasing or decreasing porosity or permeability with the age of the cores, suggesting that the samples either are not significantly affected by dehydration and aging, or that any changes occur within a very short time after the cores are cut (Appendix Fig. 1). The one fresh core (Taloola 2, sample 89) and the oldest core (Merrimelia 3, sample 43) both had values well within the ranges determined for the other cores.

A decrease in porosity with the depth of the sample is apparent from the porosity against depth crossplot in Fig. 11a. This is probably due partly to compaction effects.

Higher quartz contents and lower clay contents were noted in the samples from the more deeply buried horizons, mostly from the Birkhead Formation. A series of crossplots showing porosity plotted against mineralogy shows that as both the illite and kaolinite contents increase, the porosity increases (Appendix Fig. 2). The opposite trend can be seen in the crossplots of porosity and quartz content.

The increase in quartz content was previously attributed to the more silty nature of the samples, but in light of the decrease in porosity, may instead be due to quartz overgrowths infilling the main pores. This would account for the reduction in porosity of some of the Birkhead Formation samples as can be seen in the SEM Micrographs in Fig. 10a.

Alternatively, a decrease in quartz content and an increase in clay content will increase the proportion of micro-porosity, perhaps resulting in the higher values of porosity measured in these samples.

The porosity against pore radii plot shows the expected trend of decreasing porosity with pore radii (Fig. 11b).

It was surprising that permeability showed no correlation trend with mineralogy (Appendix Fig. 2). A decrease in permeability might have been expected with an increase in clay content. No regular variation of permeability can be seen with increasing depth, pore radii, or porosity (Fig. 11c, 11d and 11f).

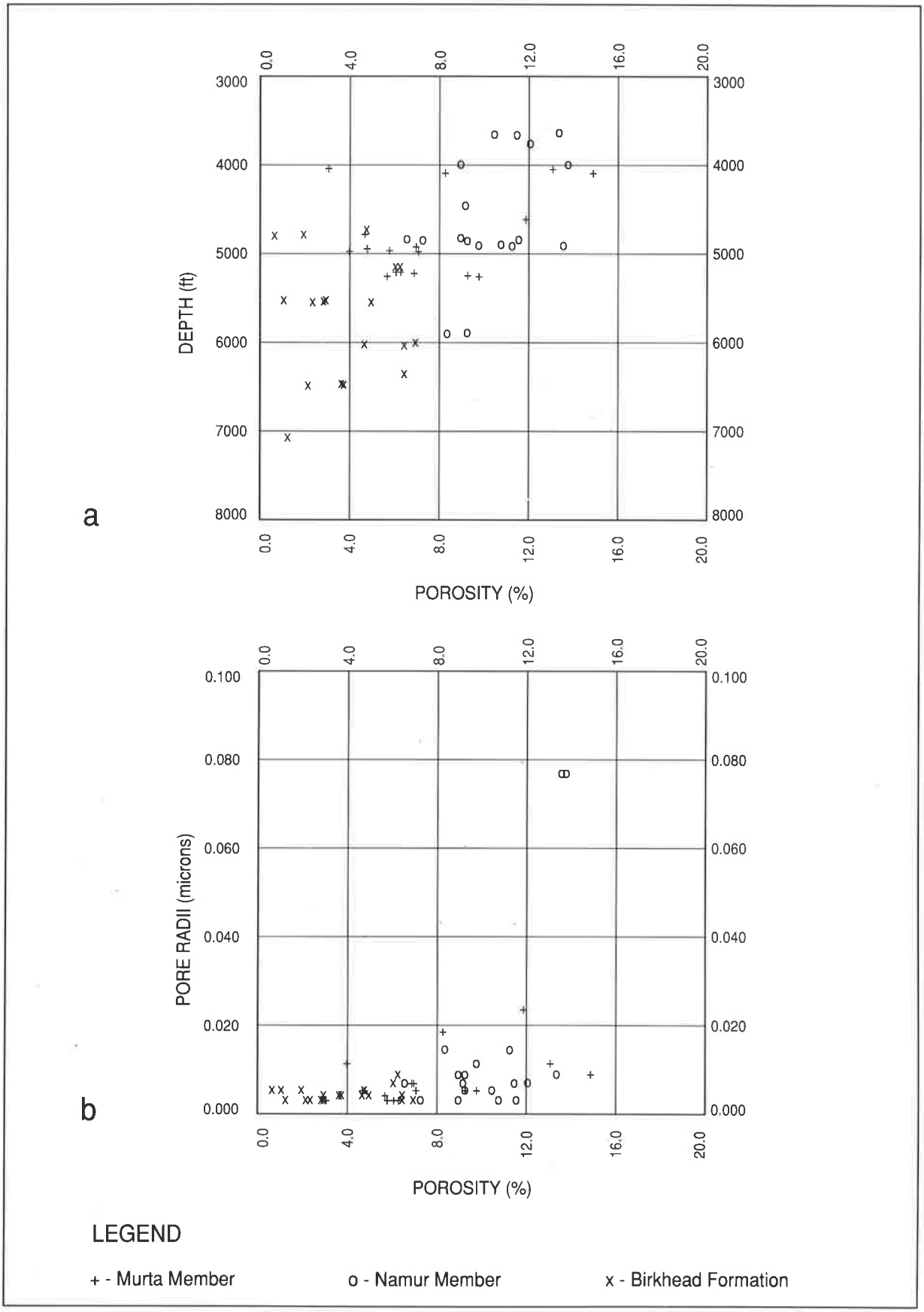

FIG. 11 : Crossplots of Porosity against a) the Depth of Origin of the Sample and against b) the Pore Radii.

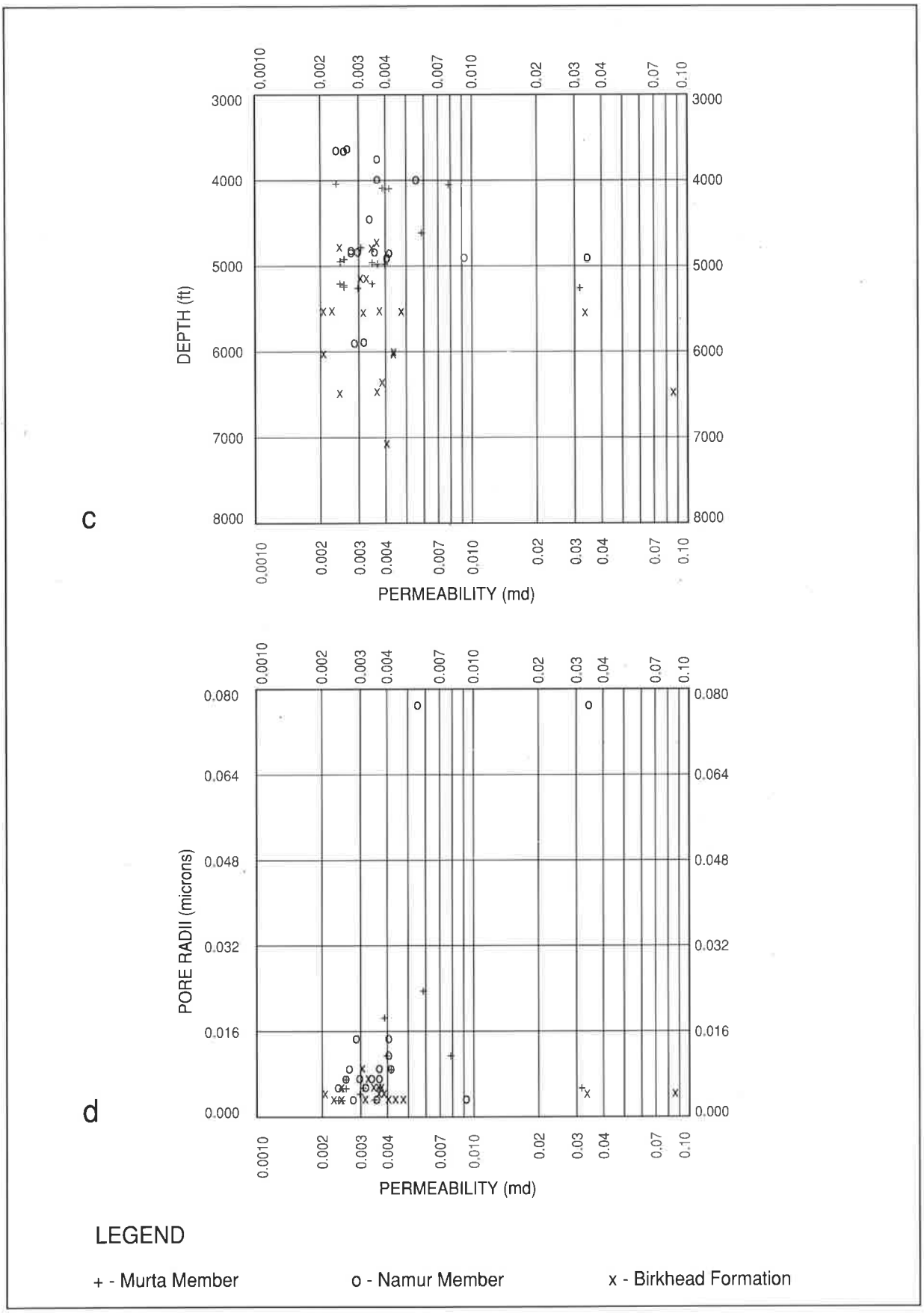

FIG. 11 : Crossplots of Permeability against c) the Depth of Origin
CONT. of the Sample and against d) the Pore Radii.

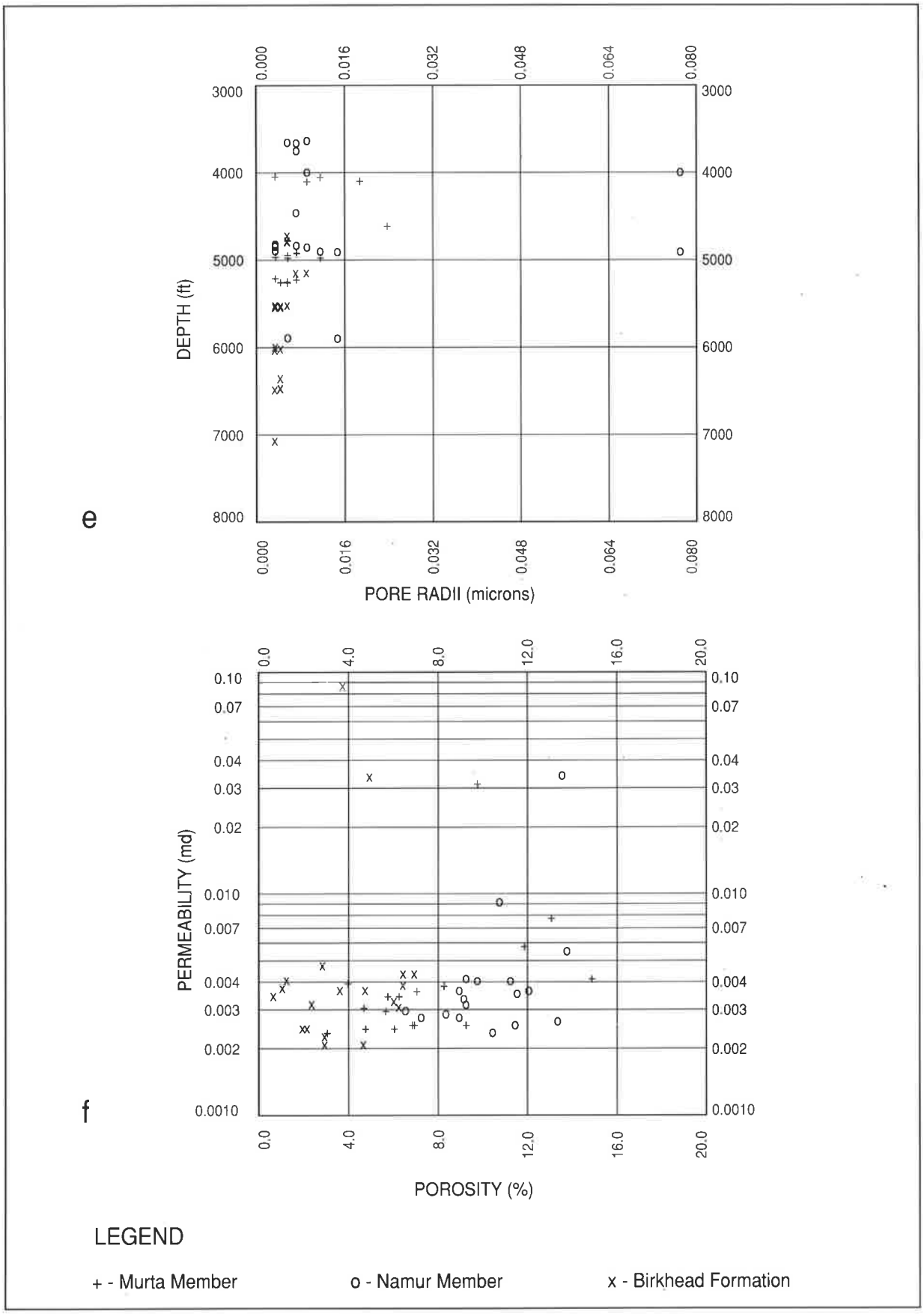

FIG. 11 : Crossplots of e) the Depth of Origin of the Sample against the Pore Radii and f) Porosity against Permeability.

CONT.

6. CAPILLARY PRESSURE MEASUREMENTS

6.1 OIL MIGRATION AND ENTRAPMENT THEORY

To understand how capillary pressure techniques can be used to evaluate seal capacity, it is necessary first to consider how secondary hydrocarbon migration and entrapment occurs. Secondary migration is the movement of hydrocarbon droplets or filaments upwards through a sedimentary sequence from the source rock to a trap. The following description is in part, a summary of papers by Berg (1975), Schowalter (1979), Schowalter and Hess (1982), Downey (1984) and Jennings (1987), incorporating the ideas and equations of others such as Purcell (1949).

The upwards migration of hydrocarbons through porous and permeable rocks is primarily due to buoyancy forces resulting from the density differences between the hydrocarbon fluid and the water. Globules or filaments of the less dense oil or gas displace water from pore spaces as they migrate through the rock. The resistant forces to this upwards migration are the capillary forces, which preferentially hold the water in the pore spaces in a water-wet rock.

Capillary pressure was defined by Leverett (1941) as the "pressure difference between the oil phase and the water phase across a curved oil-water interface". The equation for capillary pressure, if the rock is entirely water-wet and the fluid boundary is spherical, is as follows :

$$Pc = \frac{2\gamma}{R}$$

Where :

Pc - capillary pressure

γ - interfacial tension between the oil and water

R - radius of the pore throat

Berg (1975) defined capillary pressure as "the pressure difference across the interface between two immiscible fluids". When a fluid other than the wetting fluid is introduced, the above equation becomes:

$$Pc = \frac{2\gamma \cos\theta}{R}$$

Where :

θ = the angle of curvature of the fluid surface

When the injecting fluid is water (wetting fluid) $\theta = 0$ and $\cos\theta = 1$, the equation reduces to the first equation.

The pressure required to force oil into the pore spaces displacing water is termed the displacement pressure. The factors affecting this displacement (or threshold) pressure are :

1) the interfacial tension of the fluids
2) the wettability of the rock - which controls the angle the oil-water interface makes with the grain surfaces
3) the radii of the largest interconnected pore throats

This is shown diagrammatically in Fig. 12 where a filament of hydrocarbon is migrating through a porous and permeable rock which has cylindrical pore throats.

6.1.1 INTERFACIAL TENSION

The interfacial tension is the property of an interface between two immiscible fluids, that causes it to be elastic, with a tendency to contract. It results from the "mutual attraction of like molecules within each fluid and the attraction of dissimilar molecules across the interface of the fluids" (Schowalter, 1979, p. 734). The units of measurement

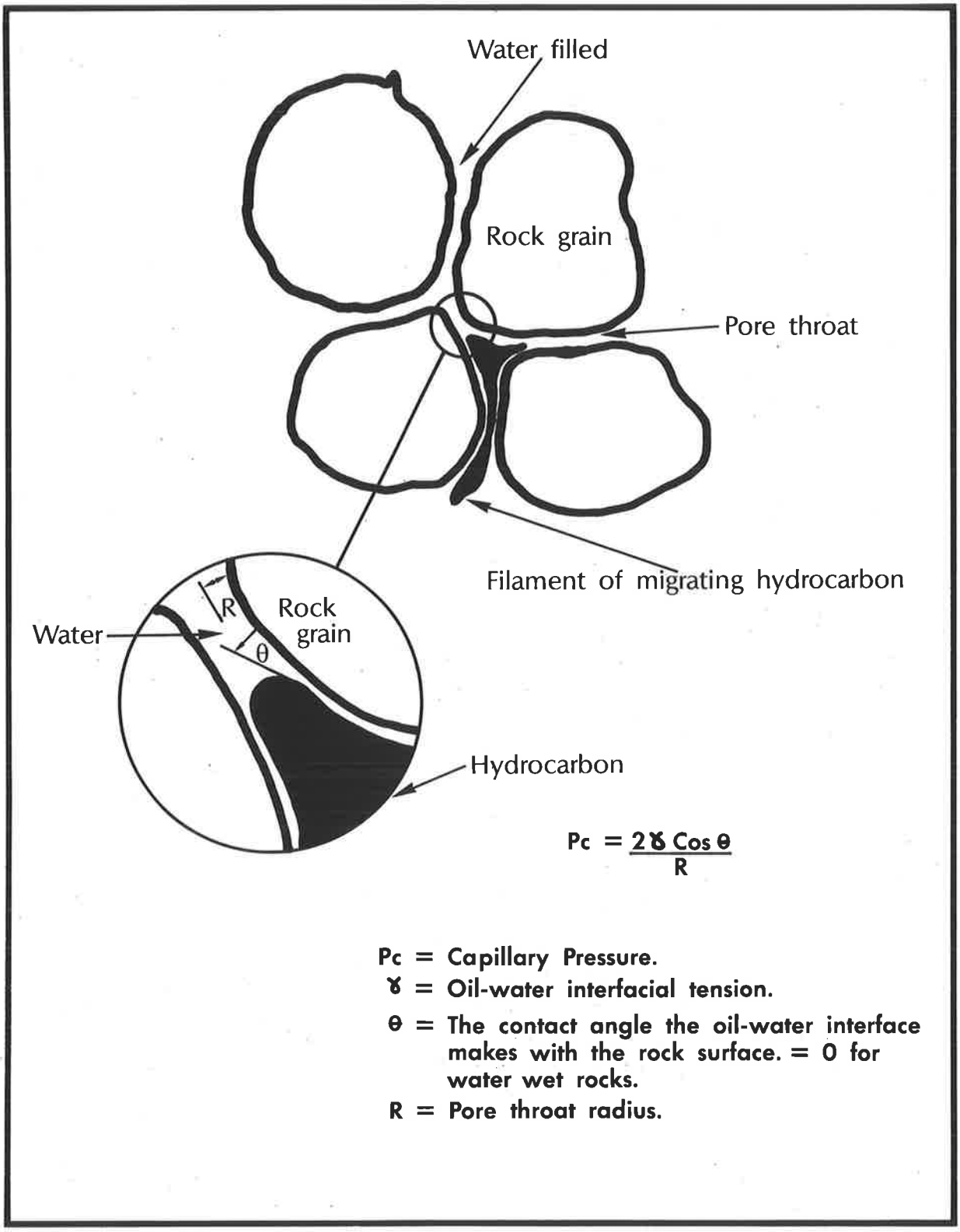

Fig. 12 Diagrammatic representation of an oil filament migrating through a water saturated rock.

are usually dynes per centimetre. Average values of interfacial tension are around 25 dynes/cm at surface conditions for medium-gravity oils (Berg, 1975).

Interfacial tensions can vary with temperature and with pressure. However, at pressures greater than 1500 psi, the effect of pressure on the measurement is much less than that for temperature (McCaffery, 1972, Michaels and Hauser, 1951).

6.1.2 WETTABILITY

The wettability of a rock is the affinity the surfaces of the grains have for the surrounding fluids. The fluid with the surface energy that is closest to that of the rock grains will be the wetting fluid. Usually the wetting fluid in sedimentary rocks is water. Water will spread out over the grain surfaces and be the fluid preferentially held in the pore spaces in a water-wet system. A change from being a completely water-wet system to a partially oil-wet system will effect the capillary pressure curves and can significantly lower the displacement or threshold pressure (Anderson, 1987).

6.1.3 TRAPPING MECHANISMS

If the interfacial tension increases or the pore radii decrease, the displacement pressure will increase and the rock will be a better seal. As the pores and pore throats become smaller, a greater force must be exerted by the oil in order to displace the water held in the pores by capillary action.

In a laterally confined structural or stratigraphic situation, a trap will be formed where the upwards buoyancy force of the oil is insufficient to displace the water in the pores of the sealing interval. Oil will move into the largest connected pores first, then into the next largest pores as the pressure increases. Oil will move laterally and vertically along the bounding surface of the seal, filling the trap, as described by England et al. (1987).

As more oil is added to the accumulation and the hydrocarbon column increases, the buoyancy force also increases. The maximum force occurs at the highest point on the accumulation, where the column is greatest.

If the seal is competent and laterally continuous, the trap can be filled to its structural spill point. Oil will then spill out into the next trap at the same reservoir level. If the seal is not laterally continuous, the structure will only be filled to a level that corresponds to the extent of the seal. This can be the point at which a good seal passes laterally into a poor seal which can either hold no oil or a significantly smaller column than the good seal. The excess will leak into the next reservoir above.

For vertical migration to occur, a network of continuous filaments of oil passing through the largest connected pore throats of the seal is required to form a pathway. The pressure at which the formation of this network of oil filaments takes place is termed the threshold or breakthrough pressure. Unless this pathway is formed, it is believed by several authors (Schowalter, 1979, Thomas et al., 1968) that no oil will leak upwards. Experiments performed by Thomas et al. (1968), showed that no leakage of fluids occurred from core plug samples over a period of three to ten days while the pressure remained below the threshold pressure.

If the threshold pressure of the seal is exceeded, the pressure exerted by the oil pool will decrease as oil leaks upwards. A large proportion of the oil may escape before the pressure has dropped sufficiently to allow water to imbibe back into the pore spaces, breaking the oil filament and halting migration (Schowalter, 1979). This filament of migrating hydrocarbon will be broken when there is insufficient pressure from the pool below to force more hydrocarbons upwards.

Schowalter (1979) summarised the results of several workers and suggested that approximately half the total column of oil will leak before the pressure will be too low

to allow migration to continue. In contrast to this, Watts (1987) suggested that only a small drop in buoyancy pressure may be required to allow the imbibition of water back into the seal, halting migration. This implies that oil will leak in many small, discrete amounts, rather than a few large episodes and that the reservoir may remain close to its maximum fill as defined by the extent of the seal.

6.1.4 RELATING THRESHOLD PRESSURE TO CAPILLARY PRESSURE MEASUREMENTS

Threshold entry pressure and hence seal capacity can be determined directly from capillary pressure measurements performed in a laboratory. The easiest and quickest method is to use air and mercury as the wetting and non-wetting fluids respectively. Mercury is forced into the pore spaces at increasing increments of pressure and the threshold pressure is then determined from one of several methods from the pressure versus mercury saturation curves. The oil column required to exert this pressure on the seal can then be calculated from this value, using simple equations. The calculated oil column can then be compared to known field hydrocarbon column heights.

This sort of analysis is relatively easy and is particularly useful in fine grained rocks where examination by conventional core analyses and thin section microscopy is difficult.

6.2 CAPILLARY PRESSURE METHODS

The one inch (2.5 cm) diameter core plugs were divided into approximately half inch length wafers. One set was used for the special core analysis (capillary pressure measurements) and the others were used for the conventional porosity and permeability measurements.

The determination of capillary pressures was performed using air and mercury. Although using fluids similar to those in the reservoir would appear to offer greater accuracy, air

and brine or oil and brine methods take much longer to perform in finer grained rocks, due to an increase in stabilisation at time at each increase in pressure. An additional problem with either air and brine or oil and brine methods is that reservoir fluids can have a wide variation in properties. Many different synthetic brines and oils must be produced in the laboratory from analyses conducted on actual samples from well tests. It was decided that the air and mercury method of capillary pressure determination would provide accurate results without having to create a suite of different brine and oil samples.

There is much documentation on the validity of using air-mercury capillary pressures and converting the results to oil and water or gas and water (Pickell et al., 1966; Thomas et al., 1968; Omoregie, 1986), particularly for strongly water-wet rocks. It is common practice within the oil industry to take this approach.

Wafers of core plugs were placed in high pressure core holders. Mercury, the non-wetting phase, was injected into the end of the core plug at increasing increments of pressure. For these tests, mercury was injected at pressures ranging from 5 to 33,000 psi. Air, the wetting phase, was displaced by the mercury in varying amounts, depending upon the pressure. The volumes of the fluids were continuously recorded and displayed by computer as both numeric data and graphically. A plot of mercury saturation versus pressure was produced for each sample. Histograms of the accessible pore throat size distribution were also produced. These plots are displayed in the report by Gearhart (1988).

The mercury and air capillary pressure data must then be converted to the equivalent pressures that would occur under reservoir conditions. Some knowledge of the fluid properties is required. Properties such as density are obtained from routine analyses of samples taken during drill-stem or production tests.

6.3 DETERMINATION OF THRESHOLD ENTRY PRESSURE

There are several methods for determining the threshold pressure for various rock types from capillary pressure methods. For permeable reservoir rocks the displacement pressure, (the minimum pressure required to force the mercury through the sample) can be determined easily from the plots of mercury saturation versus pressure. For rocks with moderate to high permeabilities, this displacement pressure is relatively low.

Once the displacement pressure is reached, non-wetting saturations increase greatly with only a small increment of pressure, producing an almost flat plateau. This is shown graphically in Fig. 13 and is described by Jennings (1987). A line from the plateau of the capillary pressure versus mercury saturation curve is extrapolated onto the axis of the plot and the value of displacement pressure is read directly (Schowalter, 1979). This value represents the pressure at which sufficient non-wetting fluid is forced into the sample enabling a continuous filament of mercury to be formed across the length of the plug. At this pressure, migration or leakage can occur. Estimating the threshold pressure from the curve in this way should be reasonably accurate.

However, this method does not work well in tighter reservoir rocks and is particularly difficult to use in cap-rocks. The plateau can be poorly defined, with the pressure versus saturation curves showing a gradual increase in mercury saturation with pressure as shown in Fig. 13.

An alternative method must be adopted for use with low permeability rock samples. The following methods of determining threshold pressure by Thomas et al. (1968), Rudd and Pandey (1973) and Schowalter (1979) are discussed.

Thomas et al. (1968) determined the threshold pressures for several samples of cap-rock. The samples were initially immersed in water and then gas was injected at

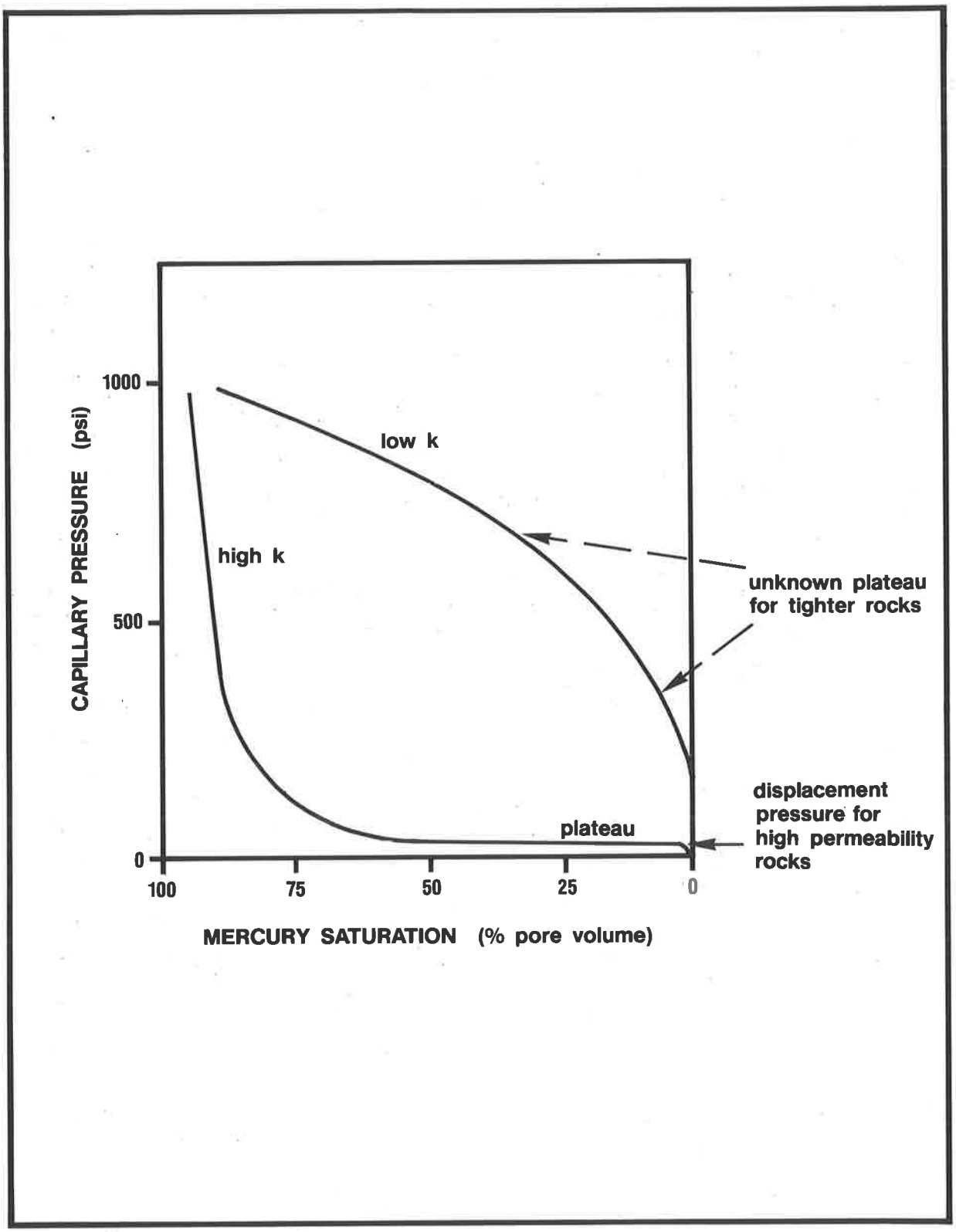

Fig. 13 Typical capillary pressure curves.

increasing increments of pressure. The flow of water from the core plugs was measured as the gas was forced into the samples. After each increment of pressure, the flow would eventually cease as equilibrium was reached. The threshold pressure was interpreted to have been reached when a continuous flow of water, eventually followed by the injected gas, was observed out of the end of the core plug.

Further capillary pressures tests using mercury and air, instead of water and gas, were performed on the same core plug samples for comparison. Plotting the mercury-air capillary pressure against the mercury saturation and extrapolating the line between 5 and 30 per cent mercury saturation to the axis, gave a value of threshold pressure in reasonable agreement with those determined from the previous experiments.

Rudd and Pandey (1973) suggested that for both mudstones and carbonates, threshold pressures can be reached at non-wetting phase saturations of less than 10 per cent and some could be as low as 3 per cent. Such low saturations indicated to them that migration was occurring along discrete localised pathways, possibly even micro-fractures within the mudstone laminations.

Capillary pressure experiments by Schowalter (1979) also showed that for a variety of rock types, including silty shales, an oil saturation of around 10 per cent should be sufficient to form a continuous filament of oil across the sample, allowing migration to occur. His experiments included a nitrogen and water analysis, similar to Thomas et al. (1968) and mercury and air measurements. He determined that the threshold pressure had been reached in the mercury and air system when electrical conduction across the sample was detected, indicating that a continuous filament of mercury was present. He noted that lower saturation values were obtained for the tighter rocks in his study.

The determination of threshold pressure by the Gearhart Laboratory for the samples in the present study, follows the method presented by Thomas et al. (1968). A linear

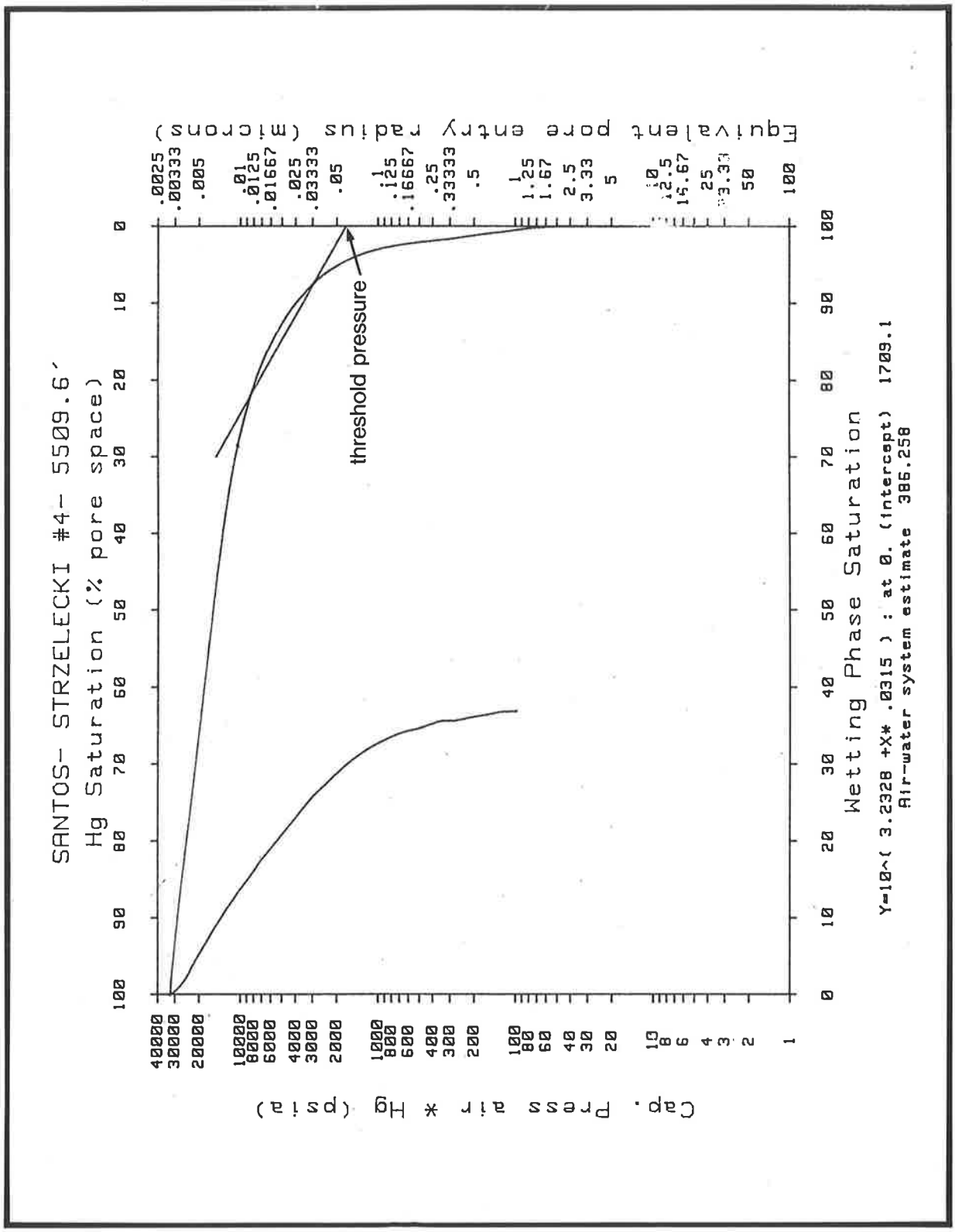

Fig. 14 Determination of threshold pressure.

regression line has been drawn between the points of 5 and 30 per cent mercury saturation and extrapolated to the axis, where the threshold entry pressure was read. The values of threshold pressures determined from this method gave the lowest value of any of the above methods and yet the values are all still relatively high (Table 5).

For several low-permeability samples in this study, the mercury saturation values at the determined threshold pressure were quite low (around 5 per cent). Based on the work by Schowalter (1979), the method adopted for this study appears to give reasonable results for the samples analysed.

6.3.1 CONVERSION TO RESERVOIR CONDITIONS

The values of threshold entry pressure conducted with air and mercury in the laboratory can be converted to values that represent the actual conditions in the reservoir by utilising the equation below.

Conversion of AIR-MERCURY Capillary Pressure Data to OIL-WATER at Reservoir Conditions.

$$\frac{\mathbf{Pc\ (LAB)}}{\mathbf{Pc\ (RES)}} = \frac{\mathbf{T \cos \theta\ (LAB)}}{\mathbf{T \cos \theta\ (RES)}}$$

Where :

Pc = the capillary pressure (psi)

T = the interfacial tension (dynes/cm)

$\cos \theta$ = cosine of the angle of curvature of the interface (or cosine of contact angle)

The use of the above equation requires a knowledge of the properties of the fluids. The oil-water threshold pressures calculated by the above method are summarised in Table 5. The interfacial tension and the angle of curvature of the interface are known for the standard laboratory fluids, but these values must be estimated to approximate reservoir conditions.

TABLE 5 - THRESHOLD PRESSURES

A) HG - AIR THRESHOLD PRESSURES IN PSI

FORMATION SEALS	MINIMUM	MAXIMUM	AVERAGE
MURTA MEMBER	999	5950	2828
NAMUR MEMBER	637	11204	3720
BIRKHEAD FORMATION	1396	4381	2550
TOTAL	**637**	**11204**	**3011**

B) OIL - WATER THRESHOLD PRESSURE IN PSI

CONVERSION = HG-AIR THRESHOLD PRESSURE * 0.0597

FORMATION SEALS	MINIMUM	MAXIMUM	AVERAGE
MURTA MEMBER	60	355	169
NAMUR MEMBER	38	669	222
BIRKHEAD FORMATION	83	261	157
TOTAL	**38**	**669**	**180**

6.4 FACTORS AFFECTING THE DETERMINATION OF THRESHOLD PRESSURES AT RESERVOIR CONDITIONS

Capillary pressures can be affected by both the properties of the rock and the properties of the fluids. A knowledge of the chemical characteristics of the oil and water in the reservoir will improve the accuracy of the final maximum oil column height calculations.

The equation given above, used to convert the laboratory measurements of threshold pressure to reservoir conditions, requires an estimate of the interfacial tension and the angle of curvature of the interface between the oil, water and the rock surface.

The standard laboratory values of interfacial tension and the cosine of the contact angle for a mercury air system are known to be 480 dynes/cm and 0.765 (θ = 140 degrees), respectively, from laboratory measurements (Keelan, 1982).

The interfacial tension values for the water and oil in the reservoir are not easy to establish as the values vary with the chemical properties of the fluids. Interfacial tension values are not routinely measured for Eromanga Basin oil samples.

The mean value of interfacial tension measured for several Texas oils by Livingston (1938) is 21 dynes/cm. Hocott (1938) found that interfacial tensions were influenced by the density of the oils, with a decrease in interfacial tension with increasing API of the oil. His measurements of interfacial tension ranged from 25 to 31 dynes/cm at atmospheric conditions. More recently, McCaffery (1972) measured the behaviour of interfacial tension of n-dodecane, n-octane and refined oils with water, under varying conditions of pressure and temperature. The values of interfacial tension for these fluids are fairly high, ranging from 50.8 for the n-octane and water system to 52.1 dynes/cm for the n-dodecane and water system. Although they are not directly applicable for estimating the values for the Eromanga Basin crude oils, the relative change with increasing pressure and temperature, to simulate reservoir conditions may be useful.

In general, interfacial tensions decrease with increasing temperature. A decrease of around 0.122 dynes/cm per degree Celsius (0.03 dynes/cm/°F) was measured for the n-dodecane and water system by McCaffery (1972). Schowalter (1979), summarised some of the work performed on both pure hydrocarbon/water and crude oil/water systems, concluding that interfacial tensions on average decrease by approximately 0.1 dynes/cm for each degree Fahrenheit increase. However, a small increase in interfacial tension is observed with an increase in pressure (Watts, 1987). McCaffery (1972) found that this increase was in the order of 2 dynes/cm for an increase in pressure of 4750 psi for a n-dodecane and water system. Experiments by Hocott (1938), showed that for several crude oils the interfacial tension increased by 3 to 8 dynes/cm when the pressure was increased from 0 to 2000 psi.

Only one combination of oil and water from the Eromanga Basin has been analysed. The interfacial tension of an oil sample from the Hutton reservoir in the Jackson Field was determined under reservoir conditions. This measurement was reported to be 21.9 dynes/cm (Core Laboratories, 1989). The reservoir temperature of the Hutton Sandstone measured by logging tools is approximately 210°F at the depth of the oil pool. The reservoir pressure determined from many formation drill-stem tests is close to 2000 psi. A value of 20.4 dynes/cm was reported by Schowalter and Hess (1982) for a crude oil and water combination from South Dakota under similar reservoir conditions.

The above measurement of water/oil interfacial tension for the Jackson Field has been used for the remainder of the samples. As API gravities of oil samples are routinely measured and as interfacial tensions tend to decrease with an increase in API gravity, (Hocott, 1938; Schowalter, 1979) relative values could be determined. However, there is scope for error in estimating these values, which could ultimately result in a poor calculation of hydrocarbon column height. Several different values were tried but as all the values of threshold pressure determined for reservoir conditions were all quite high, these further refinements were considered to have little effect on the final conclusions.

A constant value of 21.9 dynes/cm has been used. However, not all of the properties of the rock affecting the capillary pressure measurements need to be measured or estimated and some assumptions can be made about the angle of curvature of the interface between the fluids.

The Eromanga Basin rocks studied are considered to be water-wet, meaning they have a preference for water over oil and have water molecules in close contact with the rock surfaces. This is a reasonable assumption as all rocks of this type are believed to have been initially water-wet when they were deposited. Wettability can be altered after deposition by interactions with hydrocarbons or fluids introduced during drilling or core handling (Anderson, 1986). However, due to the relatively impermeable nature of the samples it can be assumed that the grains have had insufficient contact with drilling and other fluids to alter this initial wettability. Hence, the contact angle term (cos θ) can be neglected as it has a value of 1.0 under these conditions (Anderson, 1987).

6.5 CALCULATION OF MAXIMUM HEIGHT OF OIL COLUMN

The theoretical oil column heights have been calculated using the following equation : Conversion of OIL-WATER Threshold Pressures to Oil Column Height:

$$H = \frac{Pc\ (RES)}{(\rho w - \rho o) * 0.433}$$

Where :

Pc (RES) = the capillary pressure at reservoir conditions (psi)

H = height of oil column above zero capillary pressure (feet)

ρw = density of water (gm/cc)

ρo = density of oil (gm/cc)

0.433 = unit conversion factor

The density of water within the Eromanga Basin sequence is very close to 1.0 as the total dissolved solids measured are rarely above 8000 mg/l. The changes in density with increasing pressure and temperature experienced in reservoirs are small for water due to its relative incompressibility compared to oil. Oil densities measured under surface conditions must be corrected to reservoir conditions. The dissolved hydrocarbon gases associated with the oil cause a variation in values at the surface. As the Eromanga Basin oils contain very little gas, the conversion factor is close to 0.9. A list of the oil densities is given in Appendix 1, Table 2.

The threshold entry pressure (converted to reservoir conditions) for each sample has been used to calculate the theoretical oil column heights that could be attained with these cap-rocks. Table 6 lists the calculated oil column heights.

Threshold pressure measurements, after being converted to reservoir conditions, range from 38 psi to 669 psi, resulting in oil column height calculations of 288 feet up to 5,550 feet (88m to 1692m). These samples are thus all moderate to good seals. The greatest oil column heights of 5,550 and 5,324 feet (1692m and 1623m) were calculated for samples 58 and 72, the siderite cemented samples. The lowest oil column height of 288 feet (88m) was calculated for sample 90, a silty mudstone sample from the Namur Member in Taloola 2.

TABLE 6 - OIL COLUMN HEIGHT CALCULATIONS

WELL NAME AND NUMBER	CORE PLUG NO.	THRESHOLD PRESSURE Hg/Air (psi)	THRESHOLD PRESSURE Oil/Water (psi)	OIL DENSITY (gm/cc)	OIL COLUMN HEIGHT (ft)
BIG LAKE 26	1	3,844	229	0.686	1,687
BIG LAKE 26	4	2,977	178	0.686	1,307
BIG LAKE 26	5	3,026	181	0.686	1,328
CORKWOOD 1	8	2,059	123	0.700	946
GIDGEALPA 29	9	4,381	261	0.692	1,960
GIDGEALPA 30	11	2,742	164	0.692	1,227
GIDGEALPA 30	13	2,868	171	0.692	1,283
MOORARI 5	15	1,504	90	0.713	722
WANCOOCHA 4	16	3,645	218	0.717	1,775
WANCOOCHA 4	17	3,964	237	0.717	1,930
DULLINGARI 9	20	1,357	81	0.676	577
DULLINGARI 9	21	1,451	87	0.676	617
DULLINGARI 15	25	3,593	214	0.676	1,528
DULLINGARI 15	26	4,578	273	0.676	1,947
DULLINGARI 15	27	3,979	237	0.676	1,692
DULLINGARI 27	28	3,745	223	0.676	1,593
DULLINGARI 27	29	1,544	92	0.676	657
DULLINGARI 35	31	1,636	98	0.676	696
DULLINGARI 35	32	999	60	0.676	425
FLY LAKE 4	33	4,869	291	0.713	2,338
FLY LAKE 4	34	1,657	99	0.713	796
LIMESTONE CK 6	35	1,004	60	0.763	584
LIMESTONE CK 6	36	3,286	196	0.763	1,911
MERRIMELIA 3	43	1,967	117	0.681	850
STRZELECKI 4	49	1,709	102	0.745	924
STRZELECKI 4	50	2,374	142	0.745	1,283
STRZELECKI 5	51	1,916	114	0.745	1,035
STRZELECKI 5	53	1,671	100	0.745	903
STRZELECKI 5	54	1,396	83	0.745	754
CALAMIA WEST 1	56	2,126	127	0.700	977
CALAMIA WEST 1	57	772	46	0.700	355
BIALA 3	58	10,149	606	0.748	5,550
BIALA 3	59	2,975	178	0.748	1,627
DULLINGARI 29	60	4,280	255	0.684	1,867
DULLINGARI 29	62	4,172	249	0.684	1,819
DULLINGARI 32	63	2,711	162	0.684	1,182
DULLINGARI 32	64	2,730	163	0.684	1,191
GIDGEALPA 24	65	1,821	109	0.747	992
GIDGEALPA 24	66	4,775	285	0.747	2,601
MARABOOKA 1	68	1,276	76	0.718	624
MERRIMELIA 6	70	4,214	251	0.710	2,003
MERRIMELIA 6	71	4,957	296	0.710	2,356
MERRIMELIA 8	72	11,204	669	0.710	5,324
MERRIMELIA 8	73	1,193	71	0.710	567
MUDERA 1	76	3,253	194	0.718	1,590
JACKSON 2	77	2,469	147	0.705	1,153
JACKSON 3	79	4,284	256	0.705	2,001
JACKSON 3	80	5,950	355	0.705	2,780
WILSON 2	81	1,885	112	0.705	881
JACKSON 18	82	1,574	94	0.786	1,014
JACKSON 18	83	1,805	108	0.786	1,162
JACKSON 30	84	3,032	181	0.786	1,953
PITCHERY 2	86	2,611	156	0.718	1,276
TALOOLA 2	90	637	38	0.695	288

6.6 THE EFFECT OF HYDRODYNAMICS ON CALCULATED OIL COLUMN HEIGHTS

The above estimates of oil column heights are the maximum columns expected under hydrostatic conditions. Groundwater movement can have a significant effect on the amount of oil trapped below a seal if the hydrodynamic gradients are high. At regional structural dips greater than 5 degrees, buoyancy is the main controlling force in secondary oil migration. If bedding or structural dips are less than 5 degrees, hydrodynamic factors could significantly affect the trap potential (Davis, 1987).

A reduction in pressure on the seal will result from a downwards water flow, increasing the potential oil column. The reverse will occur where the groundwater movement is upwards. Studies of the hydrogeology of the Eromanga Basin have been undertaken by Habermehl (1980) and Moriarty and Williams (1982). Both authors suggest that groundwater movement through the aquifers of the Eromanga Basin is slow and in a southwest direction in the eastern part of the basin and to the southeast in the western portion. Moriarty and Williams (1982) stated that the gradients in the central part of the basin range from 1 in 2000 to 1 in 6000.

Bowering (1982) calculated the apparent dip that would be observed on an oil-water contact within the Eromanga Basin aquifers using Hubbert's equation. Using a water gradient of 1 in 3000, the equation gave a value for the amount of tilt of four minutes.

Similar methods were used by Berg (1975) to calculate the effects of groundwater movement on a stratigraphic trap, where his calculated oil column heights from capillary pressure data were far less than the actual columns observed. From production data, he inferred the presence of a tilted oil-water contact and calculated a tilt of 50 feet/mile. The additional oil column of 80 to 90 feet (24 to 27m) above the amount calculated by his work was attributed to hydrodynamic tilting. This was supported by the reported

hydrodynamic gradients of 20 to 30 feet/mile or 1 in 200 in this area.

No tilted oil-water contacts have been reported in the Eromanga Basin. Many errors are possible when measuring the depth to the oil-water contact, in part due to well deviations that are not accounted for in nearly vertical wells and the effects of permeability variations. The determination of small hydrodynamic tilts, if present, is extremely uncertain.

The variation in depth of the oil-water contact in fields such as the Jackson Field, Hutton Sandstone oil pool, is within 10 feet (3m) for all wells across the extent of the field (Fig. 17). The depth of the oil-water contact in the Jackson Field does not vary in a consistent way across the fields and the magnitude of variation is within the acceptable error. Therefore, it is considered that these oil-water contacts are essentially horizontal and that small variations are probably due to permeability effects.

It appears that the effects of hydrodynamics on the height of oil columns in the Eromanga Basin are small enough to be insignificant.

6.7 SUMMARY OF CORE PLUG ANALYSES

The main sealing intervals in the Eromanga Basin are interbedded mudstones, siltstones and fine sandstones of the Murta and Namur Members of the Mooga Formation and the Birkhead Formation. Individual mudstone layers within the sealing interval range in thickness from laminations up to several feet (1-2m).

Analyses of fifty-four core plug samples from these intervals were performed using X-Ray Diffraction, Scanning Electron Microscopy, conventional core analysis and mercury capillary pressure techniques to investigate the mineralogy and to determine the sealing capacity of these mudstones.

All of the mudstone samples are composed predominantly of quartz, kaolinite and illite with minor to trace amounts of chlorite, feldspar and siderite. A few samples contained minor amounts of smectite. In addition to the mudstone samples, four samples of hard, siderite cemented bands were analysed.

Microporosity, determined from the capillary pressure measurements, forms 90 to 99 per cent of the total porosity. Porosity occurs between the platy illite and fine mica grains as seen in the scanning electron microscope work. The kaolinite clays, although indicated to be abundant from the XRD analyses, proved difficult to distinguish with the SEM, except for the coarser grained variety, observed in some of the larger pore spaces. All samples have permeabilities less than 0.09 millidarcies, which is expected from competent sealing lithologies.

The threshold pressure measurements and the resultant calculations of potential oil column heights have shown that the mudstone layers within the sealing intervals of the Murta Member, the Namur Member and the Birkhead Formation are capable of sealing over a few hundred feet (90 m) of oil. The greatest threshold pressures were measured in the siderite cemented samples (plug nos. 58 and 72). Very little difference in the magnitude of threshold pressure was noted between mudstones and silty mudstones with formation or with depth, shown in the crossplots in Fig. 15.

Crossplots of the sample clay type against threshold pressure show that variations in clay mineralogy, either kaolinite or illite, have little effect on the magnitude of the sealing capacity for these samples (Appendix Fig. 3). This is supported by the poor correlation of mineralogy with conventional core analysis, particularly permeability (Appendix Fig. 2).

Correlation of threshold pressure with porosity shows no trends for the sample range (Fig. 15b). Crossplots of threshold pressure against permeability and pore radii (Figs.

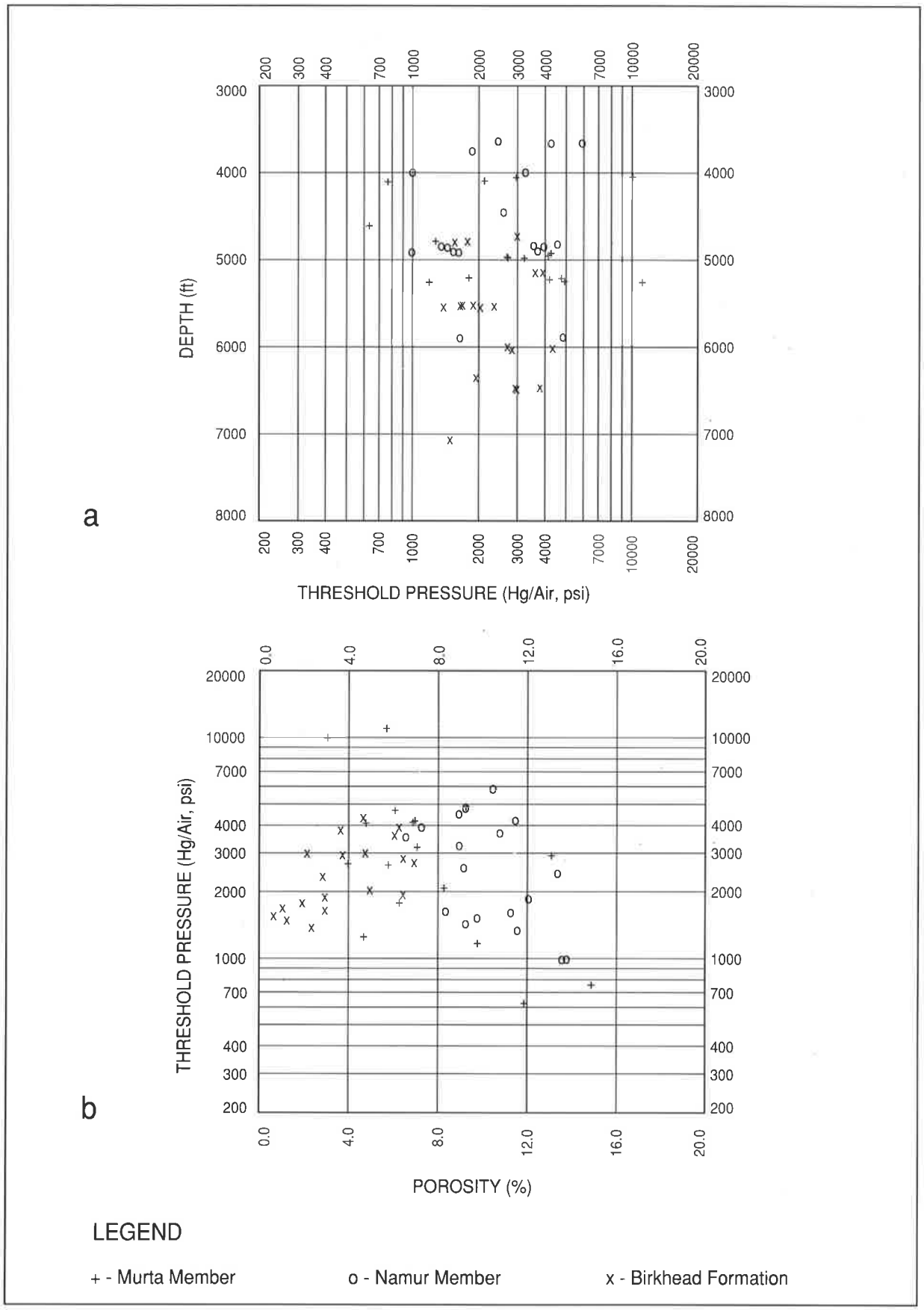

FIG. 15 : Crossplots of Threshold Pressure against a) the Depth of Origin of the Sample and against b) the Porosity.

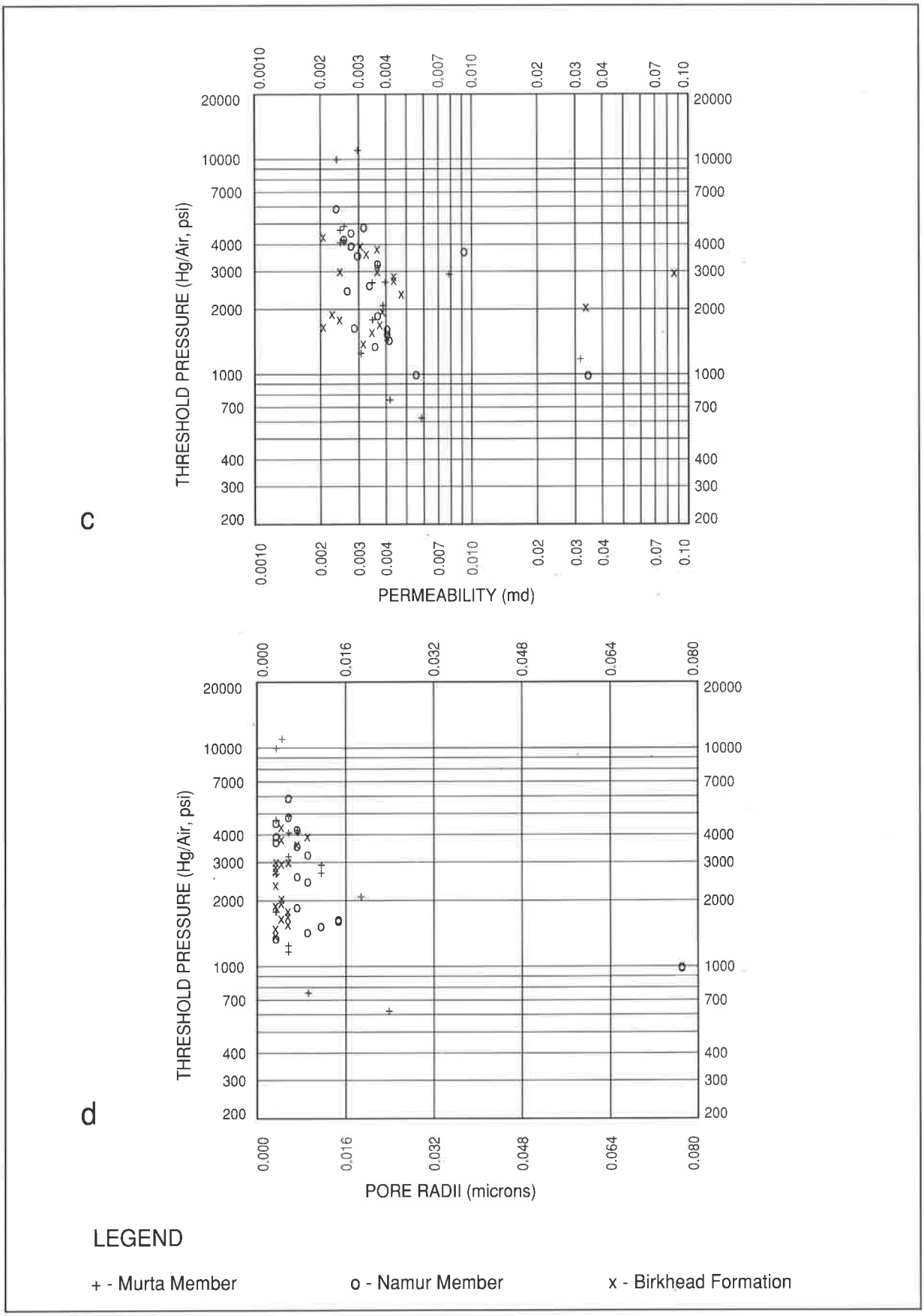

FIG. 15 : CONT. Crossplots of Threshold Pressure against c) the Permeability and against d) the Pore Radii.

15c and 15d) also show poor correlations. Two trends can be interpreted on the threshold pressure against permeability plot, which have the same direction, but have different slopes. The samples with higher permeabilities are not significantly different mineralogically nor do they have vastly differing porosity values.

According to several authors, including Thomas et al. (1968) there should be a relationship between the permeability measured from the core plug samples and the threshold pressures. Thomas et al. (1968) performed studies using air/water threshold pressures and permeability values determined for several samples of low permeability rock for the purpose of gas storage. It was suggested that in the absence of capillary pressure work, it should be possible to estimate the threshold pressure for similar rocks and fluid conditions from this relationship.

The following correlation was found by Thomas et al. (1968), from a crossplot of threshold pressure and reciprocal permeability :

$$Pt = 7.37 \times k^{-0.43}$$

Where:

Pt = threshold pressure in psi

k = permeability in md

The oil-water corrected threshold pressures for this study were plotted against the reciprocal permeabilities to see if such a trend could be observed (Fig. 15e). Both the slope determined by Thomas et al. (1968) and the exponent predicted from semi-empirical equations relating threshold pressure to permeability, are drawn on the crossplot for comparison. Several correlations could be drawn for the points plotted. For a small change in permeability, there is a large variation in threshold pressure. Therefore,

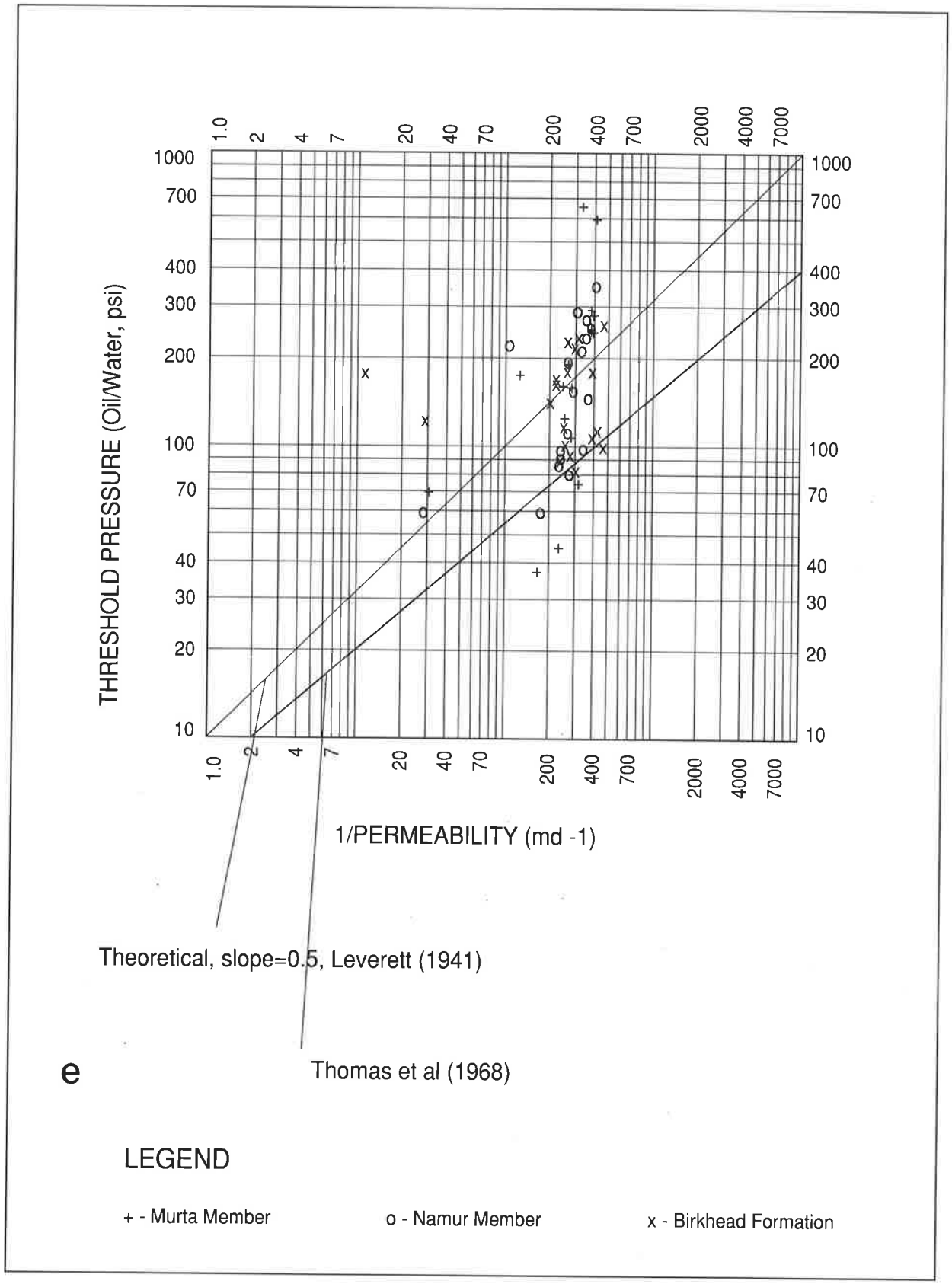

FIG. 15 : CONT. Crossplot of Threshold Pressure against the Reciprocal Permeability showing the least squares fit line found by Thomas et al (1968) and the theoretical line, predicted by Leverett (1941).

predicting the threshold pressures from reciprocal permeability from these data is not satisfactory.

The poor correlation of permeability and threshold pressure may be due to minor variations in rock properties of the samples used for the conventional analyses and those used for the capillary pressure work. There may also be some error in the determination of threshold pressure. Alternatively, effects of sample orientation may significantly influence permeability and capillary pressure measurements.

Omoregie (1986) observed that some capillary pressure data were significantly affected by orientation of core plugs. Samples not affected by the test direction were sandstones, where pore size distributions can be relatively homogeneous. However, most samples in this study contain quantities of oriented platy mica and illite clays. The grain and pore structure thus will have significant directional variation.

Omoregie (1986) also suggested that permeabilities measured in the horizontal direction are more representative of the overall pore geometry. Hence, the poor correlation of threshold pressure and permeability may also be due to orientation effects.

7. DISCUSSION AND CONCLUSIONS

7.1 DISCUSSION

This study shows that all the Eromanga Basin mudstones sampled have similar mineralogy, low permeabilities and good sealing capacity. The oil column heights calculated from the threshold pressure measurements are all greater than 288 feet (88m) with a maximum height calculated of 5,550 feet (1692m). Many Jurassic structural closures in the Eromanga Basin are subtle and are less than 200 feet (61m) from crest to spill point. The experimental results suggest that these structures should all be filled to spill below the lowest sealing interval.

However, all Eromanga Basin oil columns discovered are less than 120 feet (37m), most commonly less than 50 feet (15m) and do not always occur only below the lowest sealing interval, but can occur in multiple horizons or only towards the top of the sequence.

Eromanga Basin oil pools have been discovered trapped below the Poolowanna Formation, Birkhead Formation, Namur Member or Murta Member sealing intervals. Occasionally, small accumulations are also found below thin mudstones within the main reservoir zones. As potential sealing intervals such as the Birkhead Formation can be traced across the entire study area, it is difficult to determine what makes one mudstone a good seal and another one not.

The results obtained from this study are explained by relating the seal capacity to the actual distribution and size of some important and well-known Eromanga Basin oil pools.

7.1.1 STRUCTURES THAT ARE FILLED TO SPILL

There are only a few fields that are filled to maximum structural spill point and substantiate the findings of the capillary pressure measurements and the resultant threshold pressure determinations.

The largest Eromanga Basin oil field discovered to date, the Jackson Field, is located in ATP 259 P, Queensland. It contains 83 MMbbls of oil-in-place in the Hutton Sandstone. The oil column heights calculated from the capillary pressure measurements for the Birkhead Formation in Jackson 18 and 30 range from 1,014 feet to 1953 feet (309 to 595m). The actual structural closure and vertical oil column are both around 120 feet (37m). The reservoir consists of massive, fluvial sandstones that have high porosities and permeabilities. The excellent reservoir quality results in an oil pool with no significant transition zone (Fig. 16).

The overlying, sealing Birkhead Formation lithology is typical of that elsewhere in the basin. It consists predominantly of thin siltstones, tight sandstones and mudstones interbedded with thicker porous sandstones. Additional oil is reservoired in sandstones within this zone. The mudstone interval providing the seal to this oil pool can be identified within the Birkhead Formation from wireline logs shown in the cross section in Fig. 16. In Jackson 31, located to the south of the crest of the culmination, a sealing layer separates the Hutton oil pool from an overlying Birkhead sandstone which has been shown to be water saturated from open-hole drill-stem tests. It is this thin interval between the water saturated sandstone and the top of the porous reservoir sandstone that holds back an oil column of 120 feet (37m). The structure map in Fig. 17 shows the location of the spill point into the Jackson South area.

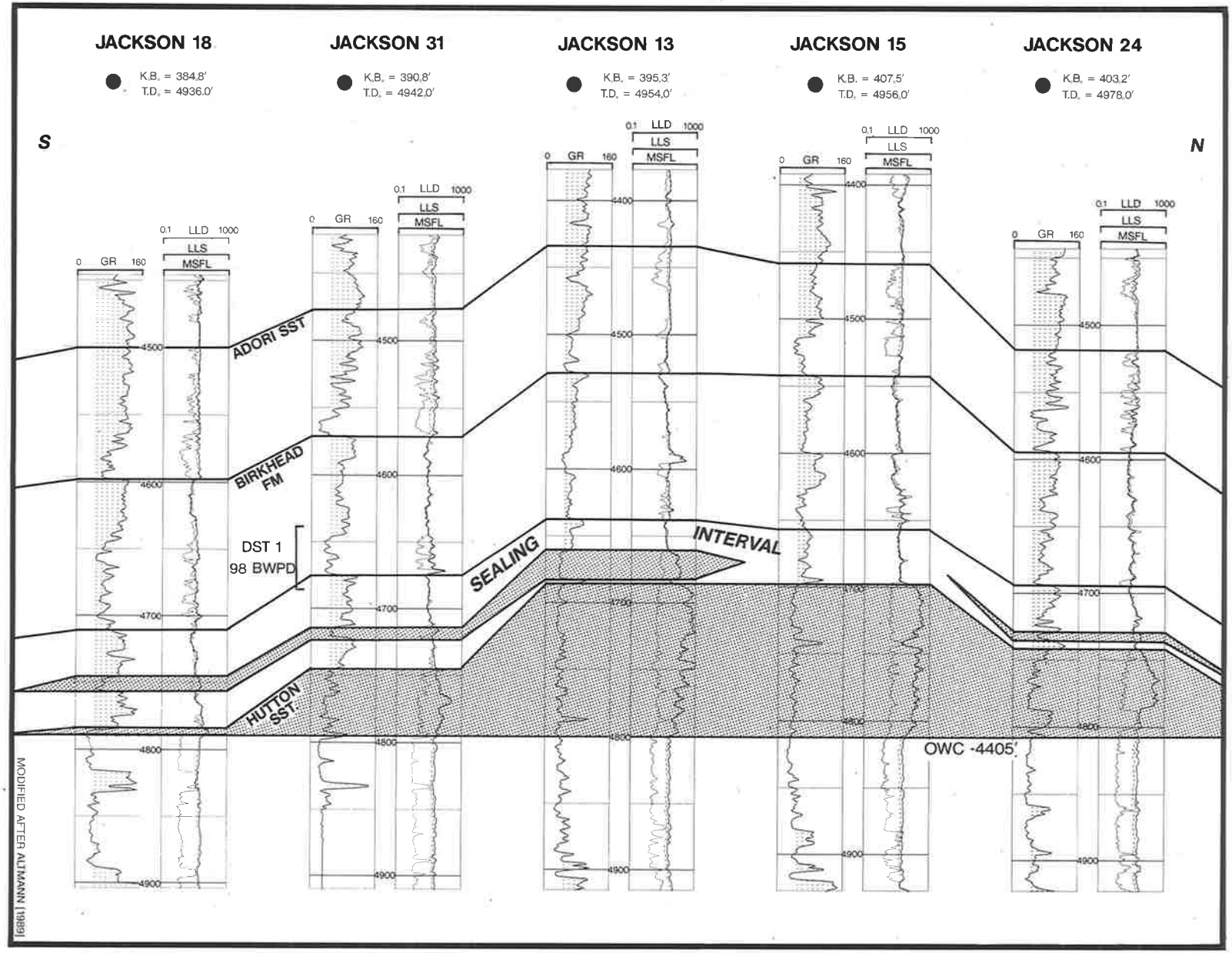

Fig. 16 Structural cross section through the Jackson Field.

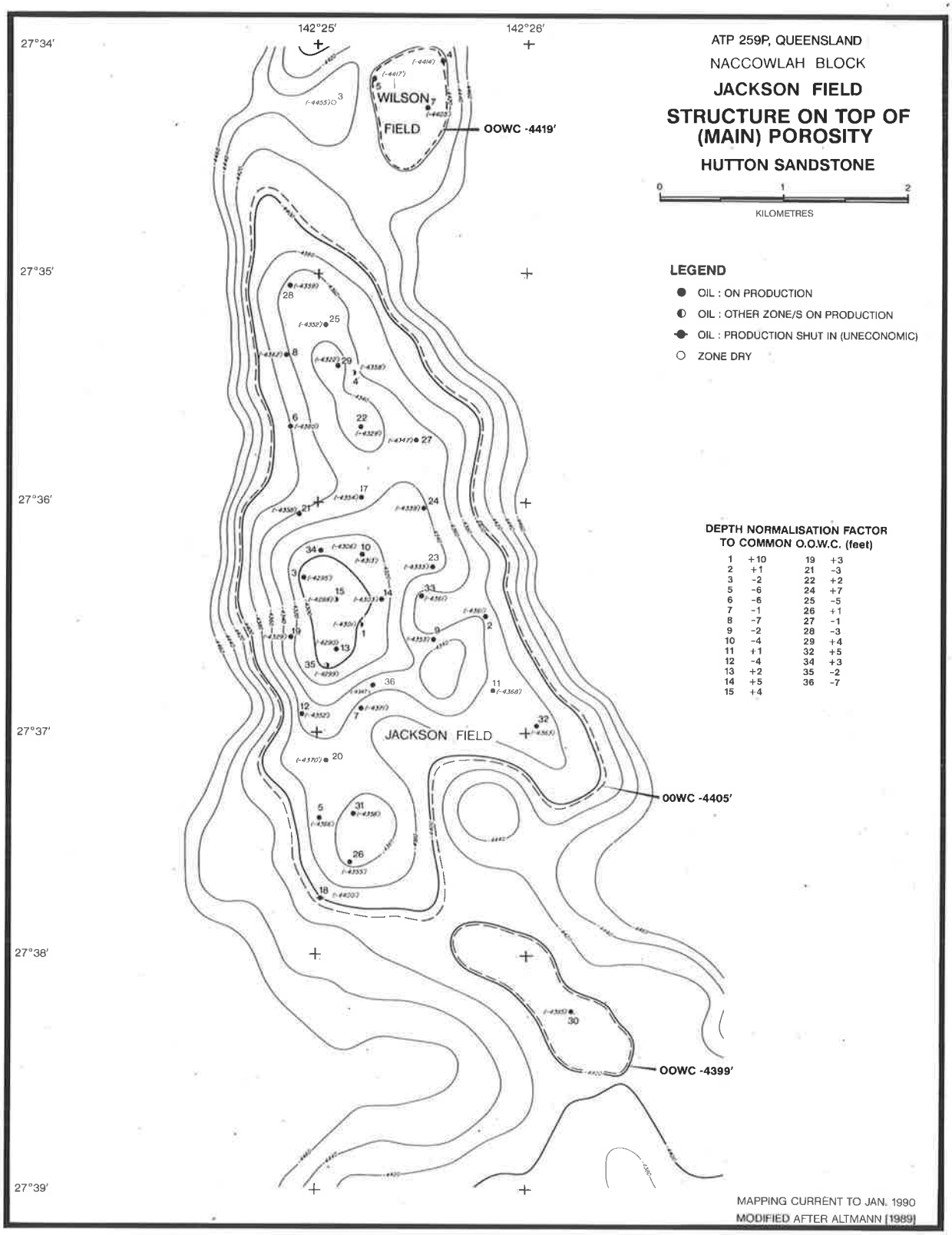

Fig. 17 Jackson Field depth structure map, Hutton Sandstone.

7.1.2 MUDSTONE SEAL CONTINUITY

Although a few structures are interpreted to be filled to structural spill (e.g. Jackson, Gidgealpa South and Bookabourdie), there are numerous fields that are only partially filled based upon current mapping.

The Taloola Field, located in the western part of the study area in South Australia (Fig. 18) contains several Eromanga Basin oil pools, one of which is a lower Hutton Sandstone oil pool (Fig. 19). The mudstone seal to this accumulation can be identified with certainty from the Taloola 2 wireline logs (Fig. 20). This 3 feet (1m) thick mudstone and siltstone bed in the lower Hutton Sandstone is trapping an oil pool with a 10 feet (3m) thick vertical column. This is much less than the currently mapped closure of the structure at this level.

The oil pool has only been intersected in one of the three wells drilled on the Taloola structure. The mudstone layer sealing the pool does not appear to be extensive, but passes laterally into siltstones and sandstones due to a facies change. The silty nature of this bed in nearby Taloola 3, can be inferred from the lower gamma ray value and the greater separation of the deep and micro-resistivity logs (Fig. 20). This lateral variation in sealing capacity has apparently provided an avenue for oil to migrate further updip.

This evidence may give an insight as to why few Eromanga Basin oil fields are filled to spill. Although the Murta Member and the Birkhead Formation have sealing intervals that will contain a certain proportion of mudstone and tight, silty mudstone, many of these may not be sufficiently continuous to form a seal over the entire structure. The thin mudstone layers may pass laterally into siltstones and sandstones, with lower sealing capacity, creating conduits and migration pathways through the interval, as pictured in Fig. 21. Either the siltstones will hold back a smaller oil column, controlled by this capacity, or the entire oil pool will leak where seal capacity approaches zero.

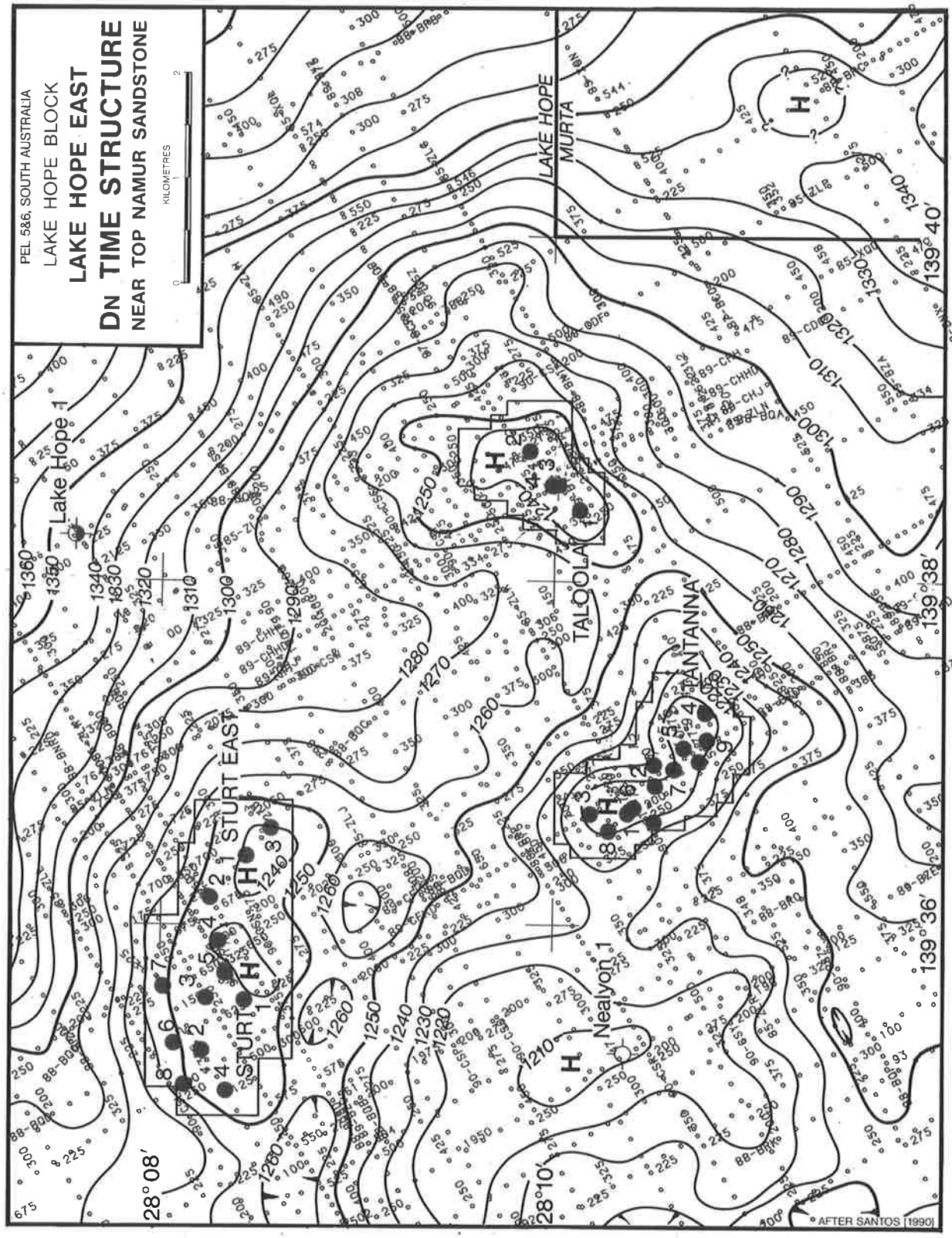

Fig.18 Time structure map of the Top Namur Sandstone Member showing the Taloola and Tantanna Fields.

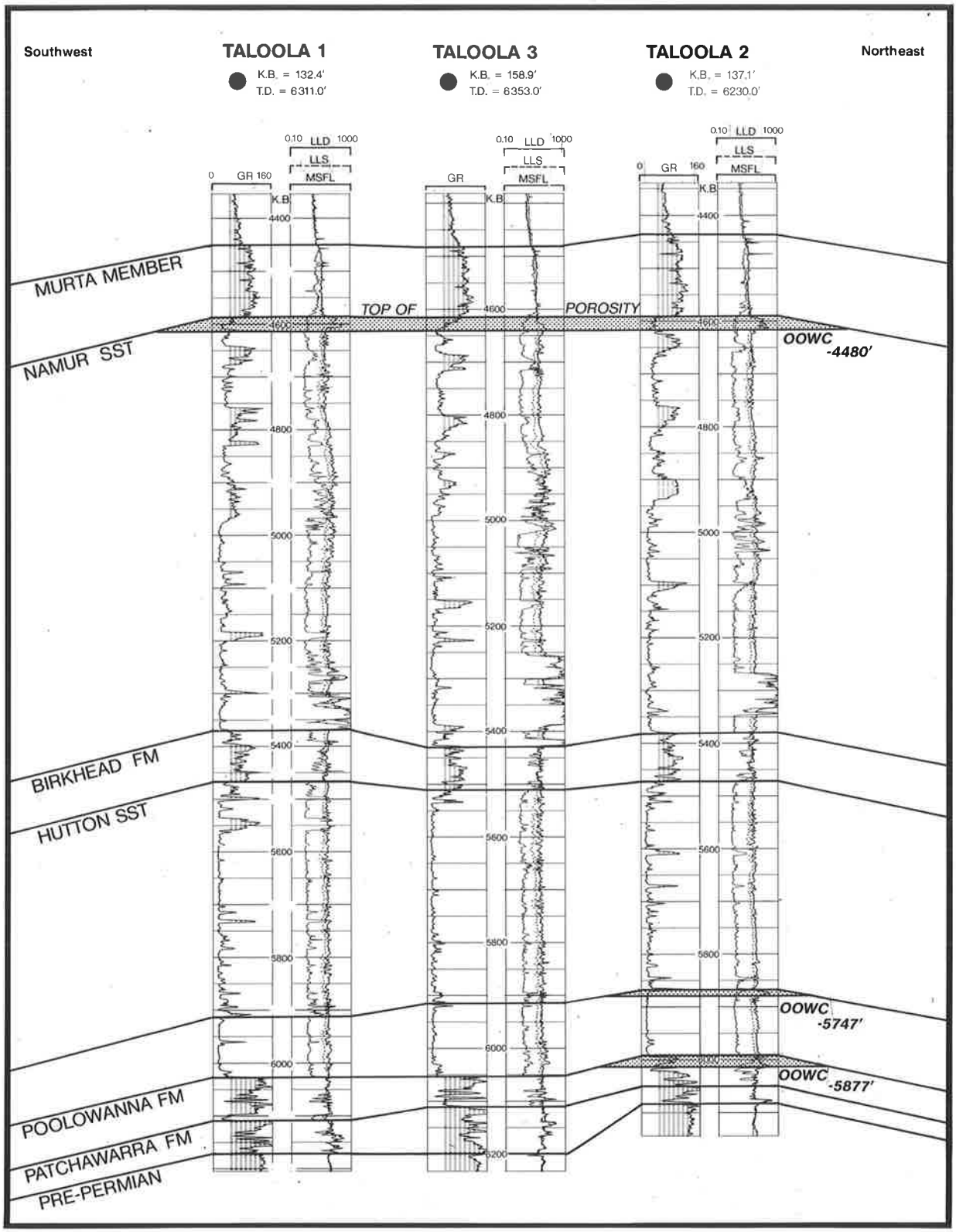

Fig. 19 Southwest to northeast cross-section through the Taloola Field showing the Namur Member, Basal Hutton Sandstone and Poolowanna Formation oil pools.

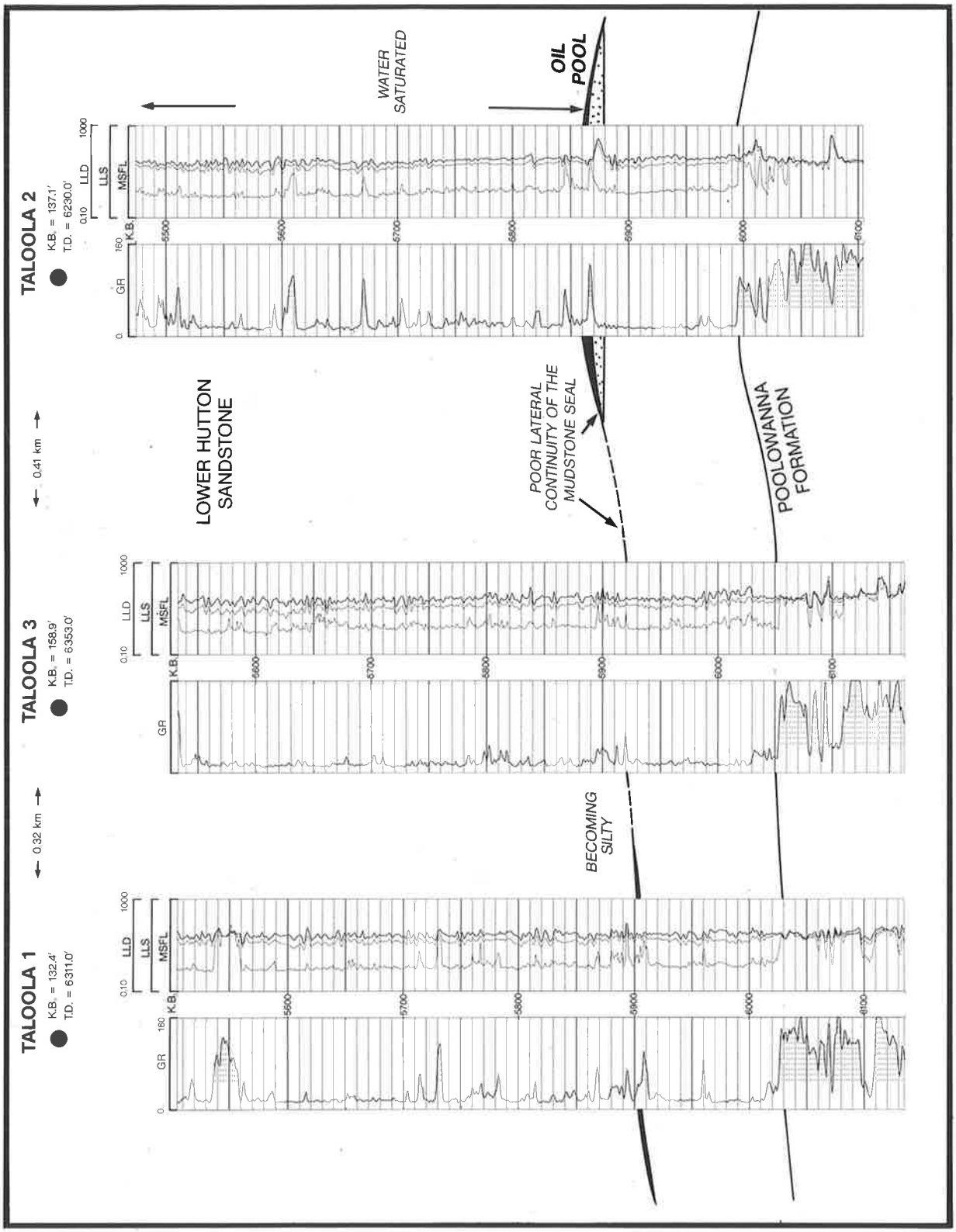

Fig. 20 Southwest to northeast structural cross section across the Taloola oil field showing the thin mudstone seal in Taloola 2 that is trapping a 10′ oil column in the lower Hutton sandstone. Lateral continuity of this mudstone is poor and it becomes very silty in the nearby Taloola 3 well.

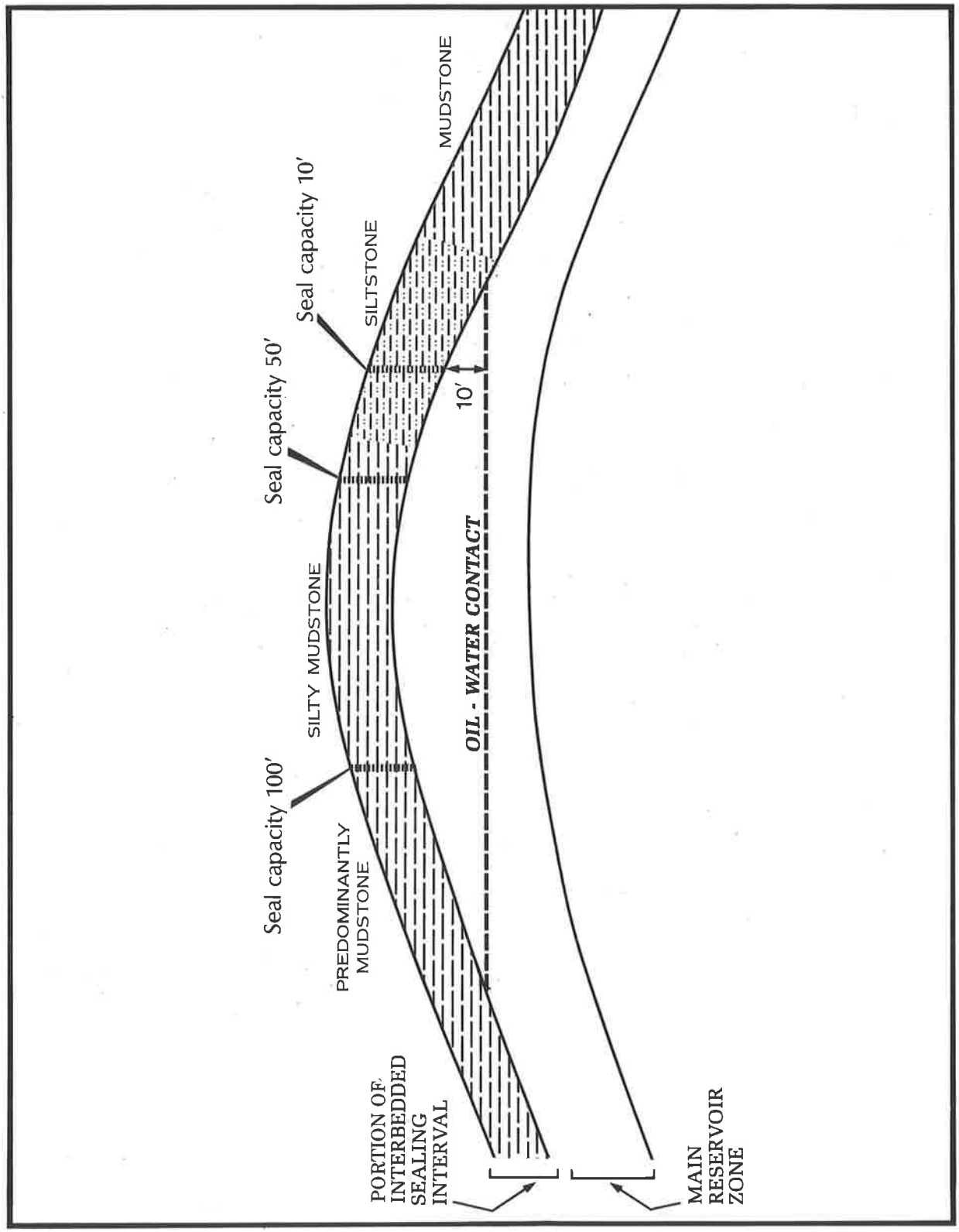

Fig. 21 Diagrammatic representation of a sealing interval and reservoir showing how the oil column can be controlled by the lateral variation in seal capacity.

It is concluded that even though thin mudstones are capable of holding back large oil columns, they must be continuous over a large portion of the field area to be the most effective. The Muteroo, Narcoonowie and Tantanna oil fields in South Australia are other examples of fields that have Hutton Sandstone oil pools that are sealed by very thin mudstone layers.

7.1.3 OIL COLUMN WASTE ZONES

In some structures with very low relief, some oil-water contacts are very close to the mapped closure. Oil columns are generally measured from the uppermost level of porous and permeable sandstone that is economic pay or 'top of porosity', down to the oil-water contact interpreted from wireline logs. That such structures are not considered to be filled to spill may be due to the incorrect identification of the top of the oil column. This may result from either a lack of well data or the existence of a waste zone that has been overlooked. A waste zone is defined by Schowalter and Hess (1982) as the region which contains non-productive or "wasted" oil, located between the trapping edge of a seal and the edge of the economic producing zone of a reservoir.

The Tantanna Field is located just to the west of the Taloola Field, in PEL's 5 & 6, South Australia (Fig. 18). Oil pools have been discovered in several horizons, one of which is the Namur Member. This Namur Member oil pool is not considered to be filled to spill. The total height of closure, measured from the top of the structure at the Namur Member level to the spill point, is approximately 90 feet (27m). An oil column of 53 feet (16m) is mapped from the top of porosity in the Namur Member to the oil-water contact at -4409 feet (-1344 m) (Fig. 22). Hence, there is an interval of 37 feet (11m) between the oil-water contact and the lowest-closing contour.

Examination of the drilling mudlog of the crestal Tantanna 1 well indicates that low porosity and permeability sandstones and siltstones with significant oil shows were

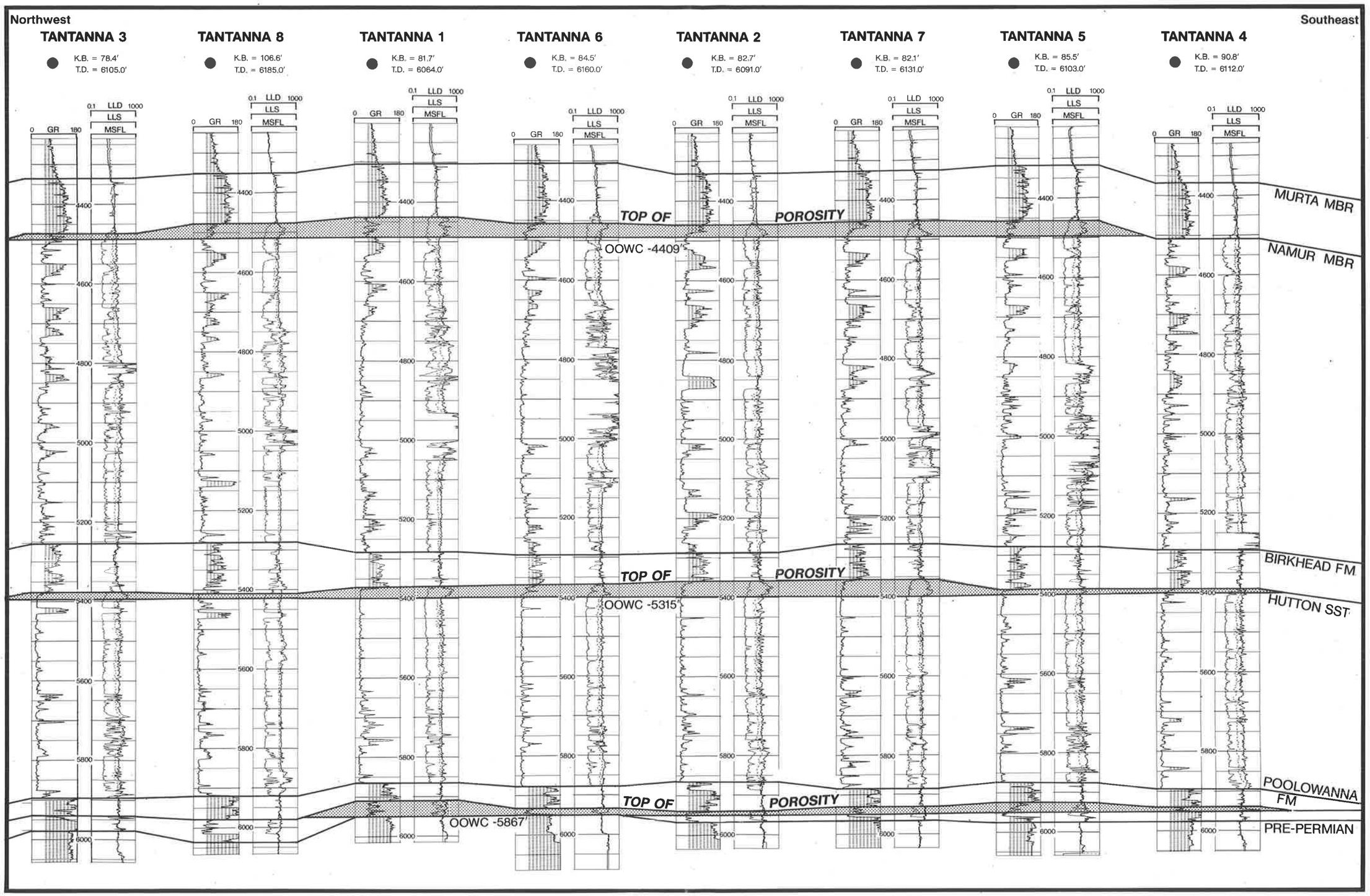

Fig. 22 Northwest to southeast structural cross section through the Tantanna Field showing the Namur Member, Hutton Sandstone and Poolowanna oil pools.

intersected above the level of top of porosity for the Namur Member. The thickness of this waste zone is approximately 30 feet (9m) in the Tantanna 1 well. When this thickness is added to the oil column height previously measured, the total vertical oil column height is very close to the mapped closure for the Namur Sandstone.

This concept is presented graphically in Fig. 23. Assuming the interbedded siltstones and sandstones have very poor sealing capacity, the first continuous mudstone within the interbedded sequence may form the seal for the total oil column.

Hence, many of the low relief structures in the Eromanga Basin may actually be filled to spill if the waste zone is accounted for in the total oil column calculations.

Attempts to measure the extent of waste zones for several other fields from cores was not possible, as most were cut below the start of the waste zone, with oil shows observed throughout the coarser grained layers. Examination of reported fluorescence shows from drilling mudlogs and daily drilling reports generally proved to be inadequate for defining the extent of the waste zones.

For the Eromanga Basin in general, the identification of sealing mudstones must be based on wireline logs as there is an insufficient number of wells with full-hole cores to enable detailed correlations to be made. Unfortunately, the vertical resolution of Gamma Ray, Neutron and Density wireline logs is not sufficient to differentiate individual sandstone, siltstone and mudstone layers in most cases. Sandstones and siltstones within the sealing intervals can also contain significant quantities of mica and k-feldspar which reduce the differences in log response between the lithologies. Hence, the individual mudstone layers cannot be resolved and mapping them from well to well is rarely possible.

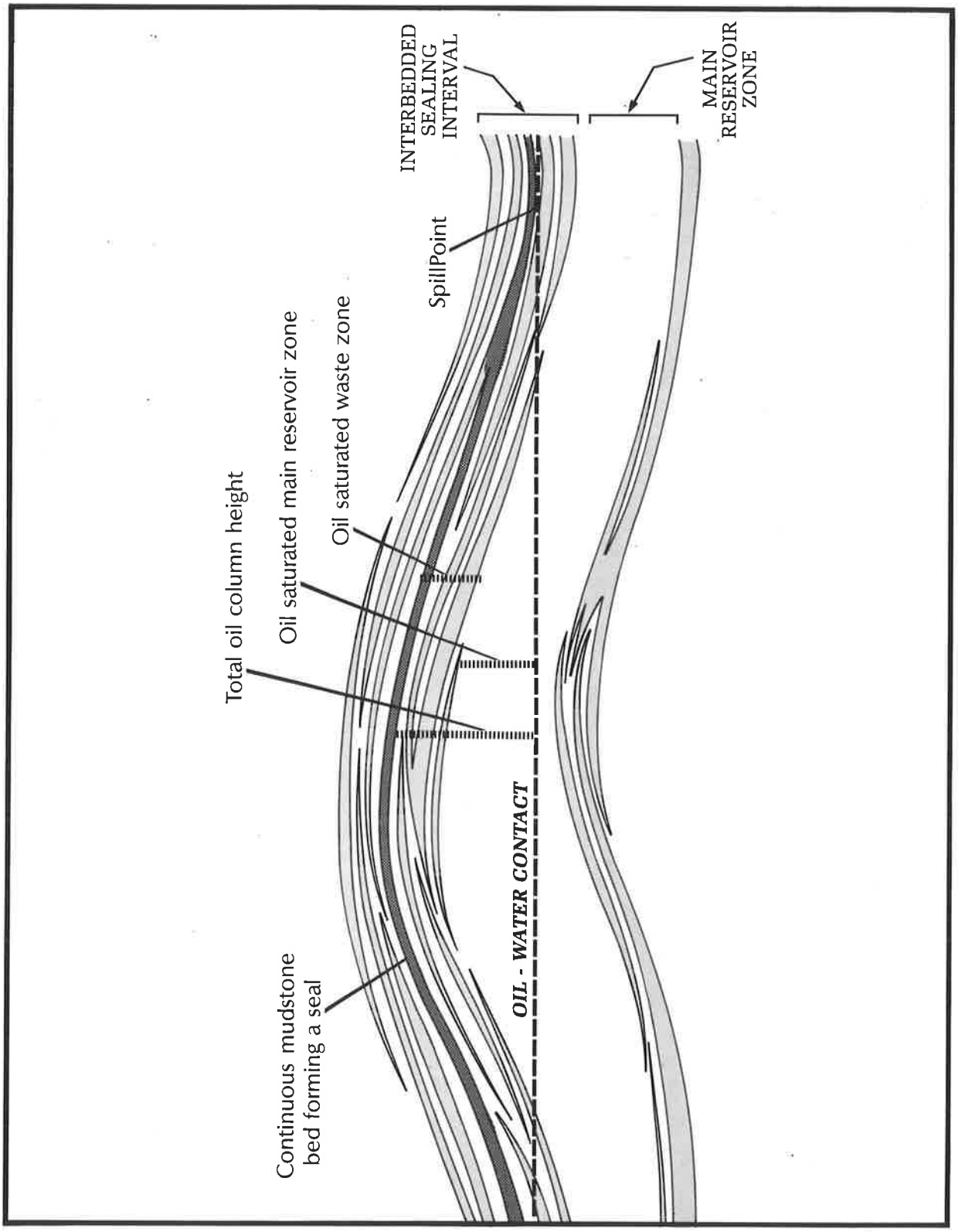

Fig. 23 Diagrammatic representation of a waste zone dependent on the lateral continuity of mudstone layers in the sealing interval.

A method whereby the individual mudstone thickness and continuity could be inferred has been investigated. It was assumed that if during deposition low energy conditions prevailed for long periods of time, greater thicknesses of mudstone would accumulate. The chance that individual layers will be far more laterally continuous will therefore be greater in these zones. If the thickness of the entire sealing interval is small, it is assumed that the individual mudstone layers will also be thin and more importantly, less likely to be areally significant.

To test this suggestion, a plot of the Birkhead Formation thickness against the volume of oil (in MMbbls) discovered in the overlying Namur and Murta Member reservoirs was made and is shown in Fig. 24a. The gross Birkhead Formation thickness has been used as an approximation of the thickness of sealing intervals within the formation. It was anticipated that the crossplot would show a trend of larger Murta and Namur oil pools associated with the thinnest Birkhead Formation sealing intervals. The crossplot in Fig. 24a does show the expected trend. As the total formation thickness decreases, the volume of oil found higher in the sequence is greater.

However, many of the fields with a thin or more sandstone-prone Birkhead Formation also have significant Hutton Sandstone oil pools trapped beneath these seals. The Jackson, Gidgealpa, Big Lake and Strzelecki Fields are examples (Fig. 24b).

There are also a number of oil pools in the Namur and Murta Members that occur in structures with thicker Birkhead Formation seals or Birkhead Formation seals that are known to be competent seals in nearby fields. The Taloola and Dullingari Fields are examples of these.

Hence, although the overall trend is apparent, other factors must be influencing the distribution of oil pools apart from the sealing interval thickness and each case must be considered individually. Attempts to use the large-scale sand-shale ratio maps to predict

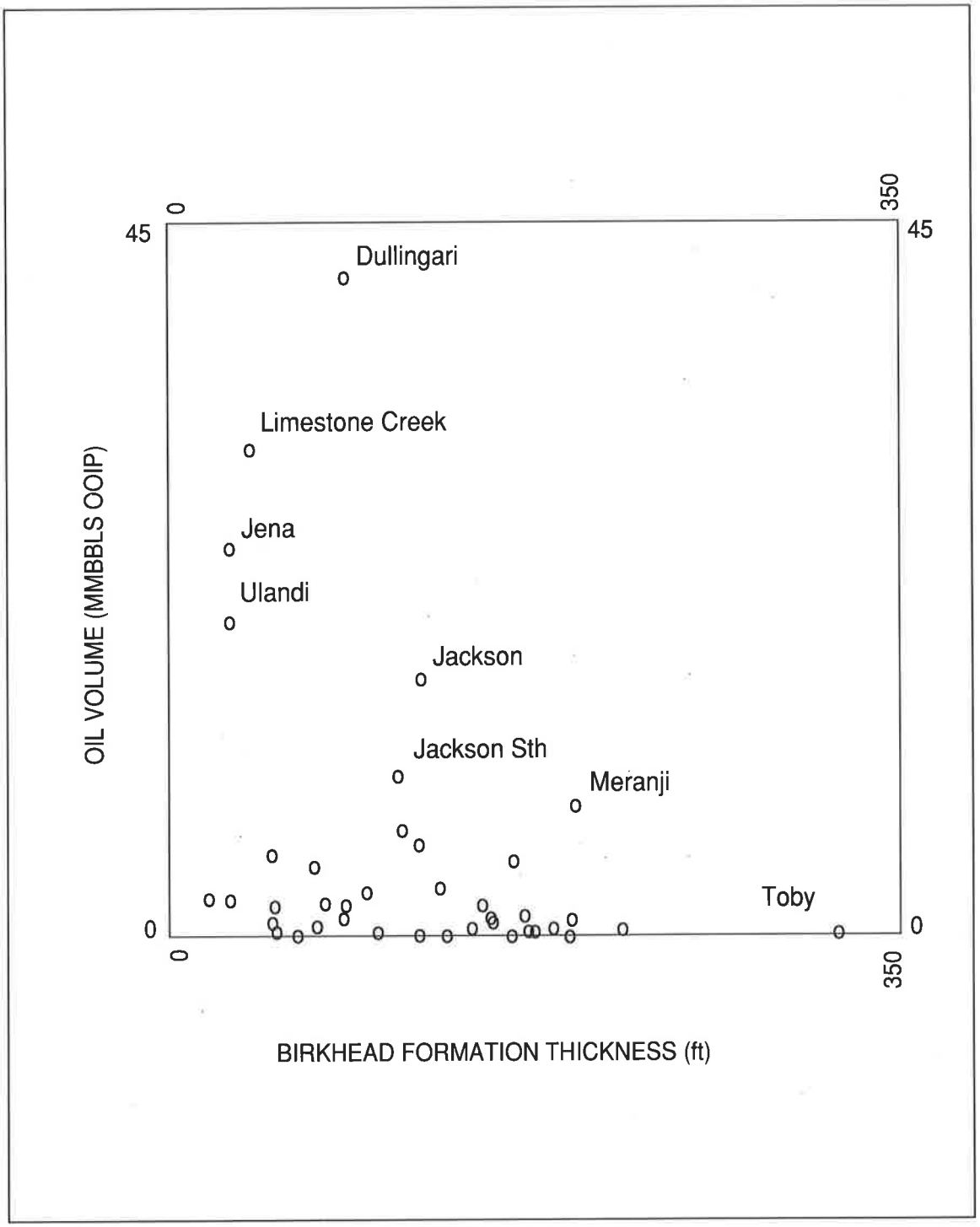

FIG. 24 a : Plot of the Birkhead Formation thickness against the volume of oil reservoired in horizons above the Birkhead Formation.

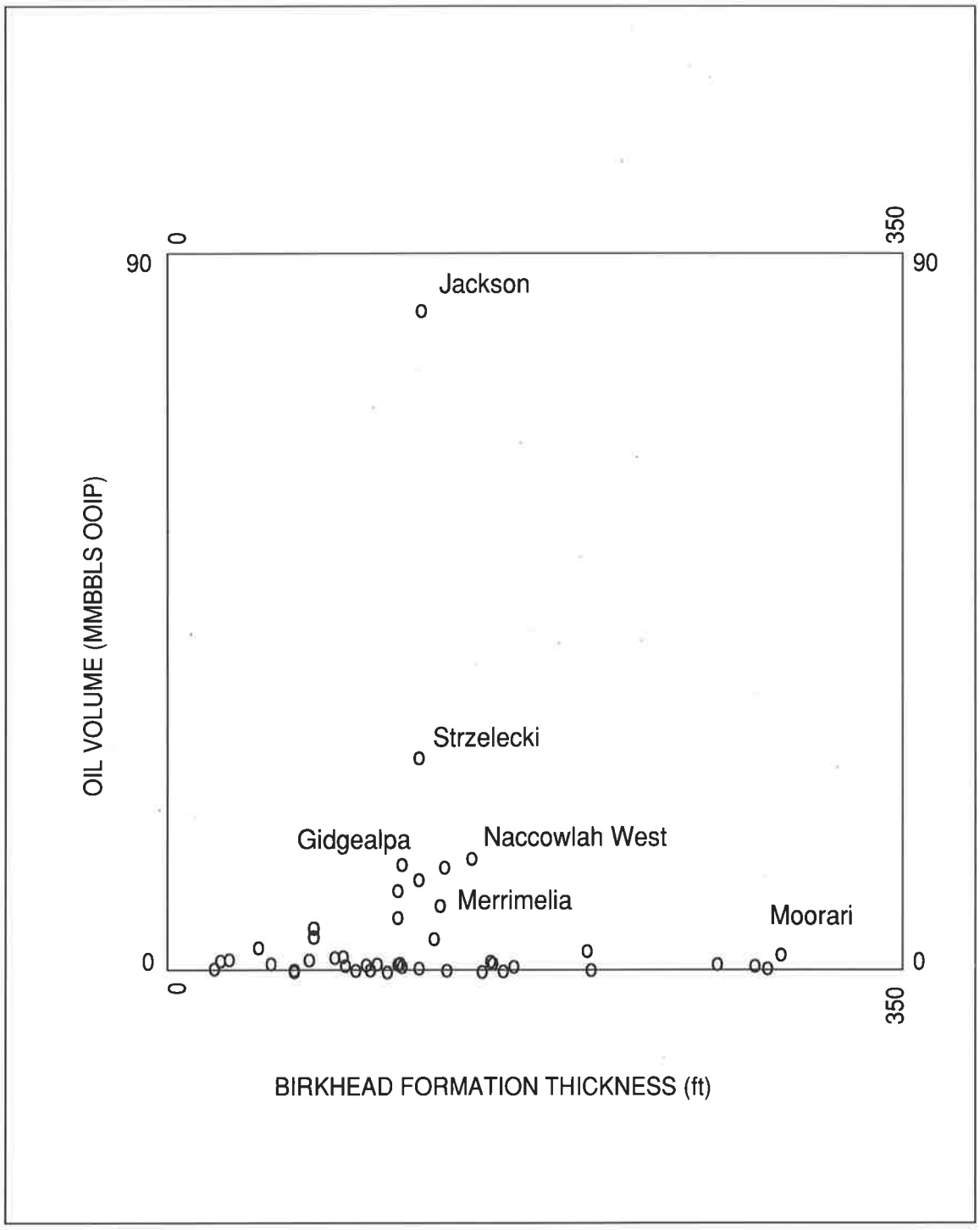

FIG. 24 b : Plot of the Birkhead Formation thickness against the volume of oil reservoired in the Hutton Sandstone below.

trap potential may not be very reliable.

The Birkhead Formation in the Taloola oil field (discussed previously) appears to be very similar to that in the adjacent Tantanna Field, except that the Hutton Sandstone does not contain an oil pool. A comparison of the two fields can be made from the cross sections given in Figs. 19 and 22. The mudstones in the Taloola Field must be breached at, or near the crest of the structure, allowing oil to leak upwards and accumulate in the Namur Member.

The lateral continuity of mudstone layers cannot be predicted from crossplots of Birkhead Formation thickness or by comparing structures that have similar stratigraphic sequences. At best, an undrilled structure can only be given a probability of intersecting oil pools in any horizon.

7.1.4 FAULTING

It has been established that a very thin mudstone layer can trap a substantial oil column, provided it is also continuous over a significant area. This continuity can be broken by faulting or fracturing, just as it can by stratigraphic variation.

However, a fault can also be a seal and prevent the migration of hydrocarbons. Harding and Tuminas (1988 and 1989) describe the mechanisms by which a fault may be either a seal or a migration pathway. It is dependent upon both the presence of fault zone material and the juxtaposition of reservoir lithologies across the fault (Allan, 1989).

The presence of sealing fault zone material such as clay smears, cataclastic gouge and mineral deposits can be determined if the well intersects the fault plane or can be inferred from well and field data. However, the sealing material or the fault throw can also diminish along strike, leaving conduits at various locations.

It has previously been mentioned that faulting is a means by which Permian sourced hydrocarbons are thought to migrate into the Jurassic reservoirs. Therefore, faulting and fracturing probably play a significant part in the migration and trapping of oil pools within the Jurassic sequence. Sprigg (1986) suggested that tectonic activity itself may also play a significant part in both hydrocarbon concentration and migration.

Unfortunately, faults that cut the Jurassic and Early Cretaceous horizons are sometimes difficult to identify and map using seismic techniques, particularly if the faults have small vertical throws. This difficulty is mainly due to the fact that many faults may be below seismic resolution and fault indications can become lost in the reflectors caused by large stratigraphic variations.

Although faults are not interpreted over many structures, in areas where major faults disrupt both the Pre-Permian basement and the Cooper Basin section, it is not unreasonable to assume that some fracturing over the crest of the structure will occur with subsequent compaction or reactivation of major faults. Significant listric faulting is present throughout the Late Cretaceous section and has been identified on many seismic lines across the basin, (Fig. 25). These faults usually sole out above the Murta Member and disappear before cutting horizons below the Namur Member, but some may extend to deeper levels.

Even if faulting through the sealing intervals can be confirmed, the lithologies within the sealing intervals that are juxtaposed across the fault plane cannot be mapped in detail due to the rapid stratigraphic variations.

There are many fields such as Big Lake and Meranji, that have oil pools in the Murta and Namur Members, overlying a thicker Birkhead Formation which should provide a good seal. It is hypothesised that in such fields, vertical migration and the size of the oil accumulations could be controlled primarily by faulting or fracturing of the lower seals.

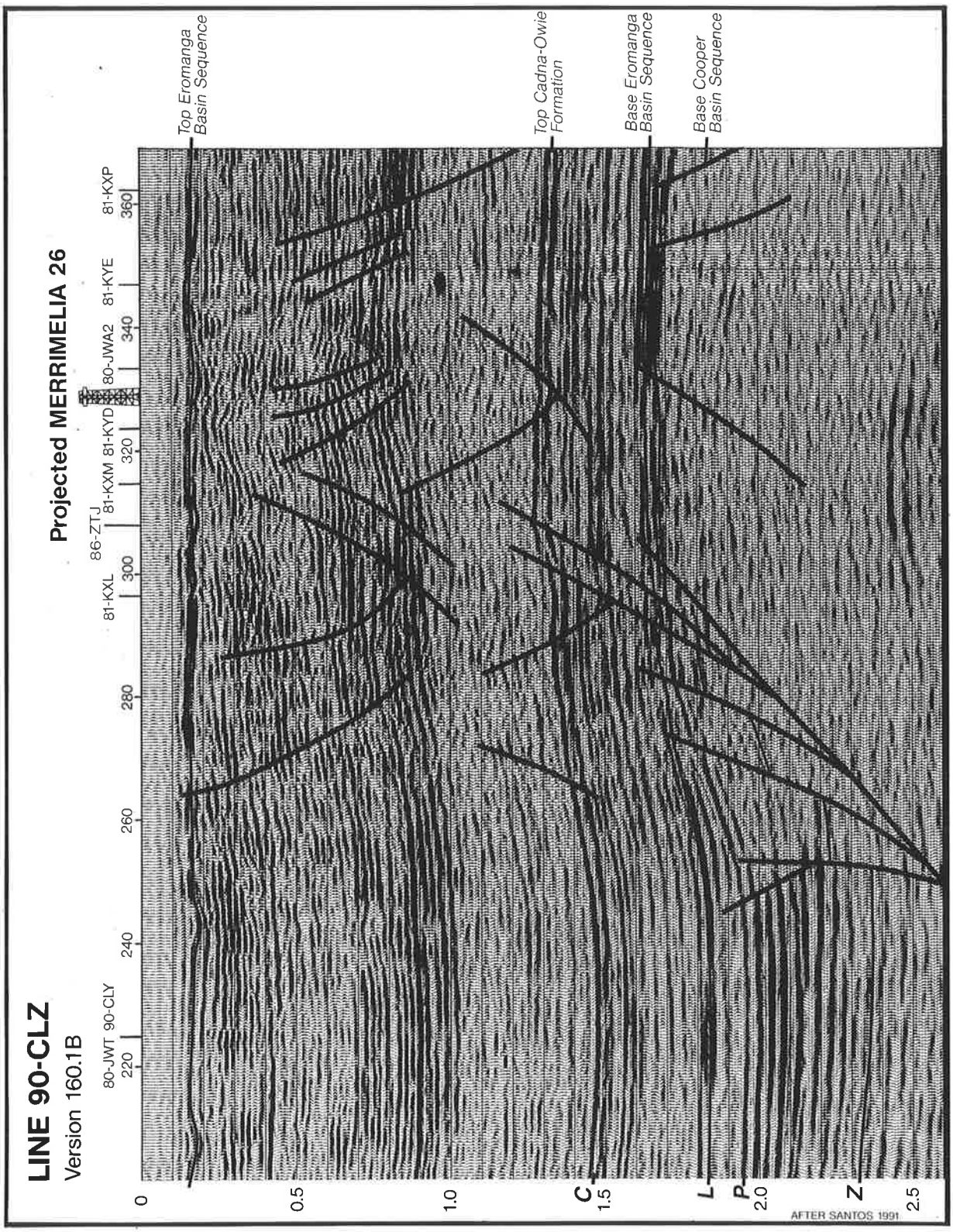

Fig. 25 Seismic dip line across the Merrimelia Field.

The Big Lake Field lies in the central South Australian part of the study area. The structure contains oil pools in the Namur Member, Birkhead Formation and Hutton Sandstone. The underlying Toolachee, Daralingie, Epsilon, Patchawarra and Tirrawarra Formations reservoirs contain large quantities of dry gas. Major northeast-southwest trending regional faults are mapped along the north-western flank and are interpreted to extend at least to the top of the Permo-Triassic Cooper Basin sequence.

In the past, while the Permian sequences in the deeper Nappamerri Trough were in the oil generative phase, significant quantities of oil were probably migrating through the sandstones around the Big Lake Field. Oil may have leaked up faults, accumulating in the Jurassic to Early Cretaceous reservoirs. Further generation of oil and gas from the deeper Nappamerri Trough would have continued to recharge the structure, forcing any remaining oil out to the basin margins. Eventually, in this thermally mature area, dry gas has been left in the Permian formations. Hence, the timing of faulting and seismic activity in relation to hydrocarbon generation and migration also appears to be very important. Gas pools would have accumulated in the Jurassic sequences in many more structures than have been identified, if faulting had developed later in the history of the basin. Present mapping at the level of the Big Lake oil pools is not sufficiently detailed to determine whether or not faulting controls the current size of the accumulations.

In the Meranji Field, located approximately 50 km to the north of the Big Lake Field, an oil pool is present in the Namur Member. The Birkhead Formation is over 130 feet (40m) thick, but there is no oil pool in the underlying Hutton Sandstone. Oil shows are observed in the Birkhead Formation, indicating that some oil may have migrated through at some stage, but no economic oil pools remain. There are very few oil shows above the Birkhead Formation however, indicating that oil migration may have been restricted to a narrow pathway. The controls on vertical distribution within the field are not known, but due to the structural complexity of the area, it is likely that faulting over the structure is involved. The throw on a fault, or some associated fractures, may be such

that in the Birkhead Formation, sandstones are juxtaposed against other porous sandstones, thus forming a conduit for oil migration. If the fault zone itself provides the pathway, oil migration could be restricted to a narrow zone.

Structures may also be completely drained of hydrocarbons due to upper level faulting. This may explain the abundance of oil shows observed in wells drilled at the crest of some structures, even though no oil accumulations have been discovered. Harding and Tuminas (1989) state that normal faults have highly variable sealing capabilities and hence it can be difficult to predict if a faulted structure will be a trap.

It is not only major faulting that can provide pathways for oil to migrate into overlying reservoirs. Due to the finely bedded nature of the sealing lithologies, a fracture with a magnitude of throw in the order of less than a few inches (0.1m), would be sufficient to breach a sealing mudstone. These fractures can occur as a result of major faulting or deformations related to dewatering or compaction in partially lithified sediments. The presence of these fine fractures cannot be proven as they are far below the resolution of seismic methods and current wireline evaluation techniques. Only rarely in full-hole cores such as that shown in Fig. 26, can they be positively identified.

If faulting can be observed in the Cooper Basin section, it does not always follow that upper levels will be breached. The Mawson and Kurunda Fields are located to the south of the Gidgealpa Field, near the Meranji Field. These two small structures contain gas and oil within the underlying Cooper Basin. Faulting is assumed to have provided conduits for hydrocarbons to migrate into the Poolowanna Formation in the Mawson Field. Although the Kurunda Field has a slightly thicker Nappamerri Formation (regional sealing mudstone-siltstone interval of Triassic age), significant faulting similarly occurs over this structure. However, there has been no oil discovered in any of the Jurassic horizons. The faults over the Kurunda Field either do not extend to the Jurassic level or do not place more porous and permeable beds in close proximity across the fault.

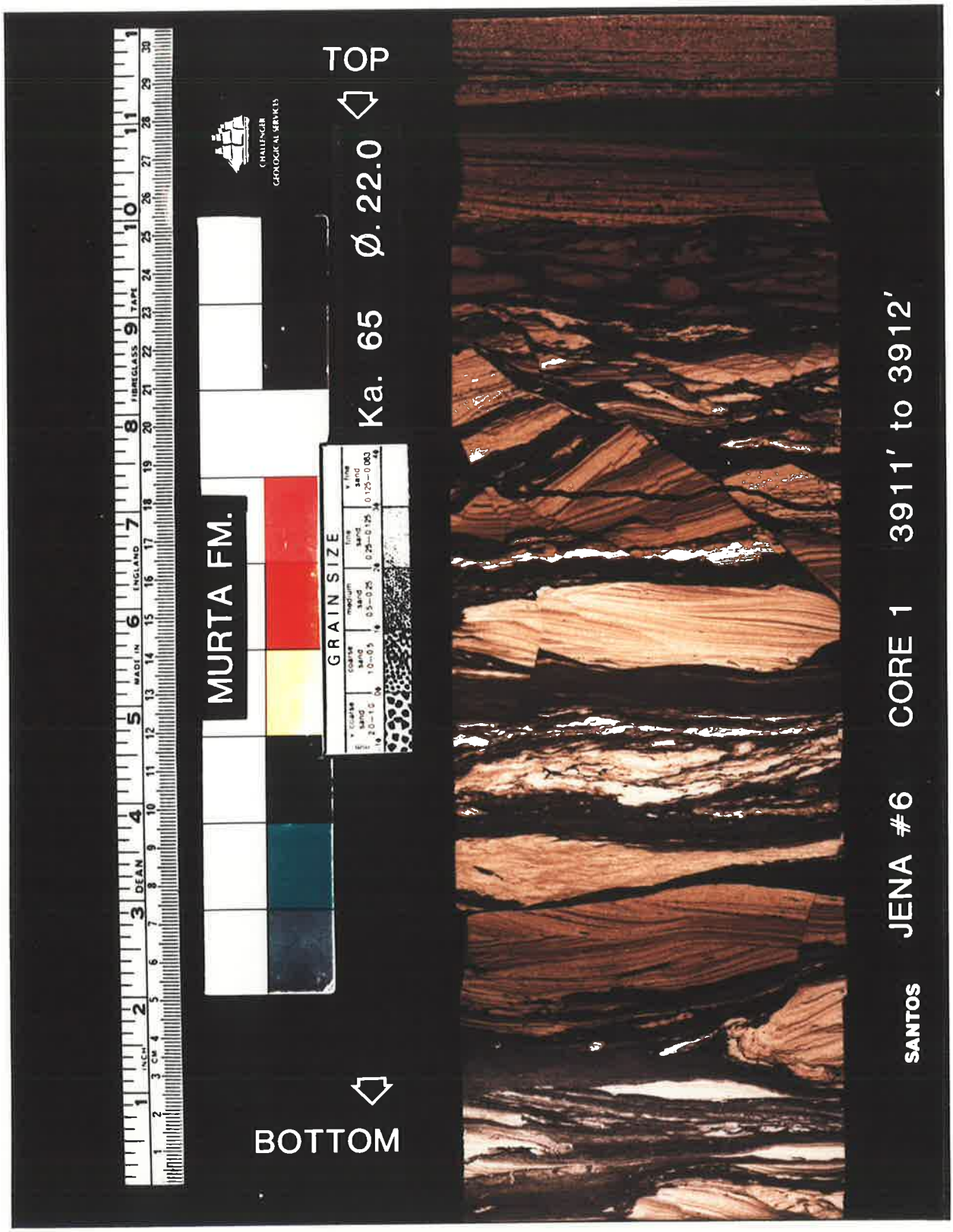

Fig. 26 Core photograph of a sealing interval showing fracturing, Jena 6.

7.1.5 STRUCTURAL TIMING

Additional structural growth after the emplacement of oil into Jurassic reservoirs could be another reason why more structures are not filled to structural spill at the lowest sealing horizon. If the rate of growth exceeds the amount of oil leaking from the Permian sequences into the Eromanga Basin traps, structures cannot be filled to spill.

The total thickness of Jurassic to Early Cretaceous sediment across the Eromanga Basin shows very little variation. Following infilling of the top Triassic erosional topography by the Poolowanna Formation sediments, subsidence was relatively constant across the entire study area. This is evidenced by the Cadna-Owie to Hutton Formation isopach which reaches a maximum thickness of approximately 1560 feet (457m) across the north of the study area and gradually thins to a minimum of 1010 feet (308m) in the south west region.

Present day structural configuration of many closures is in part the result of compaction and Tertiary uplift. If oil was migrating and trapped prior to this structuring, the difference in the total closure height versus the oil column height could be attributed to the additional relief created during the Tertiary events.

As previously discussed, re-activation of faults can also lead to faulting or fracturing of the overlying Eromanga Basin sequence, resulting in a reduction in seal continuity at a level above the existing oil-water contact. Depending upon the level of breaching, some oil may migrate further upwards or the entire oil pool might be lost.

If oil migration into overlying Jurassic structures at the Cooper Basin margins began only a relatively short time ago and is continuing at the present time, recent seismic events, rather than long term structural growth, may have the greatest influence on such accumulations.

7.1.6 OIL VOLUME AVAILABLE FOR ENTRAPMENT

A further group of oil fields may have oil column heights less than the sealing mudstones are capable of holding due to an insufficient volume of oil leaking into the Eromanga reservoir rocks. This would give the same results as the case where structural growth exceeds the supply of hydrocarbons.

Variations in source rock type and quality, lack of suitable migration pathways or small drainage areas could also account for the low volumes of oil discovered in some areas.

Potential Permian source rocks have only just entered the oil window around the margins of the Cooper Basin. In these areas, only relatively minor volumes of oil are thought to have been generated and expelled (Heath et al., 1989). Elsewhere, the amount of Permian sourced oil may be limited by a more gas-prone source rock type.

Evidence for variations in source rock type and quality is obtained from hydrocarbon distributions within the Cooper Basin. In the Gidgealpa and Tirrawarra areas, gas is trapped within the upper Patchawarra Formation and oil is reservoired in the lower Patchawarra Formation and in the underlying Tirrawarra Sandstone. This distribution can be interpreted as a difference in source type, suggesting that the various horizons are generating predominantly either oil or gas.

7.2 CONCLUSIONS

The main aim of this study was to use capillary pressure techniques to determine the seal capacity of several rock samples from the sealing intervals within the Eromanga Basin and to establish if poor seal capacity is one of the major factors controlling the distribution and size of oil pools.

The results of the mercury capillary pressure work show that all of the mudstones sampled have high threshold entry pressures, very low permeabilities and are very good seals. From observations of full hole cores and wireline logs, individual silty mudstones are often less than 3 feet (1m) thick. However, even these thin mudstones should be capable of sealing vertical oil columns from 288 feet (88m) up to several thousand feet (1700 m). Actual oil columns observed are generally less than 50 feet (15m) and commonly less than structural closure. Multiple oil pools are common in a single structure, implying that leakage from horizon to horizon has occurred.

The discrepancy between the seal capacity derived from the capillary pressure results and some of the observed oil columns is due, in part, to the poor lateral continuity of mudstone beds resulting from:

1. Rapid facies changes from mudstone to siltstone and sandstone and
2. Fractures and faults.

The juxtaposition of sandstones and more permeable siltstones across faults and fractures may have allowed the vertical migration of hydrocarbons to occur in the same way as a lateral facies change.

The continuity of thin mudstone beds does appear to control the distribution and size of some oil pools in the Eromanga Basin. It follows that structures will contain oil to

variable levels of fill and will display no consistent patterns. Some horizons are known to be filled to spill, others have oil trapped only in the waste zones and have no economic pools, and others are incapable of holding back any oil column at all.

Hence, although the mudstones are excellent seals, it is concluded that for them to be most effective, they must extend over a reasonable area of the structural closure. The level at which disruption of the seal occurs will define the level to which oil may be trapped.

Although the height of some Eromanga Basin oil columns can be directly related to the seal capacity and continuity of mudstone layers in some cases, there are many other factors that could also control the size and distribution of Eromanga Basin oil pools. These are:

1. access to Permian sourced oil via faults or breached, eroded regional mudstone seals
2. the availability of mature Jurassic or Early Cretaceous source rock that is rich enough to generate and expel significant volumes of oil
3. a sufficiently large volume of oil to fill both the porous and permeable reservoir rocks and the waste zones between the reservoir and the seal
4. structural growth and trap development prior to oil migration.

A statistical approach to identify areas that possess the above attributes will highlight regions of greater oil potential. However, the controls on many of the field examples discussed are still not fully understood.

This study has shown that the mudstones are excellent seals and the potential for large oil accumulations, whether they are structural or stratigraphic, exists. However, in this

discussion it is clear that a large range of variables must all be favourable to enable the accumulation of economic oil pools. The seal capacity and the continuity of mudstones are critical factors but which cannot explain the known distribution of all the Eromanga Basin oil fields in isolation.

REFERENCES CITED

Allan, U. S., 1989. Model for hydrocarbon migration and entrapment within faulted structures: AAPG Bull., v. 73, p. 803-811.

Altmann, M. J., 1989. Jackson Field Hutton and Westbourne hydrocarbons- in-place mapping package, Naccowlah Block, ATP 259P, Qld.: SANTOS Ltd., Adelaide (Unpubl.).

Anderson, W. G., 1986. Wettability literature survey - Part 1: Rock/oil/brine interactions and the effects of core handling on wettability: Jour. Petroleum Technology, (Oct. 1986) p. 1125-1144.

Anderson, W. G., 1987. Wettability literature survey - Part 4: Effects of wettability on capillary pressure: Jour. Petroleum Technology, (Oct.1987) p. 1283-1300.

Berg, R. R., 1975. Capillary pressures in stratigraphic traps: AAPG Bull., v. 59, p. 939-956.

Bowering, O. J. W., 1982. Hydrodynamics and hydrocarbon migration - a model for the Eromanga Basin: APEA Jour., v 22:1., p. 227-236.

Cook, A. C., 1982. Organic facies in the Eromanga Basin. In: Moore, P. S. and Mount, T. J. (eds.), Eromanga Basin symposium summary papers. Geological Society of Australia and Petroleum Exploration Society of Australia, Adelaide, p. 234-257.

Core Laboratories, Western Atlas International, 1989. Contact angle and interfacial tension measurements, Jackson 34 well, Jackson Field: Report for SANTOS Ltd., Adelaide. (unpubl.)

Davis, R. W., 1987. Analysis of hydrodynamic factors in petroleum migration and entrapment: AAPG Bull., v 71, no. 6, p. 643-649.

Downey, M. W., 1984. Evaluating seals for hydrocarbon accumulations: AAPG Bull., v. 68, p. 1752-1763.

England, W. A., Mackenzie, A. S., Mann, D. M. and Quigley, T. M., 1987. The movement and entrapment of petroleum fluids in the subsurface: Jour. Geol. Soc. London Vol 144, p. 327-347.

Gearhart, 1988. Core analysis report for cap-rock assessment: report for SANTOS Ltd., Adelaide. (unpubl.)

Gilby, A. R. and Mortimore, I. R., 1989. The prospects for Eromanga oil accumulations in the northern Cooper Basin region, Australia. In: O'Neil, B. (ed.), The Cooper and Eromanga Basins, Australia. Proceedings of the Petroleum Exploration Society of Australia, Society of Petroleum Engineers, Australian Society of Exploration Geophysicists (SA Branches), Adelaide, 1989.

Gravestock, D. I., Moore, P. S. and Pitt, G. M., (eds.), 1986. Contributions to the geology and hydrocarbon potential of the Eromanga Basin: Geological Society of Australia, Special publication no. 12.

Habermehl, M. A., 1980. The Great Artesian Basin, Australia: BMR Jour. Aust. Geol. Geophys., v. 5, p. 9-38.

Harding, T. P. and Tuminas, A. C., 1988. Interpetation of footwall (lowside) fault traps sealed by reverse faults and convergent wrench faults: AAPG Bull., v. 72, p.738-757.

Harding, T. P. and Tuminas, A. C., 1989. Structural interpetation of hydrocarbon traps sealed by basement normal block faults at stable flank of foredeep basins and at rift basins: AAPG Bull., v. 73, p.812-840.

Heath, R. S., McIntyre, S. M. and Gibbons, N., 1989. A Permian origin for Jurassic reservoired oil in the Eromanga Basin. In: O'Neil, B. (ed.), The Cooper and Eromanga Basins, Australia. Proceedings of the Petroleum Exploration Society of Australia, Society of Petroleum Engineers, Australian Society of Exploration Geophysicists (SA Branches), Adelaide, 1989.

Hocott, C. R., 1938. Interfacial tension between water and oil under reservoir conditions: AIME Petroleum Trans., v. 32, p. 184-190.

Hunt, J. W., Heath, R. S. and McKenzie, P. F., 1989. Thermal maturity and geological controls on the distribution and composition of Cooper Basin hydrocarbons. In: O'Neil, B. (ed.), The Cooper and Eromanga Basins, Australia. Proceedings of the Petroleum Exploration Society of Australia, Society of Petroleum Engineers, Australian Society of Exploration Geophysicists (SA Branches), Adelaide, 1989.

Jenkins, C., 1989. Geochemical correlation of source rocks and crude oils from the Cooper and Eromanga Basins. In: O'Neil, B. (ed.), The Cooper and Eromanga Basins, Australia. Proceedings of the Petroleum Exploration Society of Australia, Society of Petroleum Engineers, Australian Society of Exploration Geophysicists (SA Branches), Adelaide, 1989.

Jennings, J. B., 1987. Capillary pressure techniques: application to exploration and development geology: AAPG Bull., v. 71, p. 1196-1209.

Kantsler, A. J, Cook, A. C. and Zwigulis, M., 1982. Maturation patterns in the Eromanga Basin. In: Moore, P. S. and Mount, T. J. (eds.), Eromanga Basin symposium summary papers. Geological Society of Australia and Petroleum Exploration Society of Australia, Adelaide, p. 284-295.

Keelan, D.(Comp.), 1982. A course in special core analysis, Corelab Laboratories Inc., p. 3.1-3.17.

Leverett, M. C., 1941. Capillary behavior in porous solids: AIME Petroleum Trans., v. 142, p. 152-169.

Livingston, H. K., 1938. Surface and interfacial tension of oil-water systems in Texas oil sands: AIME Tech. Paper 1001.

McCaffery, F. G., 1972. Measurement of interfacial tensions and contact angles at high temperature and pressure: Jour. Canadian Petroleum Technology, v. 11, no. 3, p. 26-32.

McIntyre, S., 1987. Origin of Eromanga Basin sequence oil pools, some arguments supporting the case for a Patchawarra source: SANTOS Ltd., Adelaide. (unpubl.)

McKirdy, D. M., 1982. Aspects of the source rock and petroleum geochemistry of the Eromanga Basin. In: Moore, P. S. and Mount, T. J. (eds.), Eromanga Basin symposium summary papers. Geological Society of Australia and Petroleum Exploration Society of Australia, Adelaide, p. 258-259.

Michaels, A. S. and Hauser, E. A., 1951. Interfacial tension at elevated pressure and temperature: Jour. Phys. Chem., v. 55, p. 408-421.

Michaelsen, B. H. and McKirdy, D. M., 1989. Organic facies and petroleum geochemistry of the lacustrine Murta Member (Mooga Formation) in the Eromanga Basin, Australia. In: O'Neil, B. (ed.), The Cooper and Eromanga Basins, Australia. Proceedings of the Petroleum Exploration Society of Australia, Society of Petroleum Engineers, Australian Society of Exploration Geophysicists (SA Branches), Adelaide, 1989.

Moore, P. S. and Mount, T. J. (eds.), 1982. Eromanga Basin symposium summary papers. Geological Society of Australia and Petroleum Exploration Society of Australia, Adelaide.

Moriarty, K. C. and Williams, A. F., 1982. Hydrocarbon flushing in the Eromanga Basin - fact or fallacy. In: Moore, P. S. and Mount, T. J. (eds.), Eromanga Basin symposium summary papers. Geological Society of Australia and Petroleum Exploration Society of Australia, Adelaide, p. 313-328.

Omoregie, Z. S., 1986. Factors affecting the equivalency of different capillary pressure measurement techniques: SPE paper 15384.

O'Neil, B. (ed), 1989. The Cooper and Eromanga Basins, Australia. Proceedings of the Petroleum Exploration Society of Australia, Society of Petroleum Engineers, Australian Society of Exploration Geophysicists (SA Branches), Adelaide, 1989.

Passmore, V. L., 1989. Petroleum accumulations of the Eromanga Basin: a comparison with other Australian Mesozoic accumulations. In: O'Neil, B. (ed.), The Cooper and Eromanga Basins, Australia. Proceedings of the Petroleum Exploration Society of Australia, Society of Petroleum Engineers, Australian Society of Exploration Geophysicists (SA Branches), Adelaide, 1989.

Pickell, J.J., Swanson, B.F. and Hickman, W. B., 1966. Application of air-mercury and oil-air capillary pressure data in the study of pore structure and fluid distribution: SPE Jour., v. 6, no. 1, p. 55-61.

Purcell, W. R., 1949. Capillary pressure - their measurements using mercury and the calculation of permeability therefrom: AIME Petroleum Trans., v. 186, p. 39-48.

Richardson, J. G., Perkins, F. M. Jr. and Osoba, J. S., 1955. Differences in behaviour of fresh and aged East Texas Woodbine cores: AIME Petroleum Trans., v. 204, p. 86-91.

Rigby, D. and Smith, J. W., 1981. An isotopic study of gases and hydrocarbons in the Cooper Basin. APEA Jour., v. 21(1), 222-229.

Rudd, N. and Pandey, G. N., 1973. Threshold pressure profiling by continuous injection: AIME-SPE Paper 4597, 7p.

Santos Ltd., 1990. Regional mapping project for the Lake Hope Block, South Australia, SANTOS Ltd., (western team) Adelaide. (unpubl.)

Santos Ltd., 1991. Merrimelia Field mapping project, Merrimelia/ Innamincka Block, South Australia, SANTOS Ltd., (northern team) Adelaide. (unpubl.)

Schowalter, T. T., 1979. Mechanics of secondary hydrocarbon migration and entrapment: AAPG Bull., v. 63, p. 723-760.

Schowalter, T. T. and Hess, P. D., 1982. Interpretation of subsurface hydrocarbon shows: AAPG Bull., v. 66, p. 1302-1327.

Sprigg, R. C., 1986. The Eromanga Basin in the search for commercial hydrocarbons.In: Gravestock, D. I., Moore, P. S. and Pitt, G. M., (eds.), Contributions to the geology and hydrocarbon potential of the Eromanga Basin: Geological Society of Australia, Special publication no. 12, p. 9-24.

Thomas, B. M., 1982. Land-plant source rocks for oil and their significance in Australian basins: APEA Jour., v. 22(1), p. 164-178.

Thomas, L. K., Katz, D. L. and Tek, M. R., 1968. Threshold pressure phenomena in porous media: SPE Jour., June, p. 174-184. (AIME-SPE paper 1816).

Tissot, B. P. and Welte, D. H., 1978. Petroleum formation and occurence. Springer-Verlag, Berlin, 538 p.

Tupper, N. P. and Burckhardt, D. M., 1990. Use of the methyl- phenanthrene index to characterise expulsion of Cooper and Eromanga Basin oils: APEA Jour., v. 30, p. 373-385.

Watts, N. L., 1987. Theoretical aspects of cap-rock and fault seals for single and two phase hydrocarbon columns: Marine and petroleum geology, v. 4, p. 274-307.

APPENDIX TABLE 1 - ROUTINE CORE ANALYSIS RESULTS

WELL NAME AND NUMBER	FORMATION	PLUG NO.	POR (%)	PERM (MD)	OVERBDN PERM (MD)	PRESS (PSI)	GRAIN DENS (G/CC)	PORE RADII (MICR)	MICRO POR (%)
BIG LAKE 26	BIRKHEAD	1	3.7	0.0037	0.0001	1950	2.539	0.0046	99.0
BIG LAKE 26	BIRKHEAD	4	3.8	0.0872	0.0025	1940	2.602	0.0046	98.5
BIG LAKE 26	BIRKHEAD	5	2.2	0.0025	0.0000	1945	2.548	0.0036	97.0
CORKWOOD 1	BIRKHEAD	8	5.0	0.0340	0.0080	1669	2.680	0.0046	98.5
GIDGEALPA 29	BIRKHEAD	9	4.7	0.0021	0.0000	1800	2.678	0.0046	99.5
GIDGEALPA 30	BIRKHEAD	11	7.0	0.0044	0.0000	1800	2.647	0.0036	98.5
GIDGEALPA 30	BIRKHEAD	13	6.5	0.0044	0.0000	1800	2.662	0.0036	98.5
MOORARI 5	BIRKHEAD	15	1.3	0.0041	0.0000	2120	2.581	0.0036	96.5
WANCOOCHA 4	BIRKHEAD	16	6.1	0.0033	0.0000	1540	2.616	0.0074	98.5
WANCOOCHA 4	BIRKHEAD	17	6.3	0.0031	0.0000	1540	2.654	0.0093	98.0
DULLINGARI 9	MURTA MB	20	11.6	0.0036	0.0005	1450	2.706	0.0036	97.5
DULLINGARI 9	MURTA MB	21	9.3	0.0042	0.0002	1450	2.666	0.0093	98.0
DULLINGARI 15	MURTA MB	25	6.6	0.0030	0.0000	1445	2.607	0.0074	98.5
DULLINGARI 15	MURTA MB	26	9.0	0.0028	0.0002	1450	2.651	0.0036	99.5
DULLINGARI 15	MURTA MB	27	7.3	0.0028	0.0001	1450	2.703	0.0036	99.0
DULLINGARI 27	MURTA MB	28	10.8	0.0093	0.0002	1475	2.664	0.0036	99.0
DULLINGARI 27	MURTA MB	29	9.8	0.0041	0.0003	1475	2.686	0.0118	99.0
DULLINGARI 35	MURTA MB	31	11.3	0.0041	0.0007	1475	2.697	0.0149	99.0
DULLINGARI 35	MURTA MB	32	13.6	0.0347	0.0039	1470	2.677	0.0772	97.0
FLY LAKE 4	MURTA MB	33	9.3	0.0032	0.0000	1765	2.679	0.0058	99.5
FLY LAKE 4	MURTA MB	34	8.4	0.0029	0.0000	1770	2.633	0.0149	97.5
LIMESTONE CK 6	MURTA MB	35	13.8	0.0056	0.0006	1200	2.841	0.0772	97.0
LIMESTONE CK 6	MURTA MB	36	9.0	0.0037	0.0006	1200	2.919	0.0093	98.5
MERRIMELIA 3	BIRKHEAD	43	6.5	0.0039	0.0000	1900	2.654	0.0046	97.5
STRZELECKI 4	BIRKHEAD	49	1.1	0.0038	0.0000	1650	2.433	0.0058	97.0
STRZELECKI 4	BIRKHEAD	50	2.9	0.0048	0.0000	1655	2.597	0.0036	98.5
STRZELECKI 5	BIRKHEAD	51	3.0	0.0021	0.0000	1650	2.587	0.0036	98.0
STRZELECKI 5	BIRKHEAD	53	3.0	0.0021	0.0000	1650	2.639	0.0046	97.5
STRZELECKI 5	BIRKHEAD	54	2.4	0.0032	0.0000	1660	2.632	0.0036	97.5
CALAMIA WEST 1	NAMUR MB	56	8.3	0.0039	0.0002	1220	3.025	0.0189	98.5
CALAMIA WEST 1	NAMUR MB	57	14.9	0.0042	0.0004	1225	2.645	0.0093	89.5
BIALA 3	NAMUR MB	58	3.1	0.0024	0.0000	1210	3.295	0.0036	100
BIALA 3	NAMUR MB	59	13.1	0.0079	0.0004	1210	2.695	0.0118	99.0
DULLINGARI 29	NAMUR MB	60	7.0	0.0026	0.0000	1470	2.696	0.0074	98.5
DULLINGARI 29	NAMUR MB	62	4.8	0.0025	0.0000	1480	2.719	0.0058	100
DULLINGARI 32	NAMUR MB	63	5.8	0.0035	0.0000	1480	2.666	0.0036	98.5
DULLINGARI 32	NAMUR MB	64	4.9	0.0040	0.0001	1485	2.549	0.0118	99.0
GIDGEALPA 24	NAMUR MB	65	6.3	0.0035	0.0000	1555	3.165	0.0036	96.5
GIDGEALPA 24	NAMUR MB	66	6.1	0.0025	0.0000	1555	2.629	0.0058	99.0
MARABOOKA 1	NAMUR MB	68	4.7	0.0031	0.0000	1430	2.613	0.0058	94.0
MERRIMELIA 6	NAMUR MB	70	6.9	0.0026	0.0000	1560	2.754	0.0074	99.5
MERRIMELIA 6	NAMUR MB	71	9.3	0.0026	0.0000	1565	2.664	0.0058	100
MERRIMELIA 8	NAMUR MB	72	5.7	0.0030	0.0000	1570	3.300	0.0046	100
MERRIMELIA 8	NAMUR MB	73	9.6	0.0320	0.0030	1570	2.680	0.0058	97.0
MUDERA 1	NAMUR MB	76	7.1	0.0037	0.0000	1490	2.644	0.0058	100
JACKSON 2	MURTA MB	77	13.4	0.0027	0.0001	1090	2.673	0.0093	98.0
JACKSON 3	MURTA MB	79	11.5	0.0026	0.0000	1095	2.664	0.0074	98.0
JACKSON 3	MURTA MB	80	10.5	0.0024	0.0000	1095	2.663	0.0058	100
WILSON 2	MURTA MB	81	12.1	0.0037	0.0000	1120	2.662	0.0074	99.5
JACKSON 18	BIRKHEAD	82	0.7	0.0035	0.0000	1460	2.581	0.0058	97.0
JACKSON 18	BIRKHEAD	83	2.0	0.0025	0.0000	1430	2.581	0.0058	97.5
JACKSON 30	BIRKHEAD	84	4.8	0.0037	0.0000	1415	2.587	0.0058	96.5
PITCHERY 2	MURTA MB	86	9.2	0.0034	0.0000	1335	2.673	0.0074	98.5
TALOOLA 2	NAMUR MB	90	11.9	0.0059	0.0028	1380	2.607	0.0239	91.5

APPENDIX TABLE 2 - OIL DENSITIES

WELL NAME AND NUMBER	FORMATION	OIL DENSITY GM/CC
BIG LAKE 26	BIRKHEAD FM	0.686
CORKWOOD 1	BIRKHEAD FM	0.700
GIDGEALPA 29	BIRKHEAD FM	0.692
GIDGEALPA 30	BIRKHEAD FM	0.692
MOORARI 5	BIRKHEAD FM	0.713
WANCOOCHA 4	BIRKHEAD FM	0.717
DULLINGARI 9	MURTA MEMBER	0.676
DULLINGARI 35	MURTA MEMBER	0.676
FLY LAKE 4	MURTA MEMBER	0.713
LIMESTONE CK 6	MURTA MEMBER	0.763
THREE QUEENS 1	MURTA MEMBER	0.700
WILPINNIE 1	MURTA MEMBER	0.700
MERRIMELIA 3	BIRKHEAD FM	0.681
MULAPULA 1	BIRKHEAD FM	0.700
STRZELECKI 4	BIRKHEAD FM	0.745
CALAMIA WEST 1	NAMUR MEMBER	0.700
BIALA 3	NAMUR MEMBER	0.748
DULLINGARI 29	NAMUR MEMBER	0.684
GIDGEALPA 24	NAMUR MEMBER	0.747
MARABOOKA 1	NAMUR MEMBER	0.718
MCKINLAY 2	NAMUR MEMBER	0.710
MERRIMELIA 6	NAMUR MEMBER	0.710
MOOMBA 18	NAMUR MEMBER	0.710
MUDERA 1	NAMUR MEMBER	0.718
JACKSON 3	MURTA MEMBER	0.705
WILSON 2	MURTA MEMBER	0.705
JACKSON 18	BIRKHEAD FM	0.786
JACKSON 30	BIRKHEAD FM	0.786
PITCHERY 2	MURTA MEMBER	0.718
TALOOLA 2	NAMUR MEMBER	0.695

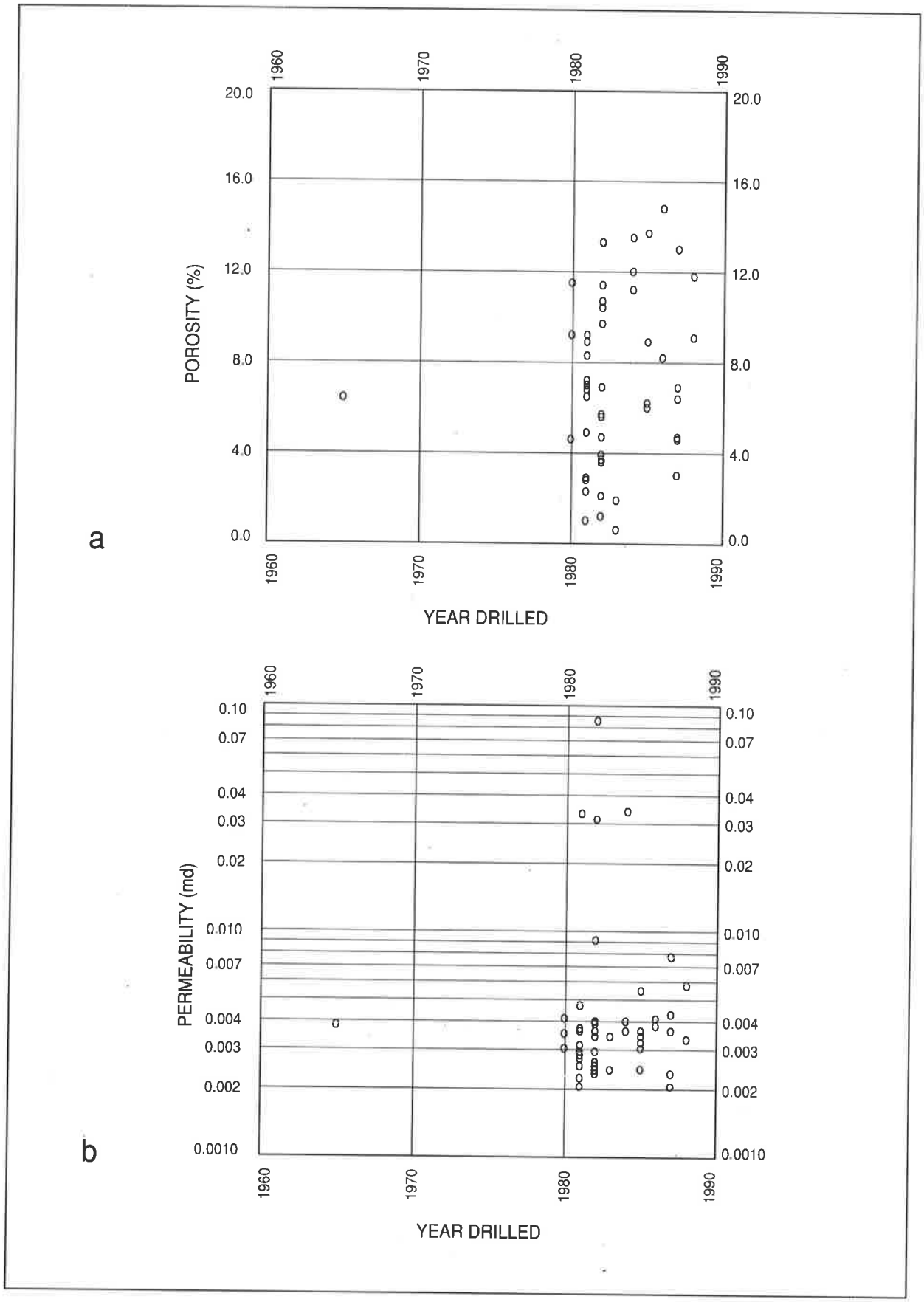

APP. FIG. 1 : Crossplots of the Year the Well was Drilled against a) the Porosity and against b) the Permeability.

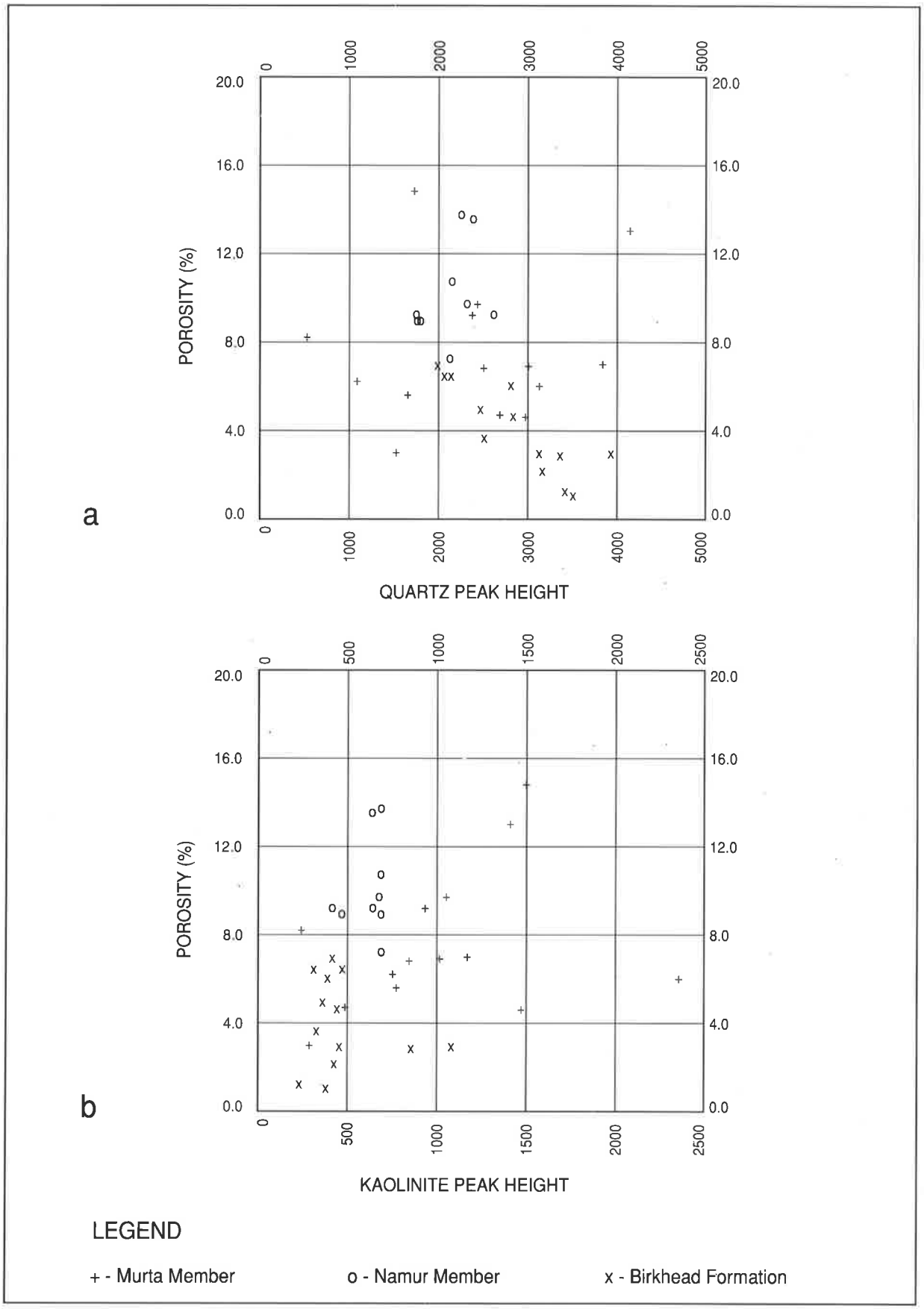

APP. FIG. 2 : Crossplots of X-Ray Diffraction Mineral Peak Heights
a) Quartz, b) Kaolinite against the Porosity.

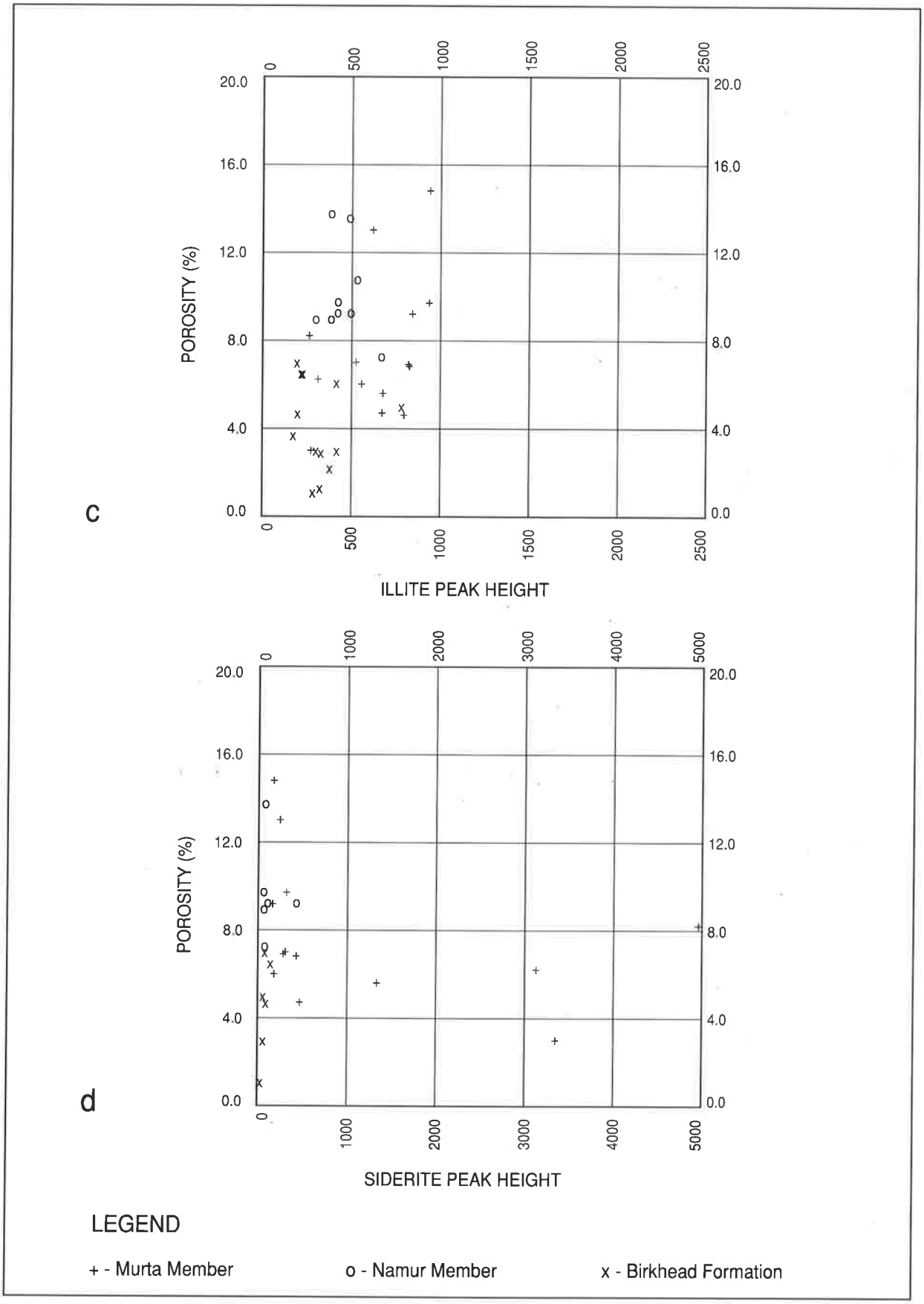

APP. FIG. 2 : Crossplots of X-Ray Diffraction Mineral Peak Heights
CONT. c) Illite, d) Siderite against the Porosity.

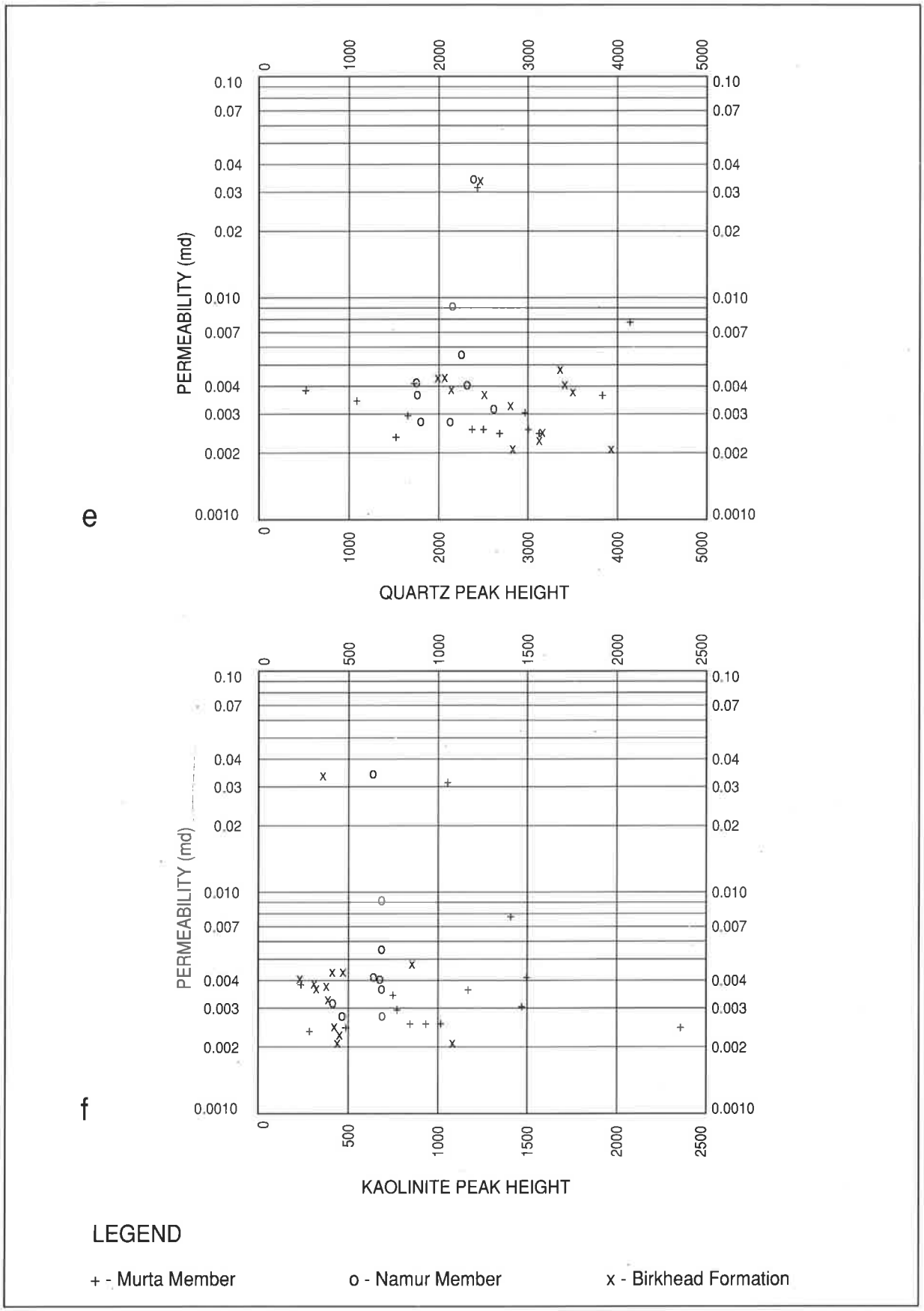

APP. FIG. 2 : Crossplots of X-Ray Diffraction Mineral Peak Heights
CONT. e) Quartz, f) Kaolinite against the Permeability.

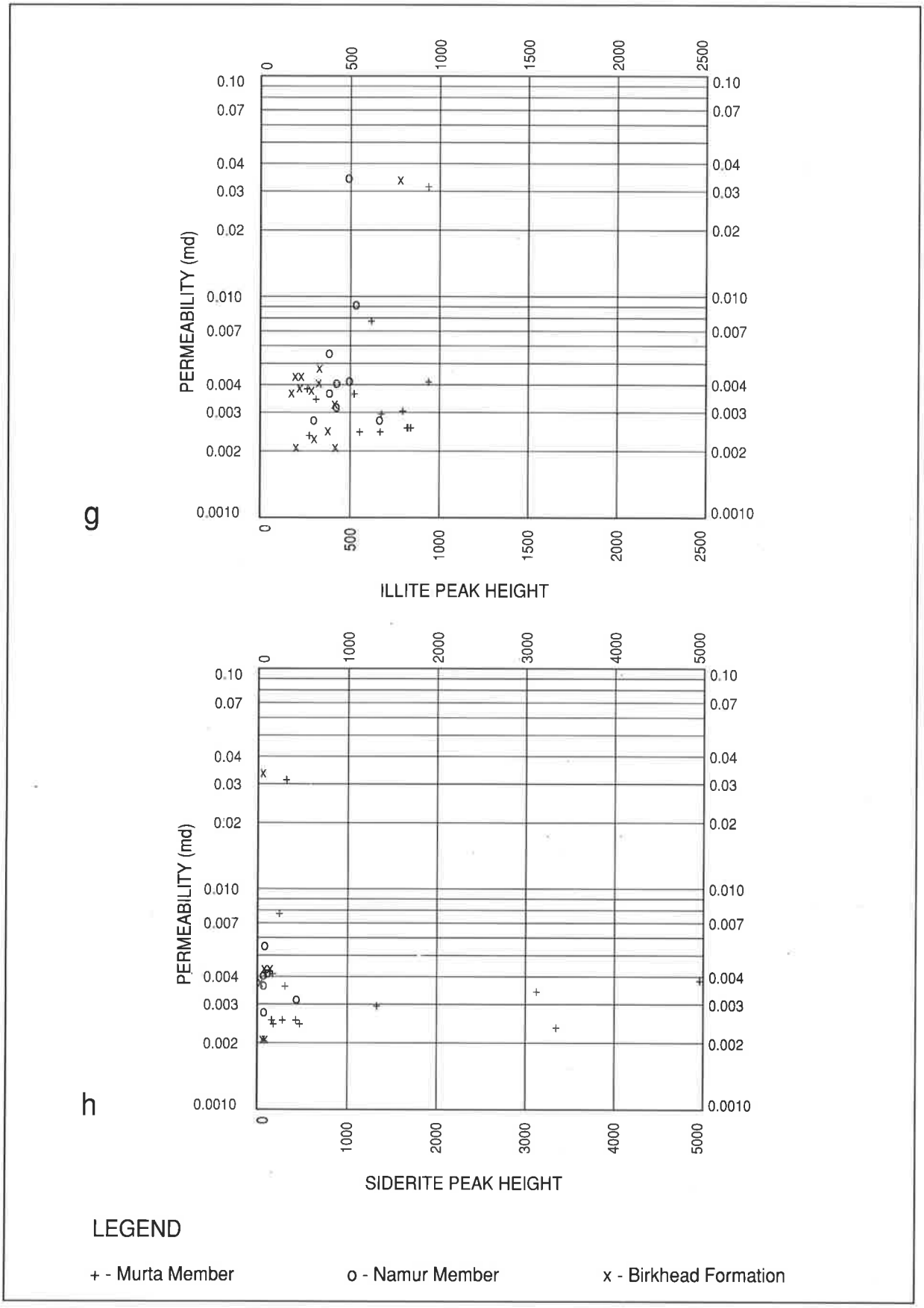

APP. FIG. 2 : Crossplots of X-Ray Diffraction Mineral Peak Heights
CONT. g) Illite, h) Siderite against the permeability.

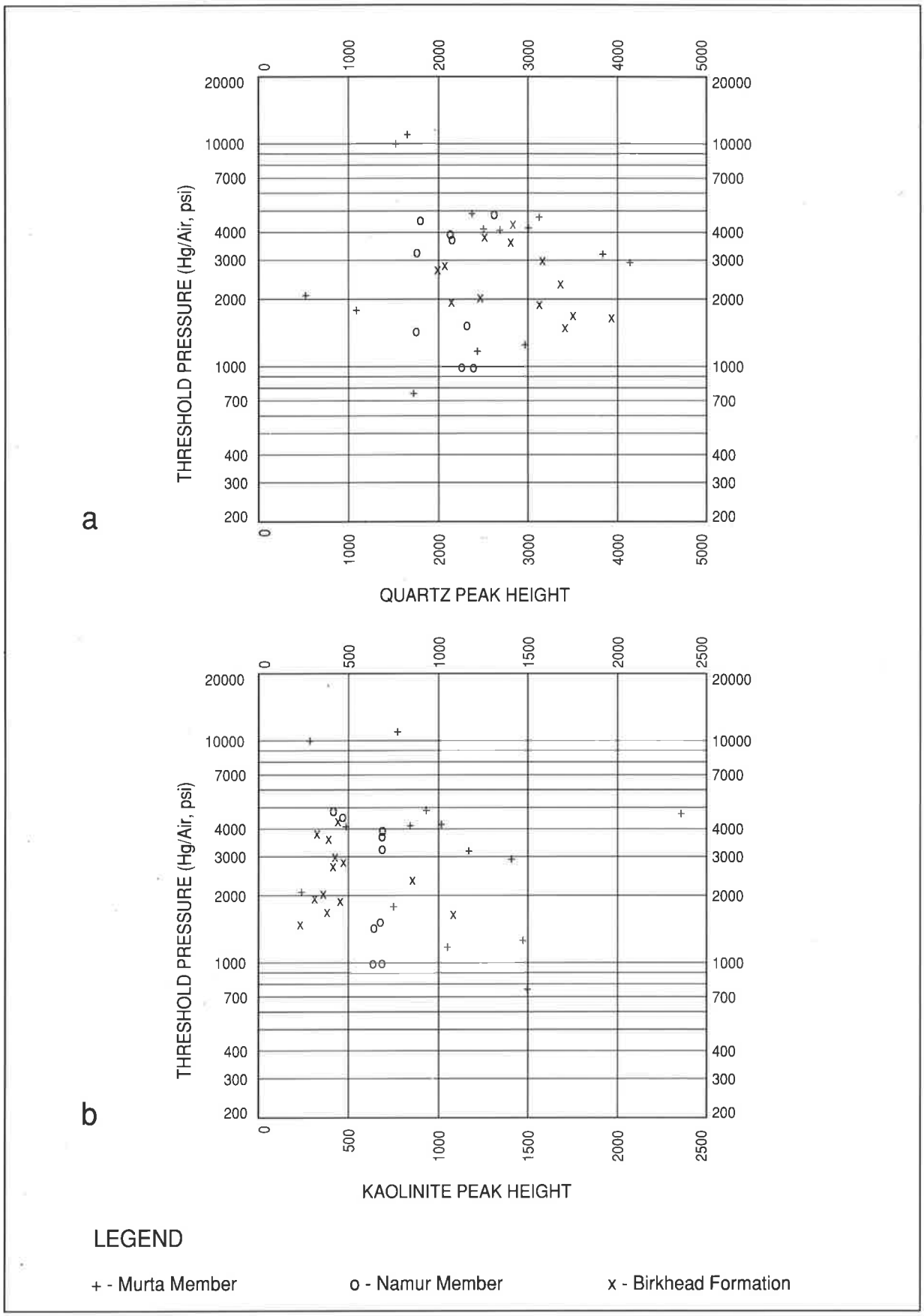

APP. FIG. 3 : Crossplots of X-Ray Diffraction Mineral Peak Heights
a) Quartz, b) Kaolinite against the Threshold Pressure.

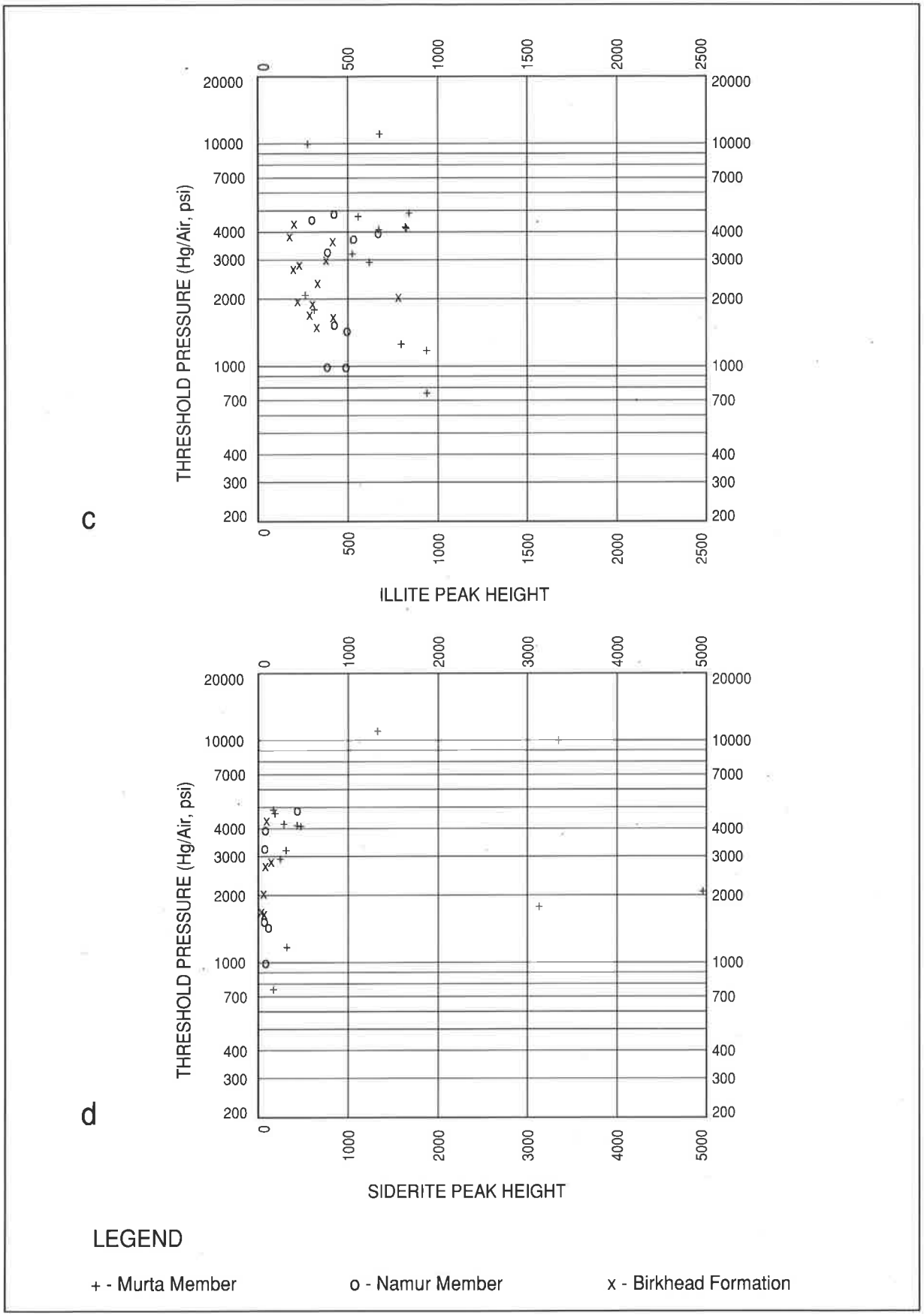

APP. FIG. 3 : Crossplots of X-Ray Diffraction Mineral Peak Heights
CONT. c) Illite, d) Siderite against the Threshold Pressure.